

UC Riverside

UC Riverside Electronic Theses and Dissertations

Title

The Design, Synthesis and Evaluation of Peptoid Heparin Inhibitors

Permalink

<https://escholarship.org/uc/item/5g32g729>

Author

Ford, Bruce

Publication Date

2011

Peer reviewed|Thesis/dissertation

UNIVERSITY OF CALIFORNIA
RIVERSIDE

The Design, Synthesis and Evaluation of Peptoid Heparin Inhibitors

A Dissertation submitted in partial satisfaction
of the requirements for the degree of

Doctor of Philosophy

in

Chemistry

by

Bruce Kevin Ford

August 2011

Dissertation Committee:
Dr. Dallas Rabenstein, Chairperson
Dr. Michael Marsella
Dr. Cindy Larive

Copyright by
Bruce Kevin Ford
2011

The Dissertation of Bruce Kevin Ford is approved:

Committee Chairperson

University of California, Riverside

ACKNOWLEDGEMENTS

There are many people who are responsible for inspiring me and who have been supportive to me in this academic journey that I would be remiss if I did not take a moment to acknowledge. I began my academic career majoring in Art. I began to draw at the tender age of two, a practice along with painting that I kept up for the duration of my life. It had always been assumed by my family and myself, that I would grow up to choose a career in Art. The practice of Art has given me many hours of satisfaction. However I realized as a young man that enjoyable and rewarding as Art is, it is very difficult to earn a living wage by it and realized that I did not want to end up another Vincent Van Gogh, penniless and dependent on relatives to support my passion, so I began to look around for something more practical that I could earn a living at while engaging my creative imagination and in the end I decided to change my academic major to Chemistry and found that I could exercise creativity in the sciences as well as in the the Arts

However such a dramatic change in academic majors required starting over from scratch and the help of many teachers along the way. I will never forget, and will always be indebted to Mr Radin, who taught me Calculus but who passed away from natural causes long before his time. No acknowledgement would be complete without thanking Dr. Cindy Kellen-Yeun, for whom I will always have the highest regard, and is one of the

most gifted teachers I have ever met. Her passion for Organic Chemistry inspired me to modify my undergraduate major from Biochemistry, for which I received a Bachelors'Degree to Organic Chemistry when I decided to pursue a Doctorate in Chemistry. She also taught me organic reaction mechanisms from scratch and much about research as well, as my undergraduate research advisor. It was also directly because of her that I decided to continue on to graduate school and to aspire to a doctorate degree in the first place.

I would also like to give credit to Dr. Michael Pirrung, from whom I continued my advanced education in organic chemistry. I am grateful for his practical tutelage in synthetic Organic Chemistry and for choosing me to design the cover art for his book 'The Synthetic Organic Chemist's Companion'. I would like to thank Dr. Eric Chronister, who came to my assistance in difficult times. I very special thanks goes to Dr. Dallas Rabenstein, always wise, even tempered, understanding, patient and is an exceptional mentor. It is Dallas who enabled me to achieve this degree through a project that I found both enjoyable and intellectually engaging.

I also want to give thanks to my family, both those surviving members and those who have passed on while I attended graduate school including my Mom, Dad and older brother Mike. And finely I would like to acknowledge Sevana Khodagholian, who was my closest friend in graduate school and remains to this day.

Bruce Kevin Ford

ABSTRACT OF THE DISSERTATION

The Design and Evaluation of Peptoid Heparin Inhibitors

by

Bruce Kevin Ford

Doctor of Philosophy, Graduate Program in Chemistry
University of California, Riverside, August 2011
Dr. Dallas Rabinstein, Chairperson

Heparin has found use as an anticoagulant in medicine for more than 70 years¹ and also plays important biological roles in addition to its involvement in the inhibition of the coagulant cascade. Since human blood has a tendency to clot in direct contact with plastics, intravenous lines are coated with heparin to inhibit coagulation during surgery, or in kidney dialysis and in other medical situations where blood is circulated extracorporeally, where it comes into direct contact with synthetic materials. Also heparan sulfate is added to the intravenous blood supply for the same purpose. Following a medical procedure of this type, it is necessary to reverse the effects of the heparin and heparan sulfate. Currently protamine is the only substance available for this purpose. Protamine is derived from natural sources and possesses immunogenic effects.

In this study, a series of peptoids, which are analogs of peptides, have been designed, synthesized² and studied with the goal of producing molecules with high binding affinity to heparin. The peptoids were produced through a solid phase synthesis methodology using a two step submonomer procedure to create each peptoid monomer unit, which were then joined together to produce a library of 18 peptoid analogs. These peptoids

were designed and synthesized with amine bearing side chains strategically located along the peptoid sequence, resulting in cationic peptoids at neutral pH. The amine side chains were also converted to guanidium groups post synthesis of the peptoid oligomers to yield a second family of cationic peptoids that are analogs of arginine containing peptides. Upon synthesis of these two related libraries of peptoids, they were studied using a variety of methods including isothermal titration calorimetry, heparin affinity chromatography, MALDI-TOF MS, and circular dichroism.

The results of these studies indicated that it is possible to synthesize high-binding affinity peptoids to heparin. It is hoped that these peptoids, by binding tightly with heparin could potentially replace the too often immunogenic side effects of protamine currently in use in medicine today.

References

1. Folkman, J., Langer, R., Linhardt, R. J., Haudenschild, C., Taylor, S. *Science* **1983**, *221*, 719-725.
2. Zuckermann, R.N., Kerr, J.M., Kent, S.B, Moos, W.H. *J. Am. Chem. Soc.* **1992**, *114*, 10646-10647.

Table of Contents

Chapter 1: Introduction	1.
1.1 Overview of the Dissertation.....	1.
1.2 Peptoids.....	5.
1.3 Structural Aspects of Peptoids.....	18.
1.4 Studies of Biological Effects of Peptoids.....	26.
1.5 Heparin and Heparin-binding Peptoids.....	31.
1.6 Anticoagulant Activity of Heparin.....	38.
1.7 Other Biological Functions of Heparin.....	43.
1.8 This Dissertation.....	44.
1.9 References.....	50.
Chapter 2: Experimental Section	55.
2.1 Automated Solid Phase Peptoid Synthesis.....	55.
2.1.1. Chemicals.....	55.
2.1.2. Peptoid Synthesizer Instrumentation.....	56.
2.1.3. Overview of Peptoid Synthesis Methodology.....	57.

2.1.4. Example Peptoid Synthesis.....	64.
2.2 Isothermal Titration Calorimetry.....	71.
2.2.1. Materials and Instrumentation.....	71.
2.2.2. Overview of ITC Titration Procedure.....	72.
2.2.3. Example of ITC Experiment.....	80.
2.3 Heparin Affinity Chromatography.....	83.
2.3.1. Overview.....	83.
2.3.2. Materials and Instrumentation.....	86.
2.3.3. Experimental Method.....	86.
2.4. Circular Dichroism.....	87.
2.4.1. Overview.....	87.
2.4.2. Materials and Instrumentation.....	89.
2.4.3. Method of Circular Dichroism.....	89.
2.5. MALDI TOF Mass Spectrometry.....	90.
2.5.1. Overview.....	90.
2.5.2. Materials and Instrumentation.....	90.

2.5.3. Experimental Methods.....	91.
2.6. High Performance Liquid Chromatography.....	91.
2.6.1. Overview.....	93.
2.6.2. Materials and Instrumentation.....	94.
2.6.3. Experimental Methods.....	95.
2.7. Lyophilization.....	96.
2.7.1. Overview.....	96.
2.7.2. Materials and Instrumentation.....	97.
2.7.3. Experimental Methods.....	97.
2.8 Solvent Evaporation under High Vacuum by Rotovap.....	98.
2.8.1. Overview.....	98.
2.8.2. Materials and Instrumentation.....	99.
2.8.3. Experimental Methods.....	99.
2.9. References	100.
Chapter 3: The Effect of Chirality and Length on Heparin- Binding Affinity.....	101.
3.1. Introduction.....	101.

3.2. The Effect of Chirality on Heparin-Binding Affinity.....	104.
3.2.1. Determination of the Chirality of the Peptoids.....	104.
3.2.2. Determination of the Effect of Chirality on Heparin Binding Affinity.....	107.
3.2.2.1. Determination of Binding Constants by ITC.....	107.
3.2.2.2. Determination of Relative Affinities by HAC.....	108.
3.2.3. Discussion.....	110.
3.3. Effect of Peptoid Length on Heparin Binding Affinity.....	110.
3.3.1 Determination of Binding Constants by ITC.....	119.
3.3.2. Determination of Relative Binding Affinities by HAC..	120.
3.4. Summary and Conclusions.....	134.
3.5. References.....	135.
Chapter 4: The Relative Binding Affinities of Peptoids Containing Ammonium and Guanidium Side Chains.....	136.
4.1. Introduction.....	136.
4.2. Measurement of Binding Constants by ITC.....	137.
4.3. Heparin Affinity Chromatography.....	138.

4.4. CD Studies on the Ammonium and Guanidinium-Bearing Peptoids with and without Heparin Present.....	144.
4.5. Discussion Regarding CD Measurements.....	153.
4.6. Summary and Conclusions.....	154.
4.7. References.....	155.
Chapter 5: A Study on the Length of Peptoid Side-Chains on Heparin Affinity	156.
5.1. Introduction.....	156.
5.2. The Effect of Length and the Carbon Chain-Bearing the Cationic Binding Site on Heparin Affinity.....	157.
5.2.1 Heparin Affinity Chromatography Results for Ammonium and Guanidinium-bearing Peptoids.....	157.
5.2.2. Relative Heparin Binding Affinities Determined by Heparin Affinity Chromatography.....	167.
5.3. The Effect of Length of the Alkyl Side Chains on Heparin-Binding Affinity.....	170.
5.3.1. Binding Constants.....	170.
5.3.2. Heparin Affinity Chromatography Results.....	176.
5.4. Heparin Affinity for Peptoids Containing Other Side Chains.....	176.

5.4.1. Introduction.....	176.
5.4.2. ITC Results for Other Side Chain-Bearing Peptoids.....	179.
5.4.3. HAC Retention Times for Other Side-Bearing Peptoids	185.
5.5. Summary.....	190.
5.6. References.....	193.
Chapter 6: Computational Results.....	194.
6.1. Introduction.....	194.
6.2. Results for the Docking of the Chiral 12-mers.....	197.
6.3. Results for the Docking of Ammonium-Bearing Peptoids to Heparin.....	198.
6.4. Results for the Docking of Guanidinium-Bearing Peptoids to Heparin.....	199.
6.5. Results for the Docking of a Benzyl-Bearing Peptoid to Heparin	199.
6.6. Discussion and Conclusions.....	200.
6.7 Summary.....	207.
6.8 References.....	208.

Chapter 7: Summary and Conclusions	209.
7.1. Introduction.....	209.
7.2. References.....	213.
Chapter 8: Future Work	214.
8.1. Introduction.....	214.
8.2. References.....	215.

List of Figures

Fig 1.1.1 Major and minor Disaccharide Repeat Units with Possible Side Chain Substituents showing the Variability of Heparin.....	3.
Fig. 1.1. 2 Representative Tetrapeptide Structure and a Tetrapeptoid Structure.....	6.
Fig. 1.2.1 Rink Amide Resin Structure.....	8.
Fig. 1.2.2 Reaction of Resin-bound, Fmoc-protected Primary Amine and Bromoacetic acid, with DIC (<i>N,N'</i> -diisopropylcarbodiimide) acting as the Activating Catalyst.....	9.
Fig.1.2.3 Second step in the Zuckermann Submonomer Peptoid Synthesis produces the first Peptoid Monomer Unit.....	10.
Fig.1.2.4 Peptoid with Monomer Abbreviations and Side Chain Structures of the Monomer Units of Peptoids synthesized and studied in this Dissertation.....	12-15.

Fig.1.3.1 Cis and Trans Peptoid Backbone Configurations.....	21.
Fig. 1.3.2 The Dihedral Angles of Peptoids.....	22.
Fig. 1.3.3 Dihedral Angles for Spe-containing Peptoid Monomer Chiral Side Chain.....	24.
Fig.1.3.4 Structure of a Chiral Peptoid designed with all Cationic Charges on one Face in Order to bind with the Anionic Groups of Heparin.....	25.
Fig.1.3.5 Molecular Model of R9-mer, with electropotential Map overlayed with cationic Groups in Blue.....	27.
Fig. 1.4.1 Protegrin-1.....	30.
Fig. 1.4.2 Lung Surfactant-B (11-25).....	32.
Fig. 1.5.1 Monosaccharides of Heparin and Heparin Sulfate with their Abbreviations and Haworth Structures.....	34.
Fig.1.5.2 The major repeating Disaccharides of the Family of Glycosaminoglycans.....	35-36.
Fig. 1.5.3 An image of a 12-saccharide Segment of Heparin.....	39.
Fig.1.6.1 The Intrinsic and Extrinsic Pathways of the Coagulation Cascade of Secondary Hemostatis.....	40.
Fig.1.6.2 The Pentasaccharide binding Sequence of Heparin for Antithrombin III.....	42.

Fig. 1.8.3 Possible Hydrogen Bonding Schemes for the Binding of an Ammonium versus a Guanidinium Group to a deprotonated Sulfonic Acid Group.....	48.
Fig. 2.1.1 Rink Amide MBHA Resin Structure.....	58.
Fig. 2.1.2 Fmoc-deprotection Mechanism mediated by Piperidine...59.	
Fig.2.1.3 Acylation through 1,3-Diisopropylcarbodiimide (DIC)-mediated Coupling between the now unprotected nucleophilic primary Amine on the Resin.....	62.
Fig. 2.1.4 Second Step in the Zuckermann Submonomer Peptoid Synthesis.....	63.
Fig. 2.1.5 HPLC Chromatogram of a 12-mer Peptoid.....	66.
Fig.2.1.6 Guanidinylation using 1-H-pyrazole-1- carboxamidine HCl.....	68.
Fig. 2.1.7 General Formula for a 9-mer Peptoid.....	70.
Fig. 2.2.1 Isothermal Titration Calorimetry Instrument Schematic...73.	
Fig2.2.2 Raw Data for the EDTA/CaCl ₂ Calibration Titration.....	77.
Fig. 2.2.3 Processed Curve using Origin 5.0 Software.....	78.
Fig2.2.4 Calibration Data for EDTA/CaCl ₂ provided by MicroCal Inc. along with the Parameters obtained and Errors.....	79.

Fig 2.2.5 Titration Curve for the Titration of 0.164 mM Peptoid H-[-N(Cad)-N(Bu)-N(spe)] ₃ -NH ₂	84.
Fig. 2.5.1 MALDI-TOF MS of a guanidylated 9-merCad.....	92.
Fig 3.1.1 Linear helical Structure of Heparin.....	102.
Fig 3.1.2 The two chiral 12-mer Peptoids produced for this Study.....	103.
Fig 3.2.1 CD Spectra for the S12-mer and the R12-mer Peptoid...	109.
Fig 3.2.2 Raw ITC Titration Data for the S-12mer.....	112.
Fig 3.2.3. Titration Curve for the S12-mer.....	113.
Fig. 3.2.4 Raw ITC Titration Tata for the R-12mer.....	114.
Fig 3.2.5 Titration Curve for the R12-mer.....	115.
Fig 3.2.6 Heparin Affinity Chromatogram for the S12-mer.....	117.
Fig 3.2.7 Heparin Affinity Chromatogram for the R12-mer.....	118.
Fig 3.3.1 Structures of the peptoids H-[(N(Orn)-N(Bu)-N(spe)] _n -NH ₂ , where n = 1 - 4.....	121.
Fig. 3.3.2 Raw ITC Titration Data for the S3-mer Peptoid.....	122.
Fig. 3.3.3 The ITC Titration Curve for the S3-mer Peptoid.....	123.
Fig. 3.3.4 Raw ITC Titration Data for the S6-mer Peptoid.....	124.

Fig. 3.3.5	The ITC Titration Curve for the S6-mer Peptoid.....	125.
Fig. 3.3.6	Raw ITC Titration Data for the S9-mer Peptoid.....	126.
Fig. 3.3.7	The ITC Titration Curve for the S9-mer Peptoid	127.
Fig. 3.3.8	Raw ITC Titration Data for the S12-mer Peptoid.....	128.
Fig. 3.3.9	The ITC Titration Curve for the S12-mer Peptoid	129.
Fig. 3.3.10	HAC Retention Times from Ammonium-bearing Peptoids from 3 to 12 Monomers in Length.....	131.
Fig. 3.3.11	Plot of HAC Retention Times vs. Ammonium-bearing Peptoids from 3 to 12 monomers in Length.....	133.
Fig.4.1.1	Guanidinium-bearing Peptoids studied in this Chapter...	139.
Fig.4.2.1	ITC Titration Curve for S9-merCadG Peptoid.....	140.
Fig. 4.3.1	HAC Retention Times for four Guanidinium-bearing Peptoids.....	141.
Fig. 4.3.2	Double Plot of HAC Retention Times vs. Peptoids from 3- 12 Monomers in Length including Guanidinium-bearing Peptoids.	143.
Fig. 4.4.1	CD Spectra of S3-mer with and without Heparin.....	45.
Fig. 4.4.2	CD Spectra of S3-merG with and without Heparin.....	146.
Fig. 4.4.3	CD Spectra of S6-mer with and without Heparin.....	147.

Fig. 4.4.4	CD Spectra of S6-merG with and without Heparin.....	148.
Fig. 4.4.5	CD Spectra of S9-mer with and without Heparin.....	149.
Fig. 4.4.6	CD Spectra of S9-merG with and without Heparin.....	150.
Fig. 4.4.7	CD Spectra of S12-mer with and without Heparin.....	151.
Fig. 4.4.8	CD Spectra of S12-merG with and without Heparin....	152.
Fig. 5.1.1	Peptoids with cationic Side Chains of Lengths from 3 to 5 Carbons in Length.....	158-159.
Fig. 5.1.2	Peptoid analogs with decreasing alkyl groups on on central monomer of the repeating trimer sequence.....	160.
Fig. 5.1.3	Peptoid Analogs with allyl and benzyl Side Chains on the central Monomer of the repeating Trimer Sequence.....	161.
Fig. 5.2.1	ITC Titration Curve for the S9-merCad Peptoid.....	163.
Fig. 5.2.2.	ITC Titration Curve for the S9-merLys Peptoid.....	164.
Fig. 5.2.3	ITC Titration Curve for the S9-mer Peptoid.....	165.
Fig. 5.2.4	Bar Graph of ITC binding Constants for Peptoids with increasing Chain Length for Ammonium-bearing Side Chains.....	166.
Fig. 5.2.5	Bar Graph of HAC Retention Times for cationic Peptoids with increasing Chain Length for Cation-bearing Side Chains.....	169.

Fig. 5.3.1 Bar Graph of estimated binding Constants for Peptoids with increasing Chain Length for central Monomer of repeating Trimer Sequence.....	173.
Fig. 5.3.2 Calibration Curve obtained from ITC binding Constants and HAC Retention Times.....	174.
Fig. 5.3.4 Bar Graph of HAC Retention Times for Peptoids with increasing central Chain Length for Ammonium-bearing and Guanidinium -bearing Side Chains.....	177.
Fig. 5.4.1 Structures for allyl and benzyl-bearing Peptoids.....	180.
Fig. 5.4.2 Titration curve for the S9-merBz peptoid.....	182.
Fig. 5.4.4 Bar graph of ITC binding Constants for allyl and benzyl Peptoids along with a S9mer included as a Reference.....	184.
Fig. 5.4.5 Bar Graph of HAC Retention Times for allyl and benzyl-bearing Peptoids with increasing Chain Length for Ammonium-bearing Side Chains.....	187.
Fig. 5.4.6 Reaction Scheme for removal of an allyl Amide protecting Group using Ruthenium (III) Chloride	192.
Fig. 6.2.1 Heparin Hexadissacharide Fragment used in docking Studies.....	201.
Fig. 6.2.2 The docking of R12-mer Peptoid to Heparin.....	202.
Fig. 6.2.3 The docking of S12-mer Peptoid to Heparin.....	203.
Fig. 6.3.1 The docking of S9-mer Peptoid to Heparin.....	204.

Fig. 6.4.1 A Guanidinium-bearing S9-mer docked to Heparin.....205.

Fig. 6.5.1 A benzyl-bearing Peptoid docked to Heparin displaying π - π Stacking with multiple aromatic Rings aligned in Rows.....206.

List of Tables

Table 1.2.1 Peptoid Designations and Sequences synthesized in this Research.....19.

Table 2.2.1 Parameters provided by MicroCal for Calibration.....75.

Table 3.1.1 The two chiral 12-mers used in the initial Study.....105.

Table 3.2.1 Binding Constants and thermodynamic ITC Parameters for the chiral 12-mers.....111.

Table 3.2.2 HAC Retention Times for the chiral 12-mer Analogs.....105.

Table 3.3.1 ITC binding Constants and thermodynamic Data for S3-mers through S12-mers.....130.

Table 3.3.2 HAC Retention Times for S3-12-mer Peptoid.....132.

Table 4.3.1 HAC mean Retention Times for Guanidinium-bearing Peptoids from 3 to 12 Monomer Units in Length.....142.

Table 5.2.1 ITC binding Data for Ammonium-bearing Side Chains of Three to Five Carbons in Length.....162.

Table 5.2.2 HAC Retention Times for Cation-bearing Side Chains of Three to Five Carbons in Length.....168.

Table 5.3.1 ITC binding Data for Ammonium-bearing Peptoids with central Side Chains of 4 Carbons down to 1 Carbon in Length.....171.

Table 5.3.2 Mean HAC Retention Times and estimated K_b from Calibration Curve shown in **Fig. 5.3.1**.....172.

Table 5.3.3 Peptoids, their HAC Retention Times and ITC derived K_b175.

Table 5.4.1 HAC Retention Times for both Ammonium and Guanidinium-bearing Peptoids with central alkyl side Chain from Four down to One Carbons in Length.....178.

Table 5.4.2 ITC binding data for Ammonium-bearing allyl and benzyl –containing Peptoids.....181.

Table 5.4.3 HAC Retention Times for Ammonium-bearing allyl and benzyl-containing Peptoids.....186.

Chapter One:

Introduction

1.1 Overview of the Dissertation

The goal of the research presented in this dissertation is to design, synthesize and study a class of oligomers known as peptoids, which are analogous to peptides but with the side chains attached to the backbone amide nitrogens as opposed to the alpha carbons as in peptides. The peptoids were designed to bind with high affinity to heparin, which is a highly-sulfated glycosaminoglycan (GAG). Heparin is used medically as a blood anticoagulant, either injected intravenously, or as an anticoagulant coating on the inner surfaces of experimental or medical devices and i.v lines such as are used in renal dialysis or during surgery that requires extracorporeal blood circulation¹. Heparin is a naturally occurring anticoagulant produced in the human body in mast cells and basophils.² The heparin used in medicine is derived from porcine intestinal mucosa and bovine lung.³ In addition to its anticoagulant properties, heparin is also known to mediate release of hepatic and lipoprotein lipases,⁴ regulate angiogenesis and growth of tumors,⁵ modulate inflammation⁶ and also possesses antiviral activity.⁷

Structurally heparin consists of linear repeating units of variably sulfated 1-4 linked uronic acid–glucosamine disaccharides (**Fig. 1.1.1.**) with molecular weights that vary from 3-50 kD, but most commercial heparin ranges from 12-15 kD.⁸ The partially sulfated ester and amine groups and the carboxylic acid groups exist in the deprotonated form under physiological pH conditions resulting in a net negative charge density that is one of the greatest in any known biological molecule⁹. In some clinical situations, it is necessary to neutralize the anticoagulant activity of heparin, for example, bleeding complications are a side effect in some 10-15% of patients given heparin. To neutralize the anticoagulant activity of heparin, low molecular weight (4.5 kD) arginine-rich proteins known as protamine are used.¹⁰ The arginine residues in protamine provide cationic groups that are able to bind with the negatively charged sulfate esters and amides through electrostatic interactions.

Protamines are derived from a variety of biological sources, including mammalian, bird, sponges, amphibians and fish, where they comprise the most heterogeneous group of sperm basic nuclear proteins and are involved with the binding of DNA around histones.¹¹

Protamine, however can cause life threatening side effects such as bradycardia, hypotension and other anaphylactic symptoms.¹² Therefore there is intense interest in developing synthetic replacements for protamine. Research on alternative neutralization agents has focused on heparin-binding peptides including synthetic peptides that have the sequence of heparin-binding domains of heparin-binding proteins.

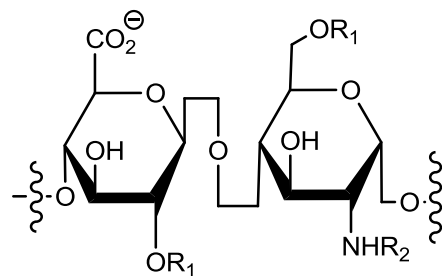
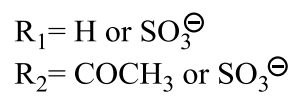
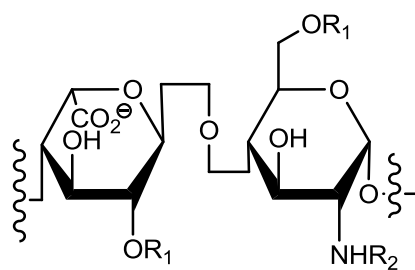
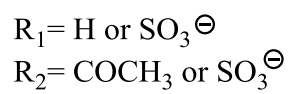


Fig 1.1.1. Major (left) and minor (right) disaccharide repeat units with possible side chain substituents showing the variability of heparin.

It was shown in 1996 by Carson¹³ and coworkers that a protein known as heparin interacting protein (HIP), which is found in human uterine epithelial cells and cell lines, binds to heparin. The amino acid sequence of the heparin-binding domain is CRPKAKAKAKDQTK,¹⁴ where C is the amino acid cysteine, R is Arginine, P is proline, K is lysine, A is alanine, D is aspartic acid, Q is glutamine and T is threonine. This sequence contains one arginine and six lysine residues that under physiological conditions would each carry a net positive charge and would account for the high binding affinity of HIP for heparin. Furthermore, modified peptides of similar sequence also have been shown to bind with high affinity to heparin and to neutralize the anticoagulant activity of heparin.¹⁴

Rabenstein¹⁵ and coworkers demonstrated significant binding affinity in two synthetic peptide analogs of the HIP heparin-binding domain shown above. The peptide analogs had the sequence Ac-SRGKAKVKAKVKDQTK-NH₂, where S is serine and G is glycine, and the same sequence containing all D-amino acids, known as L-HIPAP (L-HIP analog peptide) and D-HIPAP respectively. Both peptide analogs were found to be effective in neutralizing heparin activity using the Coatest Heparin in vitro assay, and significantly they were equally effective. The D-form was prepared since natural peptides containing only L-amino acids are unstable under physiological conditions due to degradation by proteases.

Another approach to overcome protease degradation of peptides is by the use of peptoids, N-substituted glycine oligomers, where the side chain groups are attached to the

backbone amide nitrogens rather than the central carbon of the amino acids. Representative structures of peptides and peptoids are shown in **Fig.1.1.2**. Peptoids also have the advantages that they are nonimmunogenic, pass through biological membranes more efficiently and are orally available in comparison to peptides.¹⁶

Therefore it is proposed that the synthesis and evaluation of N-lysine and N-arginine rich peptoids, i.e peptoids with side chains that will mimic the side chains of lysine and arginine, will provide bioavailable and potentially useful heparin inhibitors as a replacement for protamine as an agent for neutralization of the anticoagulant activity of heparin. These peptidomimetic heparin inhibitors would have major advantages over protamine such as resistance to protease degradation in the blood system, potential oral activity and be non-immunogenic, which greatly enhances clinical utility and reduction or elimination of protamine mediated side effects. This represents an entirely new family of molecules for this purpose.

1.2 Peptoids

Peptoids were first designed and produced by Ronald Zuckermann¹⁷ in 1992 using an approach that he referred to as submonomer synthesis. It is in general a solid phase synthesis that uses rink amide resin as a starting point. The structure of rink amide resin is shown in **Fig.1.2.1**, where the resin is represented by the sphere on the right side of the figure. In order to activate the resin, the Fmoc group must first be removed. This is achieved by reaction with piperidine.

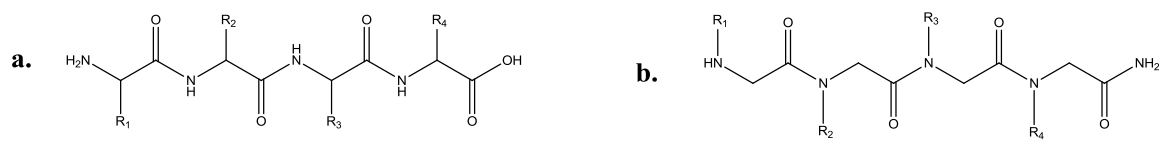


Fig. 1.1. 2. Representative tetrapeptide structure and a tripeptoid structure. Structure **a.** peptide; structure **b.** peptoid, where R_{1-4} represent variable side chains.

This leaves a primary amine which is then coupled to bromoacetic acid by use of DIC (N,N'-diisopropylcarbodiimide), which acts as an activator. The reaction scheme is shown in **Fig. 1.2.2**. This is the first step of Zuckermann's submonomer reaction and indeed the name comes from the fact that there are two steps necessary to produce the full monomer: the acylation reaction produces the bromoacetylated submonomer that is then reacted with a variety of commercially available amines, including monoprotected diamines, to form a peptoid monomer unit.

The second step in Zuckermann's synthesis is a simple bimolecular nucleophilic substitution (S_N2) shown in **Fig. 1.2.3**.

Fig.1.2.4. shows the structures of a general peptoid and the R groups attached to the backbone nitrogens of the peptoids synthesized and studied in this dissertation. Many more are possible as they only depend upon the commercial availability of amines or Boc-protected diamines. In fact, any reactive group that could be suitably protected by using Boc as a protecting group is ideal as Boc is base-nonlabile but easily removed under acidic conditions in the final cleavage step. Another desirable feature of Boc protected diamines, for example, is that following deprotection, they can then be postmodified using a suitable guanidylating agent. 1-*H*-pyrazolecarboxamide HCl in DMF stirred overnight at room temperature is especially useful giving over 65% yield of guanidylation products.

The nomenclature used in **Fig. 1.2.4.** below and in this research is derived from the side chains attached to the alpha carbon of the analogous amino acid as well as the

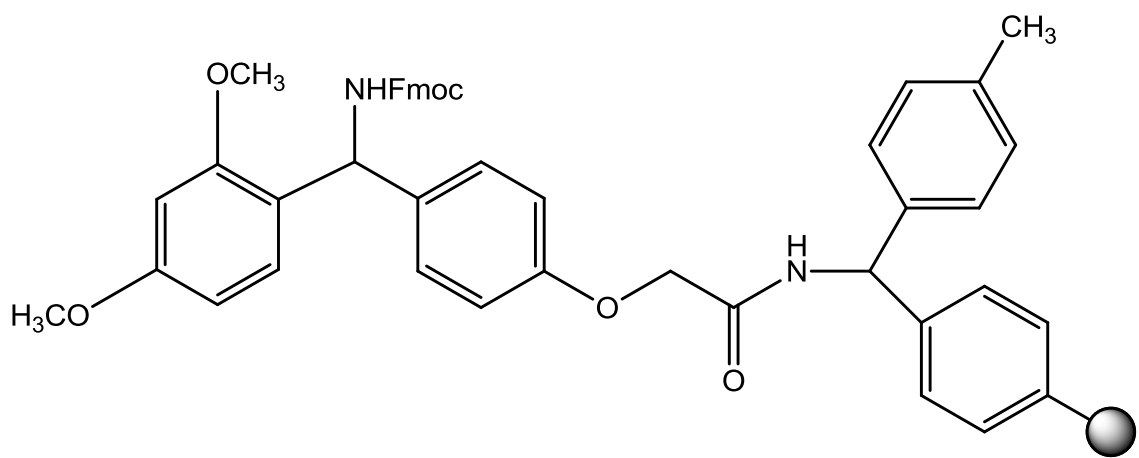


Fig. 1.2.1 Rink amide resin structure. The Fmoc protected amine is the active site of the molecule.

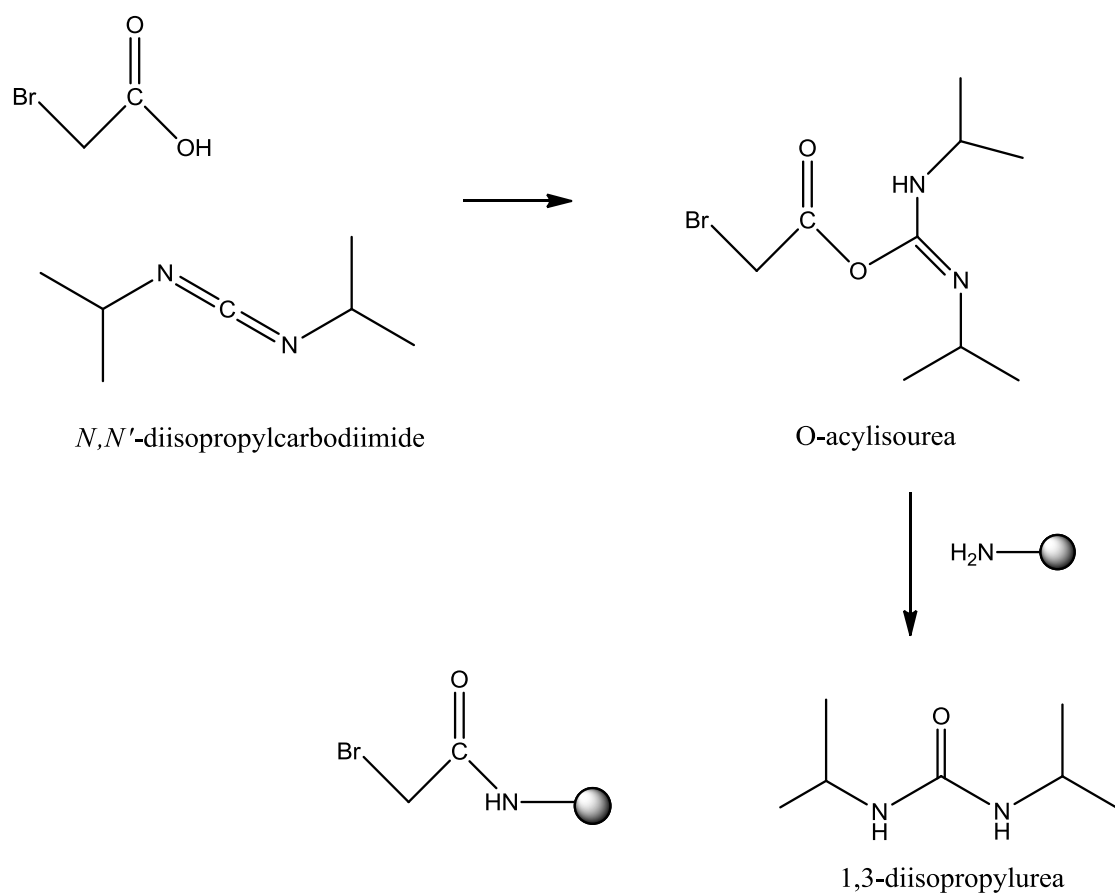


Fig. 1.2.2 Reaction of resin-bound, Fmoc-deprotected primary amine and bromoacetic acid, with DIC (*N,N'*-diisopropylcarbodiimide) acting as the activating catalyst.

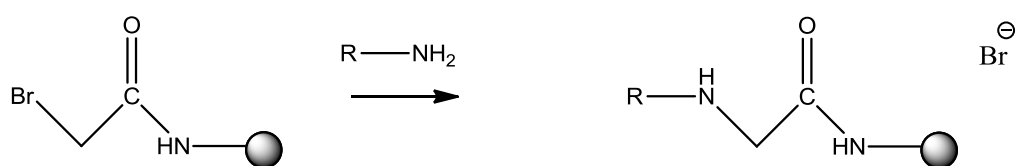


Fig.1.2.3 Second step in the Zuckermann submonomer peptoid synthesis produces the first peptoid monomer unit. The secondary amine of the peptoid monomer is ready for the next acylation reaction.

following exceptions. For example *N*(Lys) is the peptoid monomer analog of the amino acid lysine. The guanidylated form of all peptoid monomers has a G attached to the end of the name, e.g., in the above example based upon lysine the guanidinylated form is designated *N*(Lys)G. *N*(Cad) and *N*(Cad)G are derived from cadaverine, a diamine with a five carbon chain between the terminal primary amine groups. *N*(Arg) is derived from the amino acid arginine. *N*(Orn) is derived from ornithine. The alkyl series *N*(Me), *N*(Et), *N*(Pr), and *N*(Bu) is derived from the length of the carbon chain attached to the backbone nitrogen, where Me corresponds to one carbon up to Bu which denotes four carbons. Two of the monomers are derived from benzylamine and allylamine and are designated *N*(Bz) and *N*(All) respectively. The alpha chiral monomers *N*(spe) and *N*(rpe) are derived from (S)-1-phenylethanamine and (R)-1-phenylethanamine.

The two-step process is repeated to produce an N-substituted polyglycine oligomer. Since the succeeding steps involve the acylation of secondary amines instead of the primary amine of the first substitution, the concentration of bromoacetic acid in the first step is kept high. The amine concentration in the second step is typically 1 molar, but if the amine is precious then the reaction can be done at slightly lower concentration and still produce a high yield of peptoid. The final step is cleavage of the peptoid from the resin with a cocktail consisting of trifluoroacetic acid: triisopropyl silane (added as a carbocation scavenger) and water in the ratio of 95:2.5:2.5%. The time for the cleavage

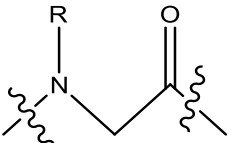
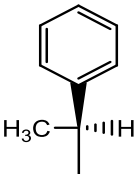
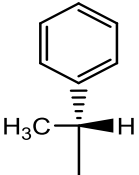
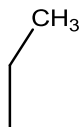
 <p>General Structure of Peptoid monomer</p>	
Abbreviation of Peptoid Monomers	Structure of the side chain R group
<i>N</i> (spe)	
<i>N</i> (rpe)	
<i>N</i> (Me)	
<i>N</i> (Et)	

Fig.1.2.4. Peptoid with monomer abbreviations and side chain structures of the monomer units of peptoids synthesized and studied in this dissertation.

Abbreviation of Peptoid Monomers	Structure of the side chain R group
<i>N</i> (Pr)	
<i>N</i> (Bu)	
<i>N</i> (Orn)	
<i>N</i> (Lys)	
<i>N</i> (Cad)	

Fig.1.2.4. Continued

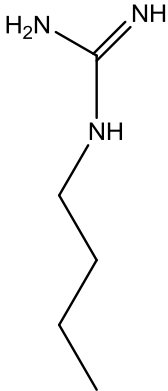
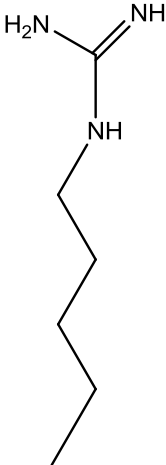
Abbreviation of Peptoid Monomers	Structure of the side chain R group
<i>N</i> (All)	
<i>N</i> (Arg)	
<i>N</i> (Lys)G	

Fig.1.2.4. Continued

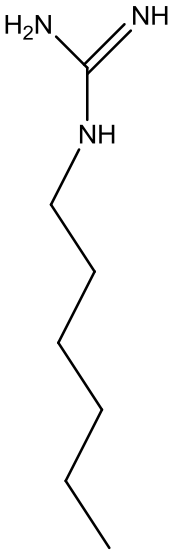
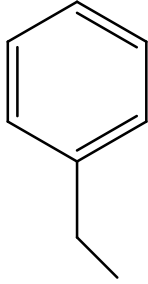
Abbreviation of Peptoid Monomers	Structure of the side chain R group
<i>N</i> (Cad)G	
<i>N</i> (Bz)	

Fig.1.2.4. Continued

from the resin and deprotection of any Boc-protected amines is 2.5 hours. Shorter times resulted in lower yields.

Various methods for the synthesis of peptoids other than solid phase automated synthesis using a peptide synthesizer have also been developed, including microwave assisted synthesis, a method of which Blackwell et al. have made extensive use.¹⁸ Peptoids can also be made manually using a syringe and some means of agitation.¹⁹ The main problem with the latter method is the time factor and repetition involved. For example a 9-mer peptoid can be produced using an automatic peptide synthesizer in 2.5 days that would take at least a week and a half manually with considerably more labor. In fact one of the advantages of synthesizing peptoids using Zuckermann's solid phase submonomer synthesis methodology is its ability to allow automated synthesis. Many brands of automated peptide synthesizers can be modified to accomplish this goal and less reagents are required than in the synthesis of peptides. Notably, HTBU is not needed to activate the coupling due to the high conversion rates using DIC in the acylation step to activate the bromoacetic acid (or some other haloacetic acid), which then reacts with the amine of the previous residue of an elongating resin bound peptoid. The solvents used are dimethylformamide (DMF) and *N*-methylpyrrolidone (NMP). The peptoids in this dissertation research were synthesized on an Applied Biosystems 433 system synthesizer using Rink amide resin.

As will be discussed below under structure of peptoids, the peptoids were rationally designed to create a secondary structure that would place all of the cationic side chains on

one face of a helix with a helical distance from residue i to $i + 3$ equal to approximately 3.1 Å; the rationale being that heparin is a linear structure with its negatively charged sulfonic acid groups on its surface.

The peptoids produced in this study along with their sequence and designation are listed in **Table 1.2.1**. Each peptoid was synthesized by the solid phase submonomer synthesis method, purified by HPLC, their identity established by MALDI-TOF mass spectrometry and their heparin binding affinity characterized by isothermal titration calorimetry and /or heparin affinity chromatography.

In addition, computations were performed on selected peptoids and in combination with heparin oligosaccharides to gain further insight into the nature of the interaction of the peptoids with heparin. The peptoids in **Table 1.2.1** produced in this study were very interesting in their resulting heparin affinity in relation to their predicted affinity. Referring to the sequences shown in **Table 1.2.1**, all peptoids were repeats of a 3-monomer sequence consisting of (starting from the C-terminal end) a chiral monomer, followed by a spacer monomer with a side chain, usually alkyl side chains but also side chains with other design features, for example allyl and benzyl groups were also used in this position, and finally a monomer with a cation-bearing side chain. Directing the choice of the monomer side chains was the desire to generate helical peptoids with all cationic side chains on the same side so as to bind with the anionic groups on heparin at physiological pH. Several design features were investigated, including the carbon chain length for both spacer monomer units and the cationic-bearing monomer.

Another design variable that was investigated was the use of guanidinium groups on the cationic side chain compared to primary ammonium groups in this position. Chirality of the alpha chiral side chain was also investigated but it was found quite early on that the S enantiomer produced peptoids with higher affinity for heparin. The final variable investigated was the overall length of the peptoid. Longer peptoids were found to bind with greater affinity to heparin. This will be discussed in detail in the experimental results section. Computational studies of free peptoids and peptoids docked with heparin are presented in Chapter 7.

Regarding **Table 1.2.1**, the first eight peptoids represent the series that was used in the investigation of heparin affinity as a function of peptoid length for both primary amine bearing peptoids and guanidylated peptoids. The remainder were synthesized for selective comparisons, with the final peptoid being the R 12-mer peptoid used in the investigation of chirality and its effect on heparin affinity.

1.3 Structural Aspects of Peptoids

As was just touched on above, much work in this research went into the study of the effect of structure, specifically changing side chains on heparin affinity. Much work has already gone into how the secondary structures of peptoids can be stabilized by changing sequences and by modifying side chains.^{20,18,21-24} A major difference between peptoids and peptides is the absence of the backbone amide hydrogen atoms in peptoids (see **Fig. 1.1.2**). In peptoids the backbone amide hydrogens have been replaced by side chains.

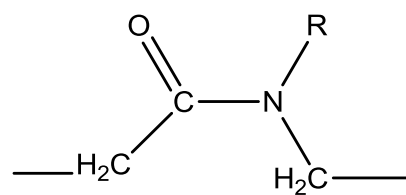
Peptoid	Sequence
s3mer	H-[N(Orn)-N(Bu)-N(spe)]-NH ₂
s3merG	H-[N(Arg)-N(Bu)-N(spe)]-NH ₂
s6mer	H-[N(Orn)-N(Bu)-N(spe)] ₂ -NH ₂
s6merG	H-[N(Arg)-N(Bu)-N(spe)] ₂ -NH ₂
s9mer	H-[N(Orn)-N(Bu)-N(spe)] ₃ -NH ₂
s9merG	H-[N(Arg)-N(Bu)-N(spe)] ₃ -NH ₂
s12mer	H-[N(Orn)-N(Bu)-N(spe)] ₄ -NH ₂
s12merG	H-[N(Orn)-N(Bu)-N(spe)] ₄ -NH ₂
s9mer(Me)	H-[N(Orn)-N(Me)-N(spe)] ₃ -NH ₂
s9mer(Et)	H-[N(Orn)-N(Et)-N(spe)] ₃ -NH ₂
s9mer(Et)G	H-[N(Arg)-N(Et)-N(spe)] ₃ -NH ₂
s9mer(Pr)	H-[N(Orn)-N(Pr)-N(spe)] ₃ -NH ₂
s9mer(Lys)	H-[N(Lys)-N(Bu)-N(spe)] ₃ -NH ₂
s9mer(Lys)G	H-[N(Lys)G-N(Bu)-N(spe)] ₃ -NH ₂
s9mer(Cad)	H-[N(Cad)-N(Bu)-N(spe)] ₃ -NH ₂
s9mer(Cad)G	H-[N(Cad)G-N(Bu)-N(spe)] ₃ -NH ₂
s9mer(All)	H-[N(Orn)-N(All)-N(spe)] ₃ -NH ₂
S9mer(Bz)	H-[N(Orn)-N(Bz)-N(spe)] ₃ -NH ₂
r12mer	H-[N(Orn)-N(Bu)-N(rpe)] ₄ -NH ₂

Table. 1.2.1 Peptoid designations and sequences synthesized for this dissertation research.

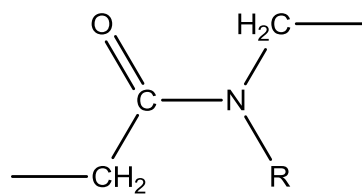
and peptides is the absence of the backbone amide hydrogen atoms in peptoids (see **Fig. 1.1.2**). In addition to the loss of hydrogen bonding that stabilizes the secondary structure of peptides, the presence of a carbon atom attached to the amide nitrogen in peptoids results in amide bonds that can undergo cis/ trans isomerism, with some of the backbone amide bonds taking up a cis configuration and others a trans configuration as shown in **Fig. 1.3.1**.²⁵ Various factors can affect the dihedral angles of peptoids. The most relevant dihedral angles are shown in **Fig. 1.3.2**.

The example above uses an aryl group directly attached to the backbone nitrogen. If the side chain is a chiral group as in S-phenylethylene (spe) as shown in **Fig.1.3.3**, then the χ dihedral angles are determined by slightly different groupings. For example, for the dihedral angle χ , since there is a methine carbon between the N_i and $N_i\text{-C-}\beta$ of the spe side chain, it would start with $ac\text{-}C_{i+1}O, N_i$. The methine carbon bridge, which also has a methyl attached would become $N_i\text{-C-}\alpha$, and the last would be the carbon on the phenyl ring attached to $N_i\text{-C-}\alpha$, which would now become $N_i\text{-C-}\beta$.

The circular dichroism spectra of peptoids with alpha chiral side chains are consistent with oligomers with a helical secondary structure.²⁶ Zuckerman's study of secondary structure and the use of chiral side chains to affect the handedness of the helices, it was found that it is critical that the first peptoid monomer residue be the chiral side chain to

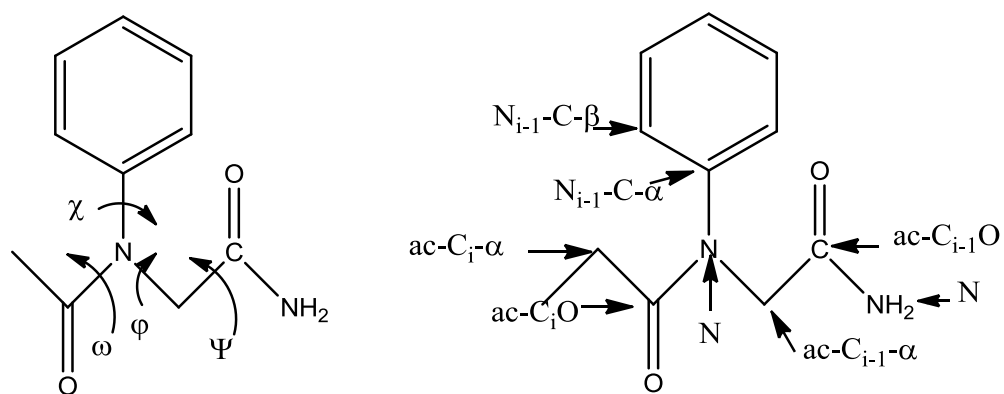


Cis Configuration



Trans Configuration

Fig.1.3.1. Cis and trans peptoid backbone configurations.



$\omega = \text{ac-C}_i\text{-}\alpha, \text{ac-C}_i\text{O}, \text{N}_{i-1}, \text{ac-C}_{i-1}\text{-}\alpha$
 $\phi = \text{ac-C}_i\text{O}, \text{N}_{i-1}, \text{ac-C}_{i-1}\text{-}\alpha, \text{ac-C}_{i-1}\text{O}$
 $\Psi = \text{N}_{i-1}, \text{ac-C}_{i-1}\text{-}\alpha, \text{ac-C}_{i-1}\text{O}, \text{N}_{i-2}$.
 $\chi = \text{ac-C}_i\text{O}, \text{N}_{i-1}, \text{N}_{i-1}\text{-C-}\alpha, \text{N}_i\text{-C-}\beta$

Fig. 1.3.2. The dihedral angles of peptoids. This nomenclature is borrowed from peptide structural studies and has been used by Rabenstein *et al.*²³ in studies of cis/trans isomerization and secondary structure of peptoids.

set the helical structure²⁷ and that the monomer with a chiral side chain repeat every three residues.

In 1997 Zuckermann *et al.* performed *ab initio* studies on chiral peptoids using Semi-empirical quantum mechanical calculations and determined that the preferred minimum energy conformation for octomers of N(spe) is in a poly proline type I helix.²⁸ A poly proline type I helix consists of all cis amide bonds resulting in a tight helix. The dihedrals in Zuckermanns peptoids associated with the minimum conformation were $\varphi = -70^\circ$, $\Psi = 165^\circ$, $\omega = 0^\circ$, and $\chi = -120^\circ$. Furthermore, a right-handed helix formed when an S-containing alpha carbon was attached to the N, while a left-handed helix formed with R chiral alpha side chains. Theoretical predictions have been confirmed by X-ray crystallography,²⁹ and NMR spectroscopy.³⁰ These techniques indicate that the peptoids containing alpha chiral side chains consist of 3-peptoid monomers per turn of the helix. It also seems to matter that the first residue be chiral, e.g. N(spe) to initiate formation of a helix.²⁰ As mentioned above, the peptoids synthesized and studied in this dissertation were rationally designed to produce a secondary structure that would place all of the cationic side chains on one face of a helix with a distance from residue i to $i + 3$ equal to approximately 3.1 Å. **Fig.1.3.4.** is a schematic of the helical structure of a 12-mer, H-[N(Orn)-N(Bu)-N(spe)]₄-NH₂ that uses N(spe) to generate a right handed helix; the structure shows the cationic residues, in this case N(Orn) aligned along one side of the helix. The purpose of placing all of the cationic charges on one face of the peptoids was so they will bind with the anionic sulfated esters and sulfamates of heparin.

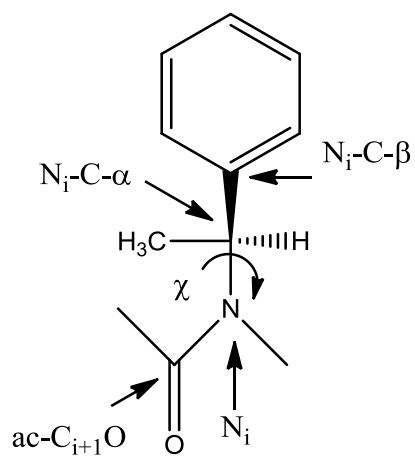


Fig. 1.3.3. Dihedral angles for a spe-containing peptoid monomer chiral side chain.

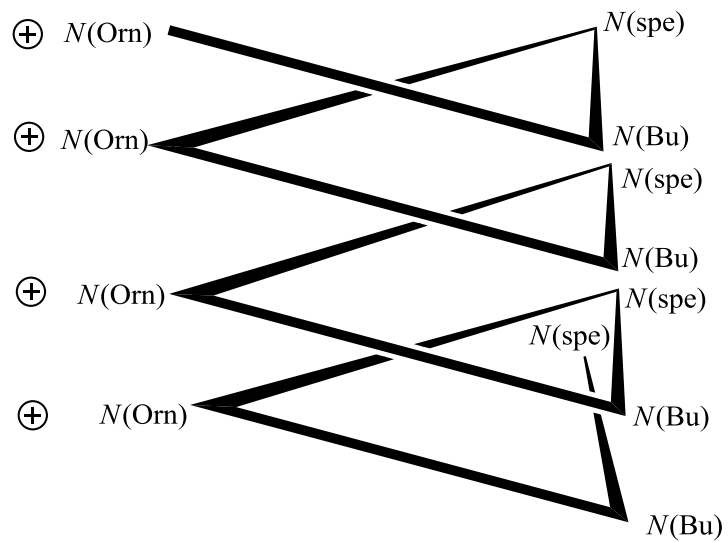


Fig.1.3.4. Structure of a chiral peptoid designed with all cationic charges on one face in order to bind with the anionic groups of heparin.

As a final example, an electropotential map surface overlaid on a molecular model was produced for the 9-mer peptoid H-[N(Orn)-N(Bu)-N(rpe)]₃-NH₂, a hypothetical peptoid that would be designated as R9-mer (**Fig. 1.3.5**). This was produced using Spartan '08³¹ and the overlay was accomplished using Acclrys Viewerlite.³² Distances between cationic groups are indicated in the structure. In this view, the minimized structure shows the charged ammonium groups on one face. Intriguing as this is, docking studies of peptoids with heparin show an alternative mode of binding to heparin as will be discussed in Chapter 7, where the results of computational studies are presented.

1.4. Studies of biological effects of peptoids.

Peptoids are becoming increasingly relevant as they are being found to possess various biological activities and more biological uses are being discovered for them. Since they possess greater advantages in many respects over their peptide counterparts, there has been great interest in duplicating the biological effects of peptides without their shortcomings. Peptides are readily degraded by peptidases that are present in both the bloodstream and in the human digestive tract. This makes them poor drug candidates.

Peptoids, in contrast, are a new synthetic development and so the human system has not had the contact on the evolutionary timescale to develop allergic reactions and has had no time to develop peptoidases. A literature search in Science Finder Scholar has turned up nothing regarding the existence of enzymes capable of cleaving peptoids. In addition they are better equipped to pass through biological membranes.³³ Early work on peptoids utilized combinatorial split pool techniques to probe biological function.³⁴⁻³⁶

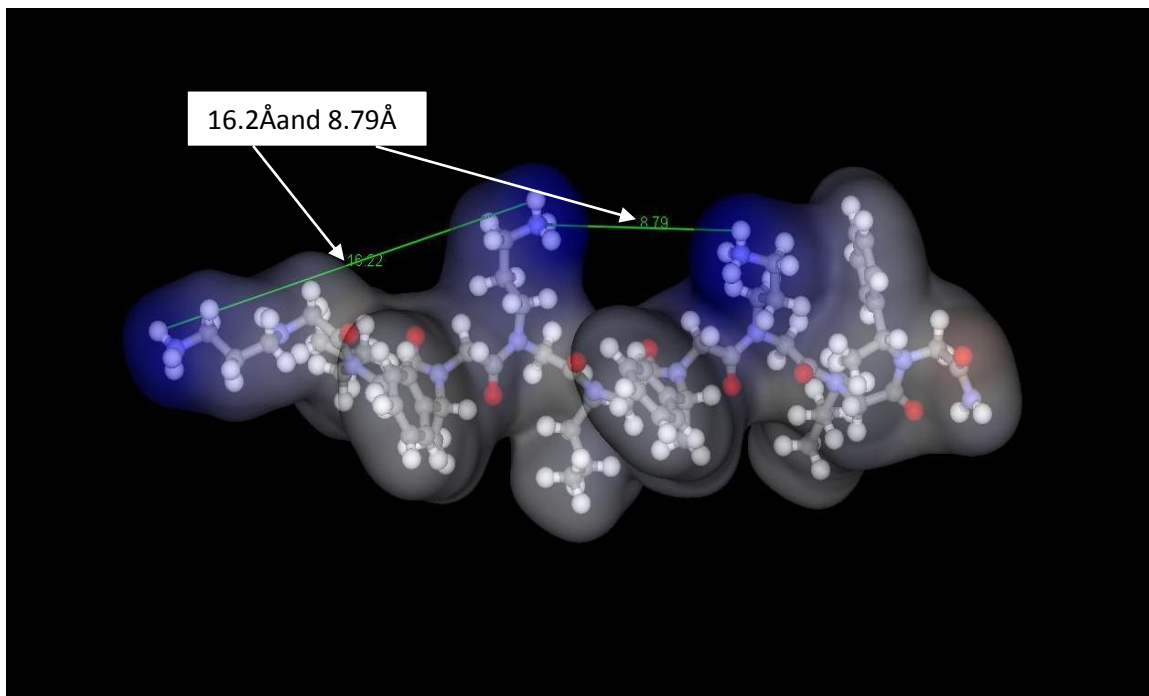


Fig.1.3.5. A calculated molecular model for the R9-mer, with an electrostatic map overlaid with cationic groups in blue. The side chain amine groups are in the ammonium form, the form present at physiological pH. The distance between the ammonium groups on the side chain of the N-terminal N(Orn) and the central N(Orn) is 16.2Å while the distance between the ammonium groups of the central and C-terminal N(Orn) residues is 8.79 Å. For comparison, distances between the anionic sites on heparin are approximately 17.5 Å and also closer distances are approximately 6 Å. These results indicate a close match between cationic sites on the peptoid and anionic sites on heparin.

Another approach that can be applied to peptoids is rational drug design using computational molecular modeling techniques. The difference in the two techniques is that in the first, large numbers of peptoid analogs are tested for a target biological function, while in the latter, the peptoid is designed as a ligand to bind to a receptor binding pocket, or as in the research presented in this dissertation, to the many sulfated esters and sulfamate groups on heparin. Potentially any peptide-binding macromolecule can be targeted by this approach or a combination of both techniques can also be applied. For example once an affinity of a peptoid for a macromolecule has been established, then a wide variety of analogs can be easily designed by modification of the side chains.

The following are examples of potential biological areas where peptoids are being studied for their biological effects. Antimicrobial peptides (AMP) are found in a wide variety of organisms as a means of protection against microbial infection.³⁷ The mechanism of action of AMPs begins with permeation of the bacterial cell membrane, which is facilitated by their amphipathic structure meaning that they contain both hydrophobic and hydrophilic regions. Their general structures consist of fairly short sequences of from 10-50 amino acids. The secondary structures have been found to be alpha helices, beta hairpins, and either looped or extended sequences. Examples are pore forming bacterial toxins such as magainins, found in the African frog *Xenopus laevis*,³⁸ and protegrins,³⁹ an example of which is seen below in **Fig. 1.4.1**.

Indolicidin, another AMP, which is derived from bovine sources has a linear amino acid sequence of consisting of NH₂-Ile-Leu-Pro-Trp-Lys-Trp-Pro-Trp-Pro-Trp-Arg-Arg-CO-NH₂ and a secondary structure consisting of an extended ribbon. The two

arginines and one lysine give it a cationic character while the aromatic residues provide the hydrophobic part of the oligomer. In all cases, AMPs have a selectivity for bacteria over mammalian organisms due to the cationic portion of the peptide, since bacterial membranes are generally negatively charged while mammalian membranes are neutral. The hydrophobic region is thought to facilitate permeability through the cell membrane thereby lysing the cell.

While AMPs possess features that would make them ideal antibiotics, peptides also have several disadvantages and this explains why many new peptide-based antibiotics have not been developed. Goodson *et al.*⁴⁰ developed a series of antimicrobial peptoid dimers and trimers that were effective against both gram negative and gram positive bacteria. While the peptoids were active at a minimum inhibitory concentration (MIC) = 5–40 μM , they were also found to be hemolytic.

The Barron group⁴¹ reported in 2003 the development of peptoid mimics of the helical antimicrobial peptide magainin-2, that possessed low micromolar activity against *E. coli* (MIC = 5–20 μM) and *B. subtilis* (MIC = 1–5 μM).

Lung surfactant mimics are another area where peptoids are finding potential use. Lung surfactant (LS) is a natural material comprised of proteins and lipids that are essential in the normal functioning of mammalian respiratory systems. They function to reduce and regulate surface tension at the air-surface interface of lungs.⁴² Deficiency in lung surfactant is a major cause of mortality in premature infants. It is also a cause of respiratory distress in children and adults. Synthetic formulations have been devised but they have been found to be problematic and less functional than extracted natural LS.

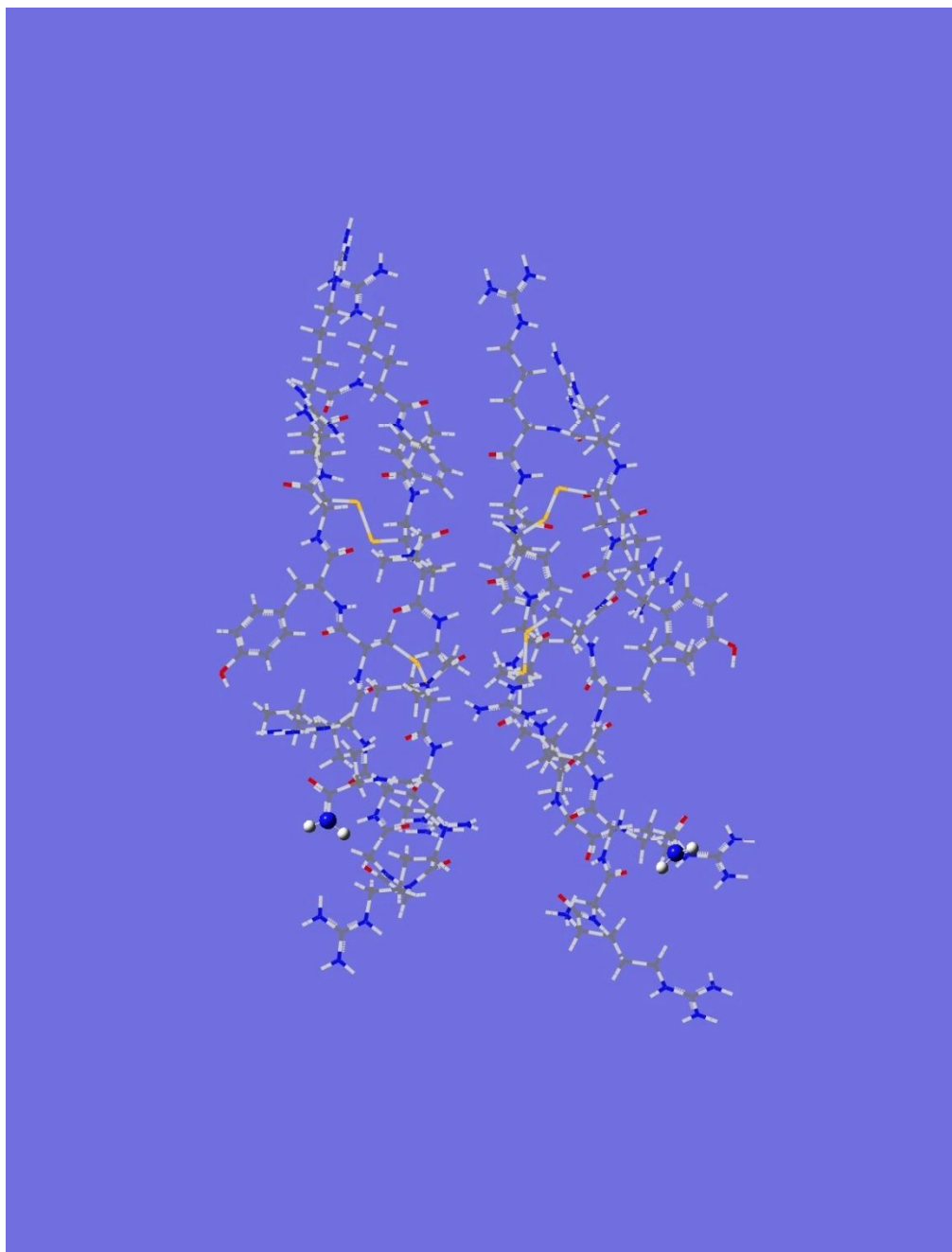


Fig. 1.4.1. Protegrin-1.⁴³ It contains 6 positively charged arginines and 4 cysteine residues in its sequence.³⁹ Its sequence is RGGRLCYCRRRFCVGVGRX (Arg-Gly-Gly-Arg-Leu-Cys-Tyr-Cys-Arg-Arg-Arg-Phe-Cys-Val-Gly-Arg-Variable).

But natural LS frequently causes an immunogenic response. This effectively eliminates their use in clinical medicine.

The Barron group has been working on peptoid-based LS mimics of the two LS proteins, which are both helical and hydrophobic in structure and composition.⁴⁴ The design strategy is to combine the two peptoids with a lipid as a formulation. The structure of a peptoid segment of Lung Surfactant B is shown in **Fig.1.4.2**. The figure demonstrates the helical structure of the natural N-terminal segment of the protein.⁴⁵ The CD spectroscopic analysis by the Barron study of the LS-B mimics in methanol displayed helical character with those containing aromatic residues showed more helicity based upon the intensity of the CD signal compared to aliphatic analogs. However evaluation of their surface-active behavior indicated that aliphatic peptoids had better activity when combined in a model lipid mixture than the aromatic peptoids causing the authors to postulate that a rigid helical structure was not necessary for lung surfactant activity.

The peptoids designed in this study were rationally designed to mimic protamine, a natural ligand for heparin. Binding of protamine by heparin mediates inhibition of the coagulant cascade. This interaction will be covered in detail in the next section.

1.5 Heparin and Heparin-Binding Peptoids

Heparin is a naturally occurring polysaccharide consisting of repeating uronic acid (1 \rightarrow 4)-D-glucosamine disaccharide subunits . The disaccharide subunits are sulfated

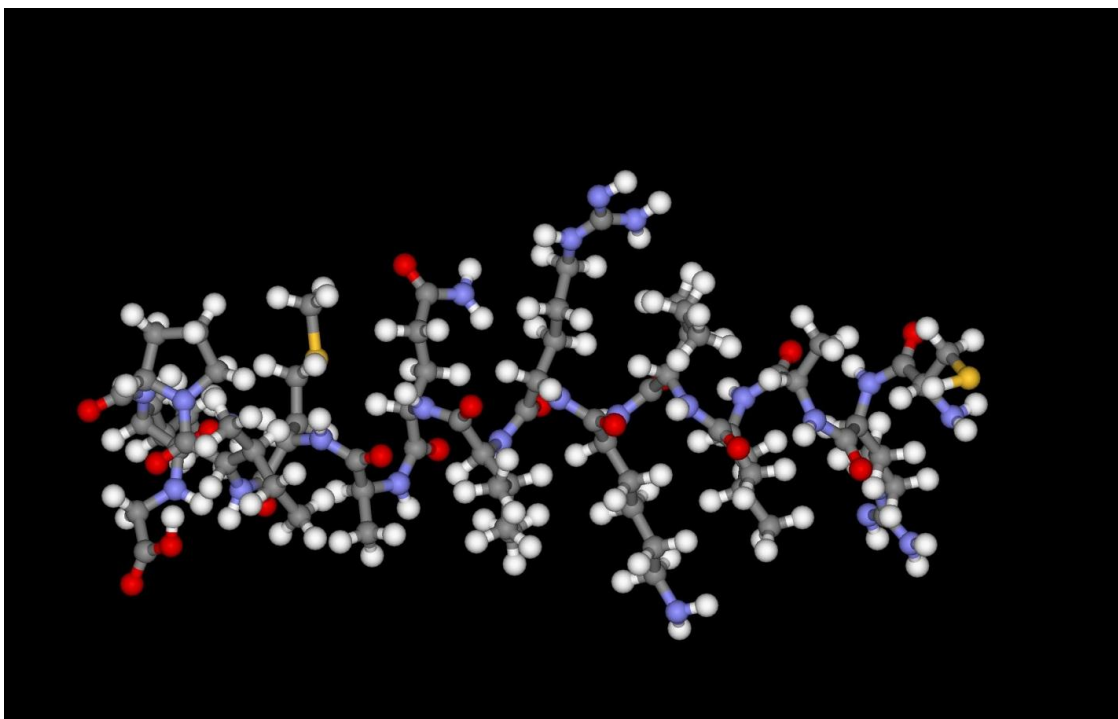


Fig. 1.4.2. Lung Surfactant-B (11-25), the sequence of which was obtained from the RCSB Protein Data Bank (designation 1KMR⁴⁶) is CRALIKRIQAMIPKG (Cys-Arg-Ala-Leu-Ile-Lys-Arg-Ile-Gln-Ala-Met-Ile-Pro-Lys-Gly). Secondary structure exhibits a helix as does the Barron peptoid mimic.

at amine and hydroxyl sites. In general heparin has a linear structure but there is great variation in the pattern of substitution on the disaccharide subunits regarding polysulfated esters and amines as well as acetyl amides. The resulting variation produces a complex and heterogeneous mixture of macromolecules. Heparin and the related polysaccharide heparan sulfate, are two members the family of glycosaminoglycans (GAGs) that also includes hyaluronic acid, dermatan sulfate, chondroitin sulfate and keratan sulfate.⁴⁷ The monosaccharides that comprise these glycosaminoglycans, together with their Haworth structures are shown in **Fig. 1.5.1**. The structures of the repeating disaccharides of the glycosaminoglycans mentioned above are shown in **Fig.1.5.2**.

Starting with the structure of a segment of heparin obtained from the RCSB Protein Data Bank, designated 1HPN, derived from molecular modeling and Accelrys Viewer lite 5.0,³² it was found that the sulfated esters lie at distances of between 6.5 Angstroms and also at a longer distance of over 10.4 Angstroms as shown in **Fig. 1.5.3**. This is important data as these anionically charged groups must be aligned with the cationic side chains of the peptoids rationally designed in this study for heparin-peptoid binding. As will be seen later, it is the addition of these two distances that provides the value of the highest density of anionic electron potential.

Heparin is produced in the human body within connective tissue mast cells. It is produced as heparin proteoglycan, which has a molecular weight of between 750 kD to 1000 kD⁴⁸. The heparin proteoglycan contains a core protein, serglycin, to which multiple heparin chains are covalently bound. Serglycin is coded by the SRGN gene.⁴⁹ These heparin polysaccharide chains are between 60–100 kD in size. The polysaccharide

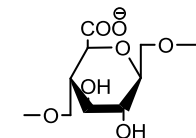
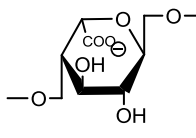
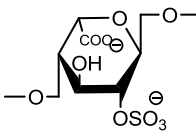
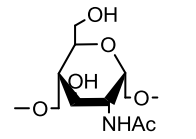
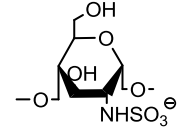
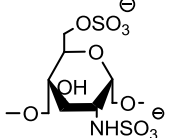
Monosaccharide	Abreveations	Structures
β -D-glucuronic acid	GlcA	
α -L-iduronic acid	IdoA	
2-O-sulfo- α -L-iduronic acid	IdoA(2S)	
2-deoxy-2-acetamido- α -D-glucopyranosyl	GlcNAc	
2-deoxy-2-sulfamido- α -D-glucopyranosyl	GlcNS	
2-deoxy-2-sulfamido- α -D-glucopyranosyl-6-O-sulfate	GlcNS(6S)	

Fig. 1.5.1. Monosaccharides of heparin and heparin sulfate with their abbreviations and Haworth structures.

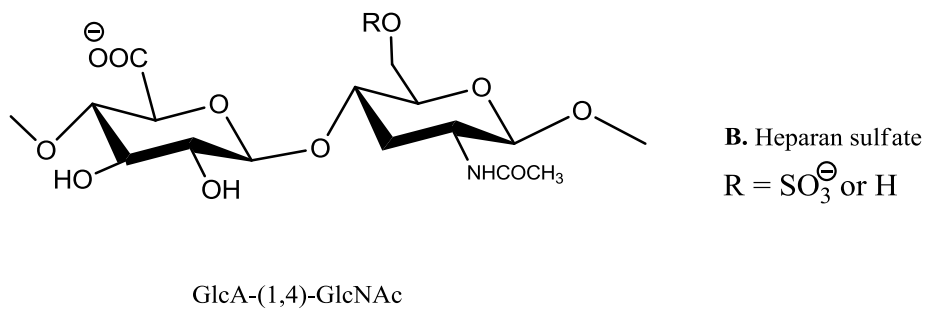
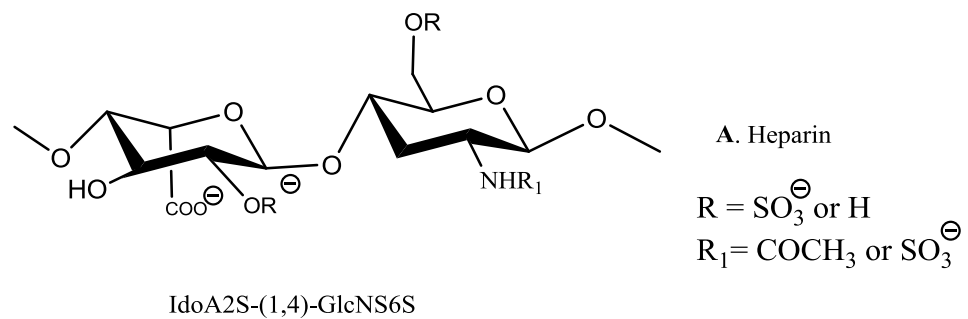
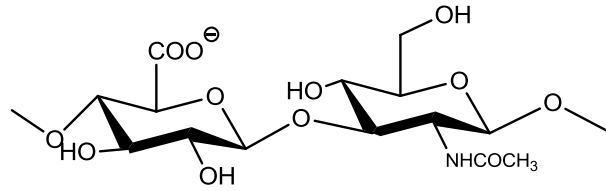
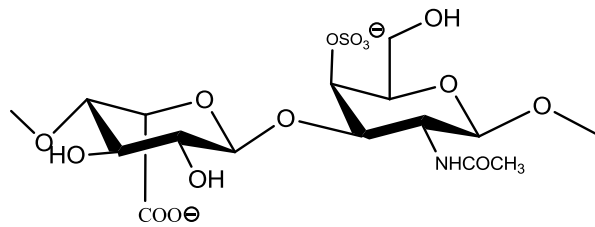


Fig.1.5.2. The major repeating disaccharides of the family of glycosaminoglycans for heparin (A), heparan sulfate (B), hyaluronic acid (C), dermatan sulfate (D), chondroitin sulfate (E) and keratin sulfate (F).



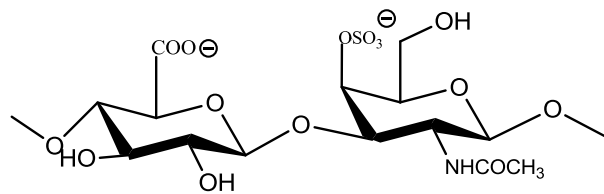
C. Hyaluronic acid

GlcA-(1,3)-GlcNAc



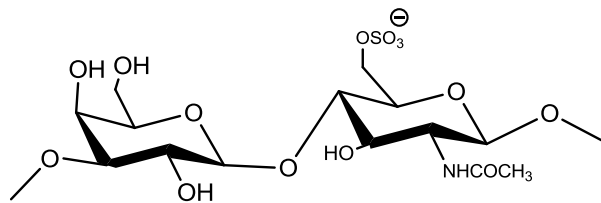
D. Dermatan sulfate

IdoA-(1,3)-GalNAc4S



E. Chondroitin sulfate

GlcA-(1,3)-GalNAc4S



F. Keratan sulfate

Gal-(1,4)-GalNAc6S

Fig.1.5.2. continued.

chains are then cleaved randomly to provide a mixture of heparin chains ranging anywhere from 5-25 kD in size. The heparin chains are then stored in the mast cells as complexes with basic proteases⁵⁰ until ready for use. At physiological pH, the sulfated ester, amide and carboxylic acid groups are deprotonated resulting in a molecule with the highest electronegative charge density of any known biological molecule.

Heparan sulfate has a similar structure to heparin but with the following difference.⁵¹ In heparan sulfate, its disaccharide subunits consist mainly of glucuronic acid (GlcA) linked to *N*-acetylglucosamine (GlcNAc); the GlcA-(1 → 4) - GlcNAc disaccharide is approximately 50% of the total disaccharide units. Heparin, on the other hand, depending on its source, consists of IdoA(2S)-GlcNS(6S) as the primary disaccharide unit in 85% of heparins from beef lung and approximately 75% of the disaccharide units from porcine intestinal mucosa.

Heparin was discovered in 1916 by Jay McLean and William Henry Howell and went into clinical trials in 1935.⁵² They were not actually looking for an anticoagulant, but recognized the potential of what they found. Since that time it has been in clinical usage especially for its anticoagulant activity. In addition to its role as an anticoagulant, it is also known to be involved in many other biological functions and these are by no means limited to the few that are mentioned here. It is involved in inhibition of angiogenesis and tumor growth,^{5,53} release of both lipoprotein lipase and hepatic lipase,⁵³ acute respiratory distress syndrome as well as asthma,⁵⁴ allergic encephalomyelitis, and many other areas where its use is either being applied clinically or is currently being studied.

1.6. Anticoagulant activity of heparin

When the epithelium of human blood vessels become exposed through damage to the cell wall, platelets become activated through a series of interrelated steps. The resulting activated platelets change shape and aggregate, with adjacent platelets resulting in a clot. This process is known as primary hemostatis.

Secondary hemostatis is more complex than primary hemostatis. The human blood coagulation cascade of secondary hemostatis involves multiple factors. It consists of two major pathways that result from the activation means involved. The two pathways are known as the intrinsic or contact activation pathway, which takes place when blood comes into contact with foreign surfaces, and the extrinsic or tissue factor pathway, which takes place when tissue is injured. **Fig. 1.6.1.** outlines the major steps in both the intrinsic and extrinsic pathways of the coagulation cascade.

The ultimate goal of the cascade is the formation of a clot at the site of injury. This process involves both primary hemostatis and secondary hemostatis simultaneously. Heparin, by binding to antithrombin, changes the structure of antithrombin and facilitates its binding to thrombin and Factor Xa, thus inhibiting the coagulation cascade.

The binding of cationic oligomers to heparin sets off a series of reactions, resulting in its well known anticoagulant activity. How this is accomplished is as follows.⁵⁵ Antithrombin III is a serpin, i.e., a serine protease inhibitor, part of a large family of enzymes that include chymotrypsin, thrombin and trypsin, all of which contain a nucleophilic serine in their catalytic site.⁵⁶ Heparin activates antithrombin III through

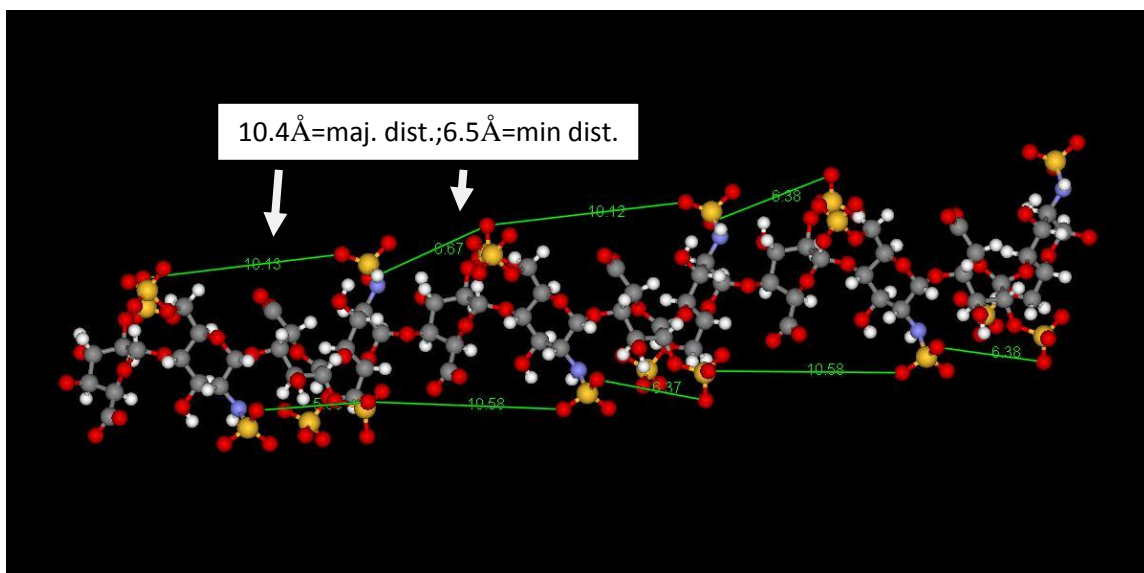


Fig. 1.5.3. An image of a 12-saccharide segment of heparin along with the distances between sulfated esters in Angstroms. The model was obtained from the RCSB Protein Data Bank and designated as 1HPN.⁵⁷ It was derived from a combination of computer molecular modeling and proton NMR.

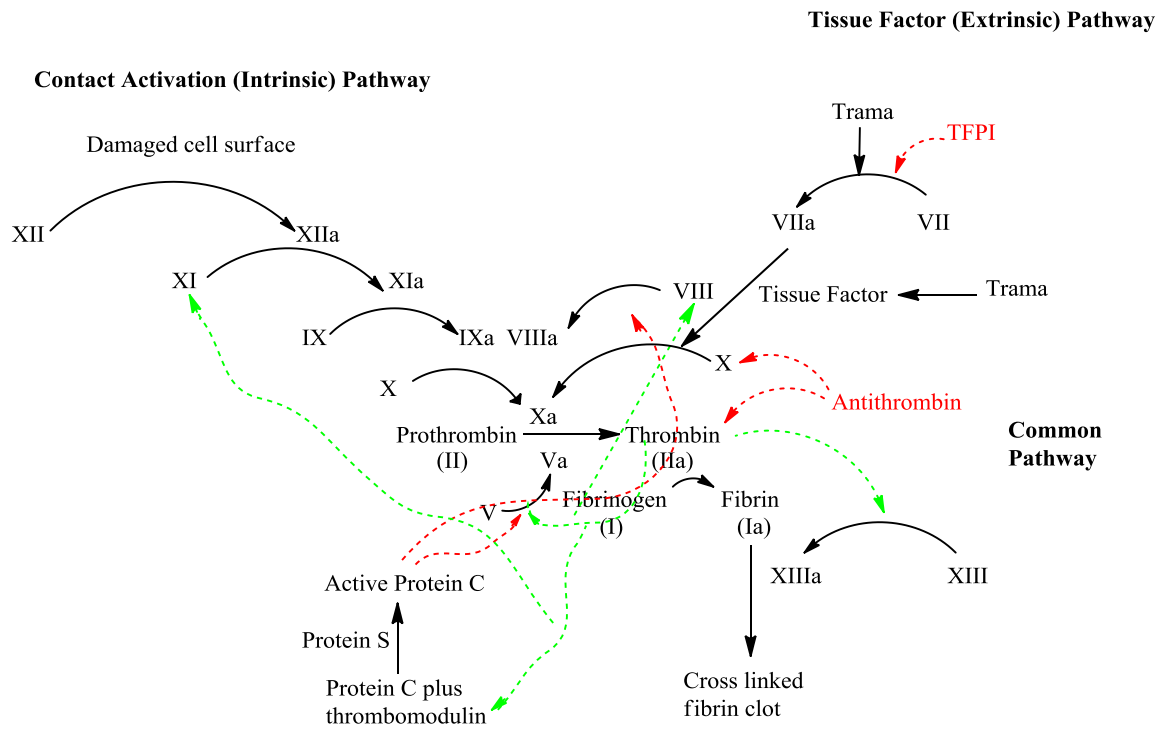


Fig.1.6.1. The intrinsic and extrinsic pathways of the coagulation cascade of secondary hemostasis. As can be seen multiple blood factors and proteins are involved. There are also feedback circuits shown by red and green dotted arrows. Antithrombin is shown in red and interferes in the cascade by interacting with both thrombin and Factor X, which is converted into Xa as shown in the above illustration.

two mechanisms. The binding of antithrombin III to heparin takes place at a pentasaccharide sequence within heparin: GlcNAc/NS(6S)-GlcA-GlcNS(3S,6S)-IdoA(2S)-GlcNS(6S), the structure of which is shown in **Fig. 1.6.2.** with the nonreducing terminus being GlcNS(6S). The third saccharide from the left in the structure is unique in that the 3-O anionic sulfate ester identified in the figure is necessary for the anticoagulant activity of heparin.

Binding of the pentasaccharide sequence of heparin is followed by an allosteric conformational change in the active site of antithrombin III, which enhances the binding of antithrombin to and inactivation of factor Xa. Factor Xa is a serine endopeptidase. The antithrombin-activated Xa then inactivates thrombin by the binding of thrombin to a site proximal to the pentasaccharide sequence of heparin.⁵⁸ It is the highly negatively charged sulfate groups on heparin that strongly bind with thrombin through electrostatic attraction.

Thrombin is essential for the coagulation cascade to go forward. Also since antithrombin binds to the highly negatively charged deprotonated sulfate esters, amides and carboxylates at physiological pH, cationic oligomers such as the peptoids produced in this study or Heparin Interacting Peptide (HIP) and other peptides that were previously studied^{13,14} can potentially interfere with the anticoagulant effect of heparin by competitive binding of heparin. Currently there is only one FDA approved drug on the market that fulfills this role, i.e. protamine or protamine sulfate,⁵⁹ which was discussed in the introduction.

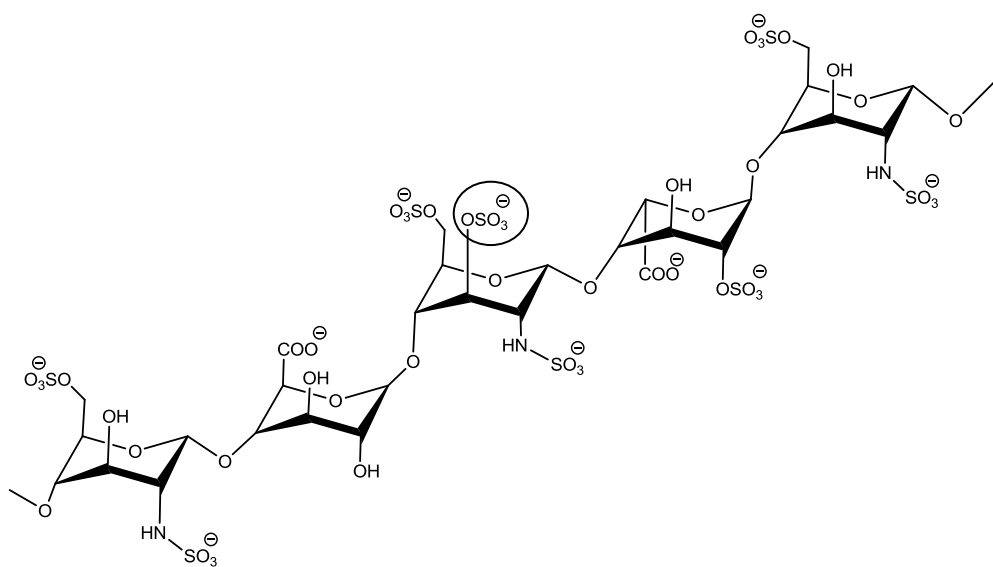


Fig.1.6.2. The pentasaccharide binding sequence of heparin for antithrombin III, shown in the chair conformation format. The 3O-sulfate group on the third saccharide from the left, which is circled in the structure is essential for the anticoagulant activity of heparin.

1.7. Other biological functions of heparin.

In addition to heparin's effect on the coagulation cascade, it also plays other biological roles in many organisms.^{51,54} To give an idea of the importance of heparin and heparin-related glycosaminoglycans, almost all cells are associated with or secrete some form of glycosaminoglycan. Also, heparin is widely conserved across the whole of the zoological spectrum of organisms including invertebrates that do not share the coagulation cascade described in the previous section. In addition it has been found that simple marine sponges use sulfated glycosaminoglycans to mediate cell-to-cell adhesion.⁶⁰ Also it is known that heparin binds to histamine in mast cells and not to the granule matrix.⁶¹ This accounts for the mobility of histamine, when secretion from the mast cell is necessary. Heparin is also secreted at the same time.

It is now known that heparin and other GAGs bind a wide variety of proteins that serve many functions having nothing to do with coagulation. In fact only one third of the chains of heparin have a high affinity for antithrombin III leaving two thirds that serve other purposes. One of the more significant roles of GAGs is in their binding to Fibroblast Growth Factors (FGF). It was found in 1991⁶² that GAGs are required in the binding of FGF's to their high affinity receptor. This is highly important since fibroblast growth factors are directly involved in the proliferation and differentiation of cells including stem cells.⁶³

Heparin plays a myriad of roles in the human body and, as stated above, throughout

the entire zoological spectrum of organisms. Viruses such as Herpes Simplex Virus (HSV) use heparan sulfate as a binding attachment point on the epithelial tissue of the eye, a study that is underway currently at Western University of Health Sciences.⁶⁴ In fact, the researchers at Western University evaluated our peptoids for activity against cellular invasion by HSV, which uses heparan sulfate to attach to membranes. They found that our peptoids did in fact interfere with HSV protein-heparan sulfate binding on target cells at very low concentrations.

1.8 This Dissertation

The central purpose of the research presented in this dissertation is to design, synthesize and study peptoid oligomers that have the ability to bind to and thereby inhibit heparin, which itself interferes with the coagulation cascade that leads to the formation of blood clots and hence in some cases can be a crucial part of the healing process. As was stated above, the only FDA approved drugs in current use for this purpose are protamine and protamine sulfate. It is of critical importance that protamine replacements be developed in order to avoid the occasionally dangerous and potentially lethal immunogenic side effects of protamine products.

Since heparin is a polyanionic glycosaminoglycan (GAG) with a high electronegative charge density, the strategy was to design and synthesize compounds that bind to heparin, and thereby block heparin's anticoagulant activity by blocking its binding to antithrombin III. Peptides are poor drug candidates *in vivo* but HIP¹³ previously discussed above, is known to contain a segment that binds to heparin. Even though the

HIP peptide by itself is not an appropriate target drug, in vitro studies⁶⁵ indicate that a portion of it has proved to be useful as a starting point that can be modified into a drug that is superior to peptides while retaining the heparin binding affinity of HIP¹³. Rabenstein *et al.*⁶⁵ designed two similar peptides designated as L-HIPAP (Ac-SRGKAKVKAKVKDQTK-NH₂) and its all D amino acid counterpart D-HIPAP that had binding constants K_b in the 10^3 to 10^4 range (dependent upon Na⁺ concentration).

Binding constants of the peptoids produced in this study were generally higher than HIP and D or L-HIPAP. The peptoids with the highest binding constants also turned out to be the most difficult to characterize in terms of binding constants by ITC. These were the guanidinylated families of peptoids. The ITC titration data did not give a reasonable fit to the modeling algorithm of the Origin 5.0 software used by the GE Healthcare/Microcal VP ITC.⁶⁶ Generally the ITC data for the guanidylated peptoids produced an anomalous dip in the fitted data points. Fortunately Heparin Affinity Chromatography (HAC) clearly demonstrated the enhanced binding affinity to heparin in comparison to primary amine-bearing peptoids.

Since it was possible to obtain binding constants from ITC data for peptoids bearing amine side chains, it was possible to compare ITC-derived K_b s to HAC retention times allowing a calibration curve of K_b versus HAC retention time to be constructed. With the calibration curve, it was possible to estimate binding constants for the guanidinylated peptoids. The heparin affinity chromatography results demonstrated consistently tighter binding and the binding constants determined from the calibration curve were higher than

the nonguanidinylated peptoids. This makes logical sense due to the greater hydrogen bonding produced by guanidinylated functional groups than primary ammonium groups. A comparison of the hydrogen bonding between a primary ammonium group and a deprotonated sulfonic ester and a guanidinium group and a sulfonic ester is shown in **Fig. 1.8.3**.

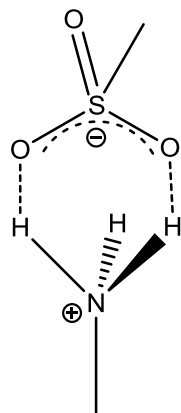
It is interesting that the peptoids developed in this study were at least 1-2 orders of magnitude greater than L-HIPAP or D-HIPAP in their binding affinity to heparin, even though they contain fewer cationic sites. In addition they were shorter than HIPAP (Ac-SRGKAKVKAKVKDQTK-NH₂)⁶⁵, which is 16 monomer units long as opposed to the peptoids, most of which are 9 units in length. It could be that the optimum length is shorter than HIPAP or more likely it is possible that peptoids studied in this dissertation are designed for optimal binding to heparin.

In the initial phase of this study, the effect of chirality of the peptoids on heparin binding affinity was studied by the synthesis of two 12-mer peptoids. One of the peptoids contained a repeating *N*(rpe) monomer unit, while the other 12-mer peptoid contained a repeating *N*(spe) monomer unit. It was determined through ITC and HAC, that the *N*(spe) bearing peptoids bound with a greater affinity to heparin. Additionally, CD was performed on both peptoids to study the secondary structure, as prior research by Zuckermann *et al.*²⁷ indicated that *N*(spe) bearing peptoids conform to a right-handed helix, while *N*(rpe) bearing peptoids were shown by CD to conform to a left-handed helix. The CD data also was consistent with the results found by Zuckermann, yielding a

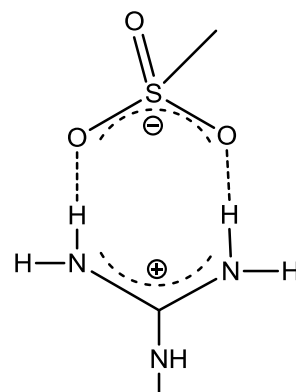
right-handed helix for *N*(spe) bearing peptoids and a left-handed helix for *N*(rpe) bearing peptoids. The ITC and HAC data for the two 12-mer peptoids, indicated that the *N*(spe) bearing peptoids possessed a greater affinity for heparin than the *N*(rpe) bearing peptoids, and so all subsequent work was done using *N*(spe) bearing peptoids. The effects of chirality of the side chains on heparin binding affinity will be discussed in Chapter Three.

Following the chirality study, a small library was produced consisting of nonguanidinylated peptoids with repeating sequences of $(N(\text{Orn})-N(\text{Bu})-N(\text{spe}))_n\text{-NH}_2$, where $n = 1, 2, 3$ and 4 producing peptoids from 3 to 12 monomers in length. Along with these, analogs were then synthesized by reaction with 1-*H*-pyrazolecarboxamide HCl to produce *N*(Arg)-containing peptoids as well. Following synthesis and purification by reverse phase HPLC and solvent removal by rotovaporation and lyophilization, all of the peptoids in this library were analyzed by ITC, CD, and HAC. The results of the study on ammonium bearing side chains will be discussed in Chapter Three, while the relative binding affinities of ammonium and guaninium bearing peptoids will be discussed in Chapter Four.

Subsequent to the length vs. heparin affinity studies, several studies were undertaken to design peptoids with different length side chains or even completely different groups as side chains, including an allyl and benzyl group. These studies all used 9-mers, except the first study investigating length. This was due to synthesis time and good results



Ammonium hydrogen bonding



Guanidium hydrogen bonding

Fig. 1.8.3 Possible hydrogen bonding schemes for the binding of an ammonium versus a guanidium group to a deprotonated sulfonic acid group.

obtained with ITC on 9-mers, and the studies were divided into the following categories in order to isolate the variables .

The first series resulted from the alteration of the length of the carbon chain linking the ammonium or guanidinium groups to the peptoid backbone. The lengths of the carbon chains studied were 3-5 carbons. The idea of lengthening the carbon chain was to assist the charge bearing groups in reaching the anionic sulfonic acid esters and amides on heparin, thereby increasing the affinity of the peptoids for heparin. The results of this study will be discussed in Chapter Five.

This study was followed by alteration of the length of the carbon chain of the central spacing monomer of the repeating trimer sequence, which consisted in all but two cases of alkyl chains from 1 to 4 carbons in length. Allyl and benzyl monomers were also tried in this position. The lengths of the central monomer were decreased from 4 down to 1 by using butylamine, propylamine, ethylamine and then finely methylamine. The idea was that perhaps a shorter chain would cause less steric interference between the chiral groups and the charge bearing groups and possibly enhance the secondary structure of the peptoid. These results will also be presented in Chapter Five. In addition, two different side chains were introduced, i.e., an allyl and a benzyl group. These were included to investigate the effect that unusual side chains in this position would have on heparin affinity. The benzyl group, for example is bulkier and the allyl group contains a pi complex, which would provide an electron dense side chain in comparison to an alkyl group. The results of heparin-binding affinities for these two side chains will be shown

in Chapter Six. In addition to these studies, it appeared valuable to use computational methods to provide potential insight into the structure of the peptoids as well as when bound to heparin.

Computational studies were therefore undertaken using Spartan '10 to investigate the secondary structure of minimized 9-mer peptoids, and Autodoc vina, designed at the Scripps Research Institute to investigate the docking of peptoids, both ammonium bearing and guanidinium bearing, to heparin. These results will be presented in Chapter Seven.

To summarize, eighteen peptoids were synthesized, purified by HPLC, and characterized by MALDI-TOF, and their interaction with heparin was characterized by isothermal titration calorimetry, heparin affinity chromatography and circular Dichroism spectrometry. The side chains of the peptoid monomers were modified to produce a variety of the peptoids with resulting changes in heparin affinity, the results of which will be summarized and conclusions presented in Chapter Eight. Future studies will be presented in Chapter Nine.

1.9 References

1. Rabenstein, D. L. *Nat. Prod. Rep.* **2002**, *19*, 312-331.
2. Guyton, A. C., Hall, J. E. *Textbook of Medical Physiology.* **2006**.
3. Linhardt, R. J., Gunay, N.S. *Sem. Thromb. Hem.* **1999**, *3*, 5-16.

4. Liu, G., Hultin, M., Østergaard, P., Olivecrona, T. *Biochem. J.* **1992**, 285, 731-736.
5. Folkman, J., Langer, R., Linhardt, R. J., Haudenschild, C., Taylor, S. *Science* **1983**, 221, 719-725.
6. Ludwig, R. J., Alben, S., Boehncke, W. *Med. Chem., Mini-Rev.* **2006**, 6, 1009-1023.
7. Lin, Y.-L., Lei, H.-Y., Lin, Y.-S., Yeh, T.-M., Chen, S.-H., Liu, H.S. *AntiViral Res.* **2002**, 56, 93-96.
8. Hirsh, J., Levine, M.N. *Blood* **1992**, 1-17.
9. Gadzekpo, V., Buhlmann, P., Xiao, K. P., Aoki, H., Umezawa, Y. *Anal. Chim. Acta* **2000**, 411, 163-173.
10. Byun, Y., Chang, L.C., Lee, L.M., Han, I.S., Singh, V.K., Yang, V.C. *ASAIO J.* **2000**, 46, 435-9.
11. Balhorn, R. *Genome Biology* **2007**, 8, 227.
12. Schick, B. P., Maslow, D., Moshinski, A., San Antonio, J. D. *Blood* **2004**, 103, 1356-1363.
13. Carson, D., Rohde, L.H., Julian, J., Babaknia, A. *J. Biol. Chem.* **1996**, 271, 11824-11830.
14. Liu, S., Zhou, F., Hook, M., Carson, D. D. *Proc. Natl. Acad. Sci. U.S.A.* **1997**, 94, 1739-1744.
15. Rabenstein, D. L., Wang, J. *Biochemistry* **2006**, 45, 15740-15747.
16. Latham, P. W. *Nat. Biotechnol.* **1999**, 17, 755-757.
17. Zuckermann, R. B., Kerr, J.M., Kent, S.B., Moos, W.H. *J. Am. Chem. Soc.* **1992**, 114, 10646.
18. Fowler, S. A., Luechapanichkul, R., Blackwell, H.E. *J. Org. Chem.* **2009**, 74, 1440-1449.
19. Hamza, M. PhD Thesis, University of California at Riverside, **2010**.
20. Fowler, S. A., Blackwell, H. E. *Org. Biomol. Chem.* **2009**, 7, 1508-1524.
21. Stringer, J. R., Ilia, A., Guzei, J., Blackwell, H. E. *J. Org. Chem.* **2010**, 75, 6068-6078.
22. Wu, C.W., Huang, K., Zuckermann, R. N., Barron, A.E. *J. Am. Chem. Soc.* **2001**, 123, 6778-6784.
23. Shah, N. H., Butterfoss, G. L., Nguyen, K., Yoo, B., Bonneau, R., Rabenstein, D. L., Kirshenbaum, K. *J. Am. Chem. Soc.* **2008**, 130, 16622-16632.
24. Fowler, S. A., Blackwell, H. E. *Org. Biomol. Chem.*, **2009**, 7, 1508-1524.

25. Rabenstein, D. L., Sui, Q, Borchardt, D *J. Am. Chem. Soc.* **2007**, *127*, 12042–1204.
26. Kirshenbaum, K., Barron, A.E., Goldsmith, R.A., Armand, P., Bradley, E.K., Truong, K.T.V., Dill, K.A., Cohen, F.E., Zuckermann, R.N. *Proc. Natl. Acad. Sci. USA* **1998**, *95*, 4303–4308.
27. Armand, P., Kirshenbaum, K., Falicov, A., Dunbrack, R.L. Jr., Dill, K.A., Zuckermann, R.N., Cohen, F.E. *Folding and Design* **1997**, *2*, 369-375.
28. *ibid.*
29. Armand, P., Kirshenbaum, K., Goldsmith, R.A., Farr-Jones, S., Barron, A.E., Truong, K.T.V., Dill, K.A., Mierke, D.F., Cohen, F.E., Zuckermann, R.N., Bradley, E.K. *Proc. Natl. Acad. Sci. U. S. A* **1998**, *95*, 4309–4314.
30. Wu, C.W., Kirshenbaum, K., Sanborn, T.J., Patch, J.A., Huang, K., Dill, K.A., Zuckermann, R.N., Barron, A.E. *J. Am. Chem. Soc.* **2003**, *125*, 13525–13530.
31. Wavefunction, Inc, Irvine, Ca, **2011** Spartan 10, Molecular Modelling software with quantum mechanical calculation functions. <http://www.wavefun.com>.
32. Accelrys. **2011**. <http://accelrys.com/products/discovery-studio>.
33. Zuckermann, R. N., Martin, E, Spellmeyer, D.C., Stauber, G.B., Shoemaker, K.R., Kerr, J.M., Figliozzi, G.M., Goff, D.A., Siani, M.A., Simon, G.A., Banville, S. C, Brown, E. G., Wang, L., Richter, L. S, Moos, W.H. *J. Med. Chem.* **1994**, *37*, 2678–2685.
34. Ng, S., Goodson, B., Ehrhardt, A., Moos, W.H., Siani, M. and Winter, J. *Bioorg. Med. Chem.* **1999**, *7*, 1781–1785.
35. Liu, B., Alluri, P. G., Yu, P., Kodadek, T. *J. Am. Chem. Soc.* **2005**, *127*, 8254-8255.
36. Peschel, A., Sahl, H.G. *Nat. Rev. Microbiol.* **2006**, *4*, 529–536.
37. http://www.nlm.nih.gov/cgi/mesh/2011/MB_Magainins
38. Jang, H., Ma, B., Nussinov, R. *BMC Structural Biology* **2007**, *7*, 21-34.
39. Goodson, B., Ehrhardt, A., Ng, S., Nuss, J., Johnson, K., Giedlin, M., Yamamoto, R., Moos, W.H., Krebber, A., Ladner, M., Giacona, M. B., Vitt, C., Winter, J. *Antimicrob. Agents Chemother.*, **1999**, *43*, 1429–1434.
40. Barron, A. E. Patch, J.A. *J. Am. Chem. Soc.* **2003**, *125*, 12092–12093.
41. Wu, X. M., R., Tang, M., Buffy, J.J., Waring, A.J., Sherman, M. A., Hong, M. *Biochemistry* **2006**, *45*, 8341-8349.

42. Notter, R. H., *Lung Surfactants: Basic Science and Clinical Applications (Lung Biology in Health and Disease)* 149 Dekker, M. Ed., New York, **2000**, 254.
43. Barron, A. E., Seurnyck-Servoss, S.L., Dohm, M.T. *Biochemistry*, **2006**, *45*, 11809–11818.
44. Kurutz, J. W., Lee, K.Y. *Biochemistry* **2002**, *41*, 9627-9636.
45. *ibid.*
46. Zaia, J. *Mass Spectrom. Rev.* **2008**, *28*, 254-272.
47. Robinson, H. C., Horner, A.A., Höök, M., Ögren, S., Lindahl, U. *J. Biol. Chem.* **1978**, *253*, 6687.
48. Schick, B. *Stem Cells* **2000**, *14*, 220–31.
49. Conrad, H. E. *Heparin-Binding Proteins*: Academic Press Ed., **1998**. 149.
50. Lever, R., Page, C.P. *Nat. Rev. Drug Discov.* **2002**, *1*, 140–148.
51. Linhardt, R. *Chem. Indust.* **1991**, *2*, 45–50.
52. Folkman, J., Crum, R., Szabo, S. *Science* **1985**, *230*, 1375.
53. Coombe, D.R., Kett, W.C. *Cell. Mol. Life Sci.* **2005**, *62*, 410–424.
54. *RCSB Protein Data Bank*, <http://www.rcsb.org/> **2011**.
55. Chuang, Y.J., Swanson, R. *J. Biol. Chem.* **2001**, *276*, 14961–14971.
56. Barrett, A. J., Rawlings, N.D. *Arch Biochem Biophys.* **1995**, *318*, 247–50.
57. Cox, M., Nelson, D. *Principles of Biochemistry*. Ed. W.H.Freeman., **2004**, 457.
58. Balhorn, R. *Genome Biology* **2007**, *8*, 227-228.
59. Parish C. R., Jakobsen, K. B., Coombe D. R., Bacic A. *Biochim. Biophys. Acta* **1991**, *1073*, 56–64.
60. Chuang, W-L., Christ, M. D., Peng, J., Rabenstein, D. L. *Biochemistry* **2000**, *39*, 3542-3555.
61. Yayon A., Klagsbrun, M., Esko J. D., Leder P., Ornitz D. M. *Cell* **1991**, *64*, 841–848.
62. Finklestein, S. P., Plomaritoglou, A. *Growth Factors*; John Wiley and Sons, Inc., New York. , **2001**. p.342.
63. Shah, A. F. A., Tiwari, V., Kim, M.J., Shukla, D. *Molecular Vision* **2010**, *16*, 2476-2486.

64. Rabenstein, D. L., Wang, J. *Biochemistry* **2006**, *45*, 15740-15747.
65. MicroCal/ G.E. Healthcare. <http://www.microcal.com>.

Chapter two: Experimental Section

2.1 Automated Solid Phase Peptoid Synthesis

2.1.1 Chemicals

The materials used for synthesis of all peptoids are given below along with their sources. Triisopropylsilane (99%), piperidine (99.5%), (R)-(+)- α -methylbenzylamine (98%) and (S)-(-)- α -methylbenzylamine (98%), N-butylamine, N-propylamine, N-ethylamine, diisopropylethylamine, and methylamine (2M in THF) were purchased from Sigma-Aldrich. N-N'-diisopropylcarbodiimide (DIC), and bromoacetic acid (97%) were obtained from TCI America. N-(tert-butoxycarbonyl)-1,4-diaminobutane, N-(tert-butoxycarbonyl)-1,5-diaminopentane and N-(tert-butoxycarbonyl)-1,3-diaminopropane were obtained from Chem-Impex International Inc. Rink amide-methylbenzhydrylamine (MBHA) resin was obtained from Novabiochem. Trifluoroacetic acid (TFA) was purchased from Chem Impex International Inc. Dimethylformamide (DMF) and methanol were purchased from Sigma-Aldrich-USA. N-methyl-2-pyrrolidone (NMP) was purchased from Alfa Aesar Inc. 1-*H*-pyroazole carboxamidine HCl was purchased from AK Scientific Inc.

2.1.2 Peptide synthesizer Instrumentation

All peptoids were synthesized by solid phase synthesis methodology with the following instrumentation: Applied Bioscience Inc 433A solid phase peptide synthesizer attached to a Macintosh PowerMac G4 876MHz computer running Applied Biosystems SynthAssist software ver. 2.0. The software was modified for the two-step submonomer method. Synthesis was run in batch mode. The rink amide resin was placed in an 8 mL reaction vessel where the first step is swelling of the resin with DMF followed by removal of the Fmoc protection group from the resin.

The primary amine solutions were placed in individual cartridges. New cartridges were used for each run to avoid swelling of the cartridges due to interaction with solvents such as NMP and DMF. The cartridges are lined up in sequence from the C-terminal end to the N-terminus of the peptoid, in a shelf on the front of the synthesizer with a spring loaded block which applies a force to the cartridges and leads into a chamber, where a dual needle assembly punctures the septum of the cartridge to remove reagents and add solvents to the cartridges under 65 p.s.i. pressure. The reagents were placed in 450 mL reagent bottles that screw into the manifold in the front of the peptide synthesizer in the following positions from left to right on the instrument. The piperidine was placed in position #1, the bromoacetic acid solution was 2M in DMF, and was placed in position #4, and the DIC was used without dilution and placed in position #8. The DMF and NMP are stored in the 4L commercial bottles placed within pressure sealed containers. N₂ was connected to the peptide synthesizer through an inlet port in the back

of the instrument by way of heavy walled gas tubing and a regulator attached to a standard 9.5" diameter by 5' gas cylinder.

The peptide synthesizer has inline filters on the right side of the instrument that require periodic changing as did the paper filters on either side of the reaction vessel. The amine solutions were all 1M in NMP with 20% DMSO to aid in amine solubility, especially in the case of some of the longer mono-Boc protected-diamines, where precipitation can clog the injection needle assembly. The cartridges had a capacity of 6 mL, and were sealed with a crimping tool using septum caps made of aluminum that allowed the needle to penetrate the cartridge to remove amine solutions and wash the cartridges with DMF during the automated process. The amines were siphoned into the reaction vessel by use of the nitrogen gas that is used to move solutions through a series of computer controlled valves during a run, which, in the case of a 9-mer, can take 2 days.

2.1.3 Overview of Peptoid Synthesis Methodology

All peptoids were synthesized on solid phase resin using Zuckermann's submonomer methodology.¹ The resin used was AAPPTEC² Rink Amide MBHA, the structure of which is shown in **Fig. 2.1.1**.

The first step in the peptoid synthesis is removal of the Fmoc group by piperidine, the mechanism for which is shown in **Fig.2.1.2**; the amine attached to the resin is shown in simplified form in the red box. The actual structure is that shown in **Fig. 2.1.1** but with the Fmoc group in the figure replaced with a primary amine upon removal by piperidine.

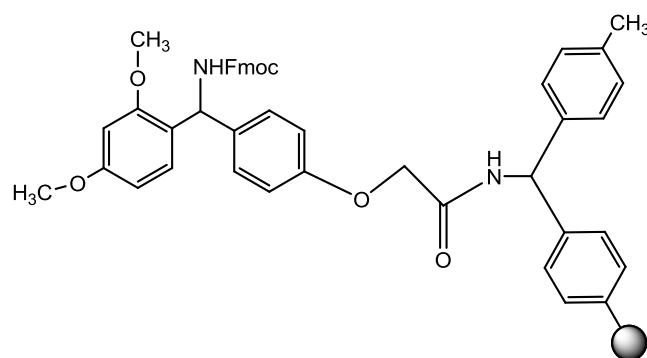


Fig. 2.1.1 Rink Amide MBHA resin structure. The active site is an Fmoc protected primary amine.³

Fmoc group

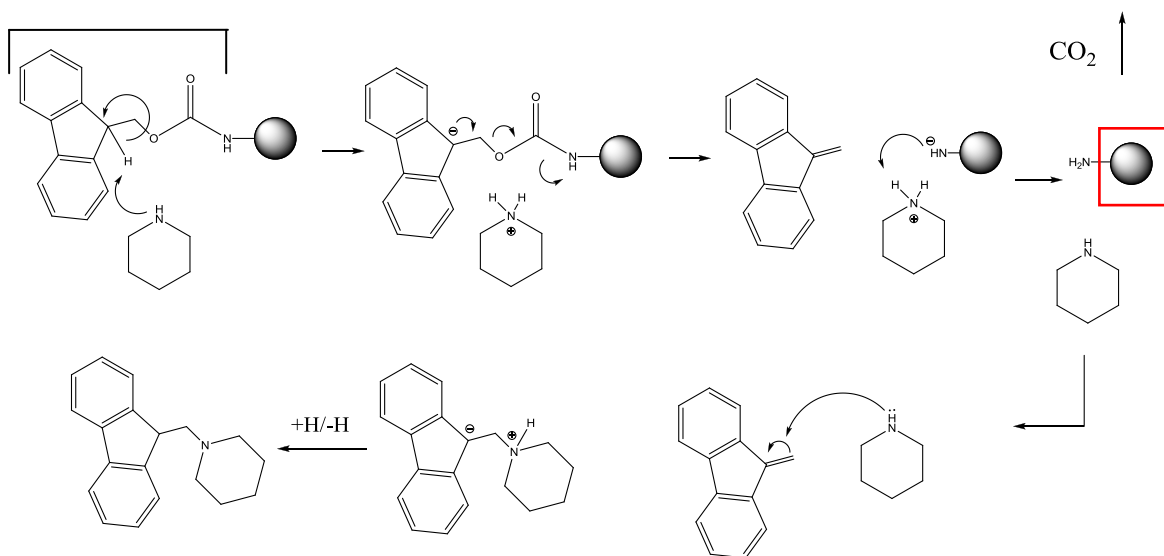


Fig. 2.1.2 Fmoc-deprotection mechanism mediated by piperidine, leading to a primary amine attached to the resin and an Fmoc-piperidine adduct. The amine attached to the resin is shown in the red box.

This and all major steps were conducted automatically by use of the peptide synthesizer described above. The resulting Fmoc-protected primary amine-resin complex was then washed automatically with DMF six times to remove the Fmoc-piperidine adduct. The primary amine attached to the resin was now free to act as a nucleophile in an acylation, where the electrophile is bromoacetic acid in what is the first part of Zuckermann's submonomer synthesis¹. The amine nucleophile was then reacted with bromoacetic acid activated by DIC at the carboxylic acid end as shown in **Fig. 2.1.3**.

This left the bromide as an excellent leaving group for an S_N2 (bimolecular nucleophilic substitution) reaction with a primary amine, the second step in the submonomer synthesis. Together the acylation reaction followed by the amine S_N2 substitution reaction produces a peptoid monomer unit. These steps are repeated sequentially to create linked N-substituted glycine monomer units until the desired resin bound peptoid is produced, at which point the synthesis automatically stops and the synthesizer display reads 'SYNTHESIS COMPLETE'. It was found that several factors were conducive to a consistently successful synthesis. In order to avoid cartridges swelling as mentioned above, the manufacturer recommended using new cartridges for each synthesis. Many failed syntheses resulted from attempting to reuse cartridges. Swelled cartridges become lodged in the shute that leads to the waste container after they are used. If the cartridge becomes stuck in the shute, the synthesis will halt and even if restarted, the synthesis will fail. Since the instrument contains a series of inert gas valves, it is essential that sufficient nitrogen is present before the synthesis is conducted.

It is equally important that sufficient solvents and reagents are loaded into the instrument to guarantee a successful synthesis.

It was found by experience that dimethylformamide (DMF) was utilized at a particularly high rate by the synthesizer. To provide an example, the synthesis of a 9-mer required at least 2 liters of DMF. The rate of NMP (*N*-methyl-2-pyrrolidone) usage was far lower. The synthesizer provides two 4-liter bottles of NMP, that are simultaneously fed into the system, and it rarely ran out. DMF is used much more frequently to repeatedly wash out the cartridges and the reaction chamber.

The following were other factors that affected the ability to produce a consistent high yield synthesis. It was found that in syntheses using the monoBoc-protected diamines with carbon chains longer than 3 carbon atoms, addition of 20% of DMSO (dimethylsulfoxide) to the NMP, which was used as the amine solvent, was necessary to avoid clogging the needle assembly. This kept the longer momoBoc-protected diamines in solution throughout the synthesis. Also, in the special case of methylamine, due to the high volatility of this amine, which is a gas in pure form, lower concentrations along with a DMF/DMSO solvent mixture were used to avoid excess swelling of the cartridges. Also in methylamine syntheses, the reaction was watched closely and methylamine containing cartridges that were going to be added later in the synthesis were kept in the refrigerator until they were needed in the synthesis. DMF was used because NMP causes a higher rate of cartridge swelling than DMF, and DMSO was added because it is known for its high solubility for many organic compounds.

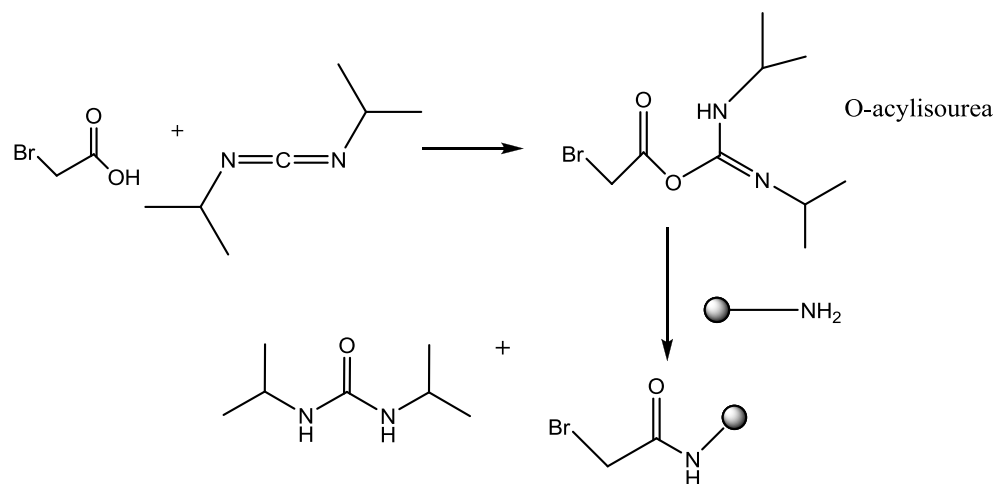


Fig.2.1.3 Acylation through 1,3-diisopropylcarbodiimide (DIC)-mediated coupling between the now unprotected nucleophilic primary amine on the resin and the bromoacetic acid by way of the activated O-acylisourea. The formation of the O-acylisourea intermediate results in an easily removable 1,3-diisopropylurea. The product of the reaction is now ready for the next step, the nucleophilic displacement of bromide by a primary amine or monoBoc protected diamine (**Fig. 2.1.4**).

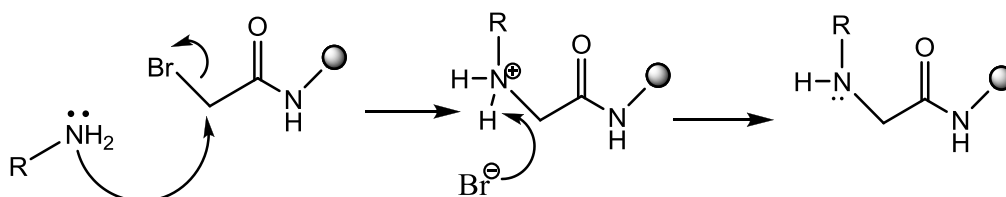


Fig. 2.1.4 Second step in the Zuckermann submonomer peptoid synthesis. The second step is a S_N2 reaction with the bromide as an ideal leaving group, which also deprotonates the resulting secondary amine. The hydrogen bromide and excess amine reagent are removed through multiple wash cycles with DMF.

Following synthesis, the resulting peptoid-resin complex is washed by vacuum filtration with methanol and allowed to dry under vacuum for 30 min.

The final step is cleavage of the peptoid from the resin through the use of TFA/TIPS/H₂O as a 95:2.5:2.5 cleavage cocktail. TIPS is triisopropylsilane and its purpose is to prevent carbocations from causing protecting groups such as Boc from reattaching themselves to primary amines. The cocktail conveniently serves a dual purpose of cleavage from the resin and removal of Boc from secondary amine-containing side chains. The products of this method are C-terminus amidated peptoids.

2.1.4. Example Peptoid Synthesis

Typically, 0.20g of 100-200 mesh rink amide MBHA resin with a substitution of 0.56 mmole/g was placed in a reaction vessel sized for a 0.10 mmol synthesis. The primary amines were placed in cartridges. Each cartridge contained 6 mL of 1M amine in either NMP or, in the case of longer Boc-protected diamines, with 20% DMSO for solubility. In the case of methylamine, DMF was used as stated above. The customized peptoid chemistry software, obtained from the Barron Research Group at Stanford⁴, was loaded on the Macintosh computer which controlled the synthesizer. The modified software contains the feature that a program can be created to accommodate the number of monomer units to be synthesized. Among the peptoids studied, 9-mers were found to yield ITC data from which binding constants could be obtained, and so 9-mers were selected as the length for analog studies, but longer peptoids were also produced by the

same method, such as 12-mers. 9-mers also were of convenient molecular weight for MALDI-TOF analysis without interference from the CHCA matrix.

Each synthesis required approximately 2.5 liters of DMF. Sufficient N₂ was also necessary to provide enough gas to run the instrument, as all of the valves on the 433A synthesizer are controlled by inert gas. For the synthesis of a 9-mer, it was found that at least 16 g of bromoacetic acid in 100 mL of DMF was necessary for the nine acylation reactions. Each acylation required 45 minutes and the nucleophilic substitution reactions required 2 hours for completion. After two days the synthesis was complete, and the resin was then washed under vacuum with MeOH. After drying for 30 minutes the granules of resin were placed in a vial with a magnetic stir bar and reacted with the cleavage cocktail for 2.5 hours.

After vacuum filtration to remove the resin, the cocktail was then removed by use of a rotovaporator leaving a viscous syrup that was taken up in 4.5 ml of deionized water in preparation for purification by reverse phase HPLC. In some cases it was necessary to add a small volume of acetonitrile or methanol to completely dissolve the solid crude peptoids prior to HPLC purification.

Normally the chromatogram contained a major peak due to the target peptoid plus minor peaks, presumably due to deletion sequences. The retention time of the major peak would depend upon the length of the peptoid and the length of the alkyl or charge-bearing side chain. The range of retention times was usually between 16 minutes

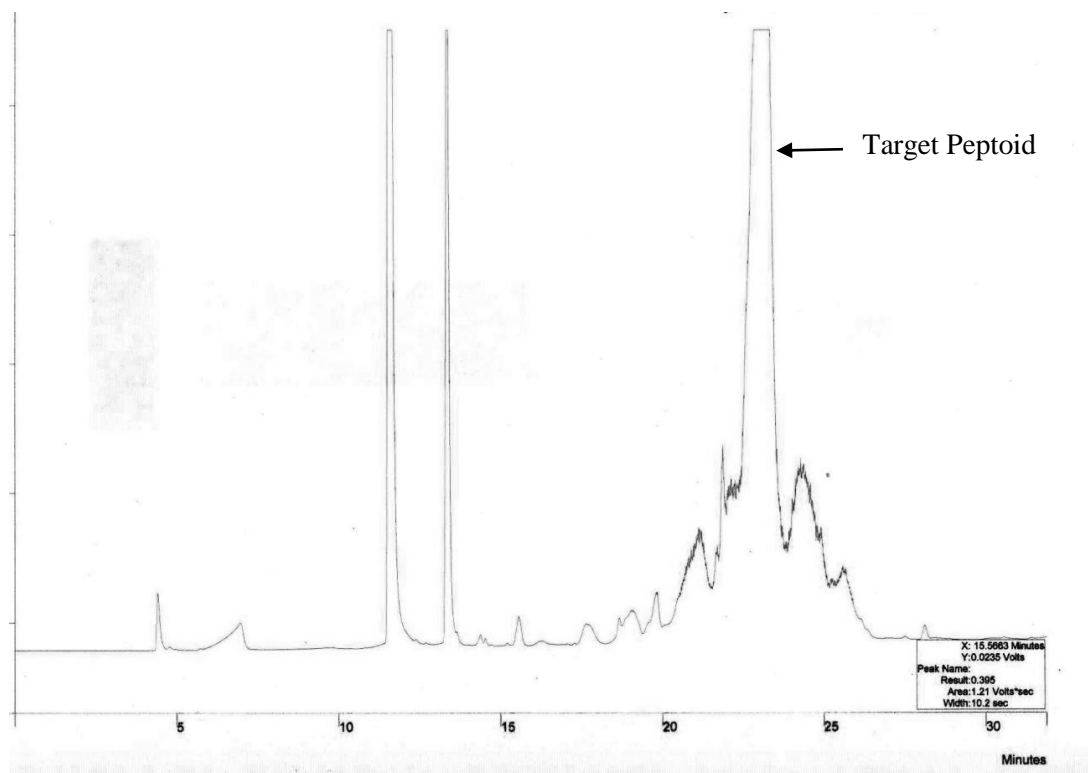


Fig. 2.1.5. HPLC chromatogram of a 12-mer peptoid with a retention time of 23 minutes.

for a 3-mer to 30 minutes for a guanidylated 12-mer. A typical chromatogram is shown in **Fig. 2.1.5**.

To purify a peptoid produced on a 0.1 mmol scale using a Waters preparatory scale column normally took between 6-9 injections to run all of the peptoid solution through the column. The typical injection volume was 650 μ L. All peptoid solutions were prefiltered through Millipore syringe filters prior to purification by HPLC.

Following purification by HPLC, the solvents were removed under a high vacuum, 2 mL of water was added and the aqueous solution frozen in dry ice, and the frozen sample was then lyophilized. Alternatively, if an oil, the peptoid oil was dissolved in methanol in a 5 mL glass vial covered with a rubber septum that was fitted to a 19/22 adapter with a syringe needle inserted allowing the methanol to be removed under vacuum in the same vial, that was then filled with 1-2 mL of deionized water. This aqueous solution was then frozen in dry ice and lyophilized to provide a white flakey or crystalline solid material. If the cationic side chains of the target peptoid were to be in the amine form, then this was the endpoint of the synthesis.

For most of the peptoids, a perguanidinylated analog was also prepared from the amine form of the peptoid by the method shown in **Fig. 2.1.6**.⁵ More than one molar equivalent of DIEA (diisopropylethylamine) was used to deprotonated the primary amine and to generate the free base of the pyrazole carboxamidine. As it turns out this reaction only works with primary amines, which in this context is fortunate as it allows the

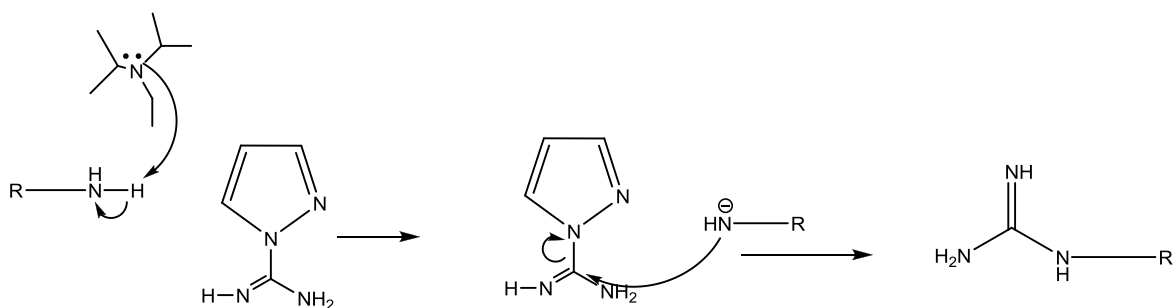


Fig.2.1.6. Guanidinylation of peptoid amine groups using 1-H-pyrazole carboxamide HCl and DIEA in DMF, conducted at room temp for 24 hours. The reaction is quenched by addition of 10:90 % TFA/H₂O until neutral pH is achieved.

reaction to be used only to modify the primary amines on the side chains and not any secondary amines, as for example on the N-terminus of the peptoid.

Upon addition of dilute TFA, the pH neutral aqueous solution of the guanidylated peptoid is purified by preparative reverse phase HPLC. In this case two major peaks appeared, one large peak with a retention time below 10 minutes and the other with a retention time approximately one minute after what was obtained with the nonguanidinylated precursor amine form of the peptoid. The second peak corresponded to the target peptoid. The solvents were again removed from the collected peak fractions under high vacuum, following which, the material was dissolved in 1-2 mL of water. The peptoid solution was then frozen under dry ice and the material lyophilized. In all cases, the products were TFA salts, with one TFA associated with each primary amino or guanidylated amine group on the molecule and with the secondary amine on the N-terminus.

The general structural formula for all of the peptoids, using a 9-mer as an example, is shown in **Fig. 2.1.7**. The general formula for the 9-mer in **Fig. 2.1.7** can be abbreviated in the following format: $H-[N(R_3)-N(R_2)-N(R_1)]_3-NH_2$. The choice of R_1 will determine the handedness of the polyproline helix as was demonstrated by circular dichroism. Specifically, spe will cause the helix to be right handed, while rpe will produce a left handed helix. To give a specific example using $R_1 = spe$, $R_2 = butyl$, and $R_3 =$ the side chain of the amino acid ornithine, which is a primary amine on the end of a three carbon

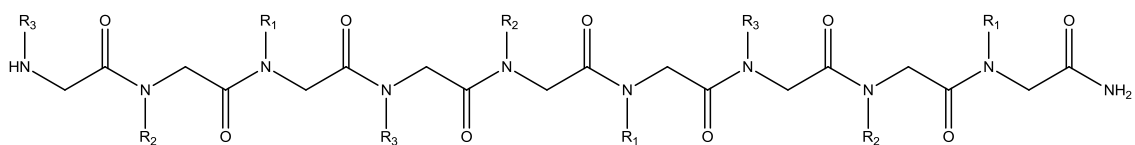


Fig. 2.1.7 General formula for a 9-mer peptoid. The 9-mer consists of a repeating trimer sequence. R_1 is a chiral unit consisting of either (*S*)-1-phenylethylamine (spe) or (*R*)-1-phenylethylamine (rpe), R_2 is an alkyl chain of 1 to 4 carbons long, or an allyl or benzyl group and R_3 is the cationic charge-bearing group, consisting of an alkyl chain of 3 to 5 carbons long terminating with either a primary amine or a guanidinium group.

chain and can be guanidylated to produce an arginine like side chain: H-[-N(Orn)-N(Bu)-N(spe)]₃-NH₂ and H-[-N(Arg)-N(Bu)-N(spe)]₃-NH₂.

2.2. Isothermal Titration Calorimetry.

2.2.1 Materials and Instrumentation

Hydrated sodium monobasic and dibasic phosphate were purchased from EMD Chemicals. Heparin sodium salt from porcine intestinal mucosa (average molecular weight of 12kDa, 180 USP units/mg, Lot 105K1114) was purchased from Sigma-Aldrich Chemicals.

Heparin-peptoid binding constants were determined by Isothermal Titration Calorimetry (ITC) using a GE Healthcare /MicroCal VP-ITC microcalorimeter controlled by a Dell PC through signal acquisition ribbons. The Windows-based Dell PC ran VPViewer and Origin 5.0 Software. A schematic of the titration cell portion of the instrument is shown in **Fig. 2.2.1**. The operation of the instrument is described in the next section. Prior to a titration, samples were degassed. A degasser unit with magnetic stirring was also purchased from MicroCal. The magnetic stirrer reduced the time to degas samples and solutions to no more than 5 minutes. After each titration, the titrated solution was removed and the sample cell cleaned. A cleaning valve was used that fit into the center port and connected to a metal tube that reached down through the center hole to the sample cell to within 2mm of the bottom of the cell. The metal tube was connected to a vacuum source and a narrow hose leading into the solution was used to clean the cell,

usually with water and methanol. The ITC instrument also has a special syringe for delivery of titrant. The syringe was cleaned with 5% Contrad 70 followed by deionized water and methanol.

2.2.2. Overview of ITC Titration Procedure

Several physical parameters can be obtained by ITC including N , the stoichiometry of the reaction, i.e., the number of ligands that are attached to the macromolecule, which is heparin in this study, K_b , the binding constant, ΔH the enthalpy of the reaction and ΔS , the entropy of the reaction, which is internally calculated by the software from K_b and ΔH since $-RT\ln K_b = \Delta H - T\Delta S$. Solving this equation for ΔS gives $\Delta S = (\Delta H + RT\ln K_b)/T$. The reaction is the interaction or binding between the ligand and the macromolecule. A schematic of the sample cell and reference cell portion of the instrument is shown below in **Fig. 2.2.1**.

The instrument measures the heat of interaction between two compounds compared to the reference cell, both of which are encased in Hastalloy⁶ to conduct heat very efficiently; the sample and reference cells and the Hastalloy are surrounded by a highly insulating material to produce an adiabatic environment. During an ITC experiment, highly sensitive thermocouples measure the temperature of the reference and sample cells. The change in temperature in the sample cell due to heat of reaction is converted into power needed to maintain a constant temperature.

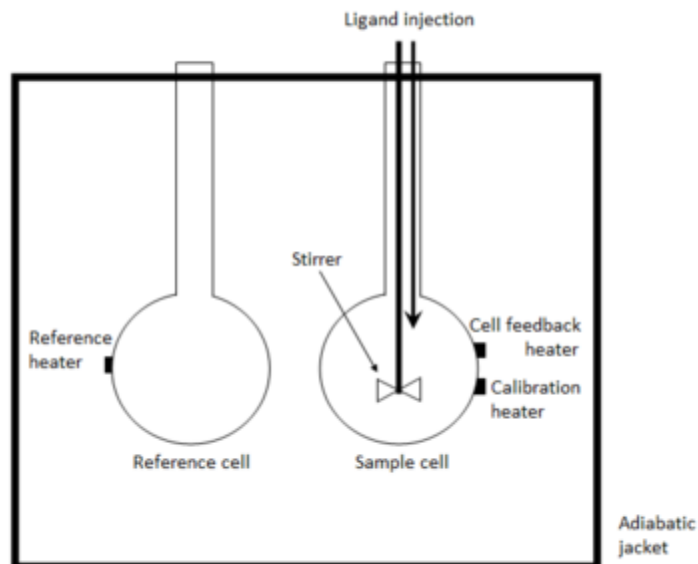


Fig. 2.2.1. Isothermal titration calorimetry instrument schematic⁷. The reference cell on the left is filled with 1.6 mL of the same buffer as is used in the main sample cell and the syringe. For our purposes, the peptoid solution was placed in the sample cell and the heparin solution was filled into the syringe. A computer connected to the VP-ITC through a pair of RS 232 connectors that control the injection rate and all other parameters and saves the resulting raw data. The binding parameters can be obtained by a nonlinear fitting of the data to a binding model using the nonlinear software program Origin, provided with the ITC instrument.

The power is monitored as a function of time, and is displayed on the vertical axis of a graph, while the horizontal axis displays the ratio of ligand to macromolecule during the titration. The resulting raw data appears as spikes either pointing upward or downward along a baseline as shown in **Fig. 2.2.2**.

If the spikes point downward as shown in the figure, then the reaction is exothermic and the enthalpy of the reaction will be negative in value. The opposite is also true, if the spikes in the raw data point upward then the reaction is endothermic and the enthalpy of reaction will be positive. Raw exothermic data will produce a titration curve that curves from the lower left corner upward and then leveling out to the upper right hand corner.⁷ Similarly, raw endothermic data will produce a titration curve that begins in the upper left hand corner and follows a curve that moves downward to the lower right hand corner. The thermodynamic parameter ΔG can be obtained from the ITC derived K_b , from **Eq. 2.2.1**. From ΔG and ΔH , ΔS can be derived from **Eq. 2.2.2**.

Eq. 2.2.1
$$\Delta G = -RT \ln K_b$$

Eq. 2.2.2
$$\Delta G = \Delta H - T\Delta S$$

The parameters obtained by fitting the data are quite sensitive to concentration and more importantly to the concentration ratio. If the concentrations are incorrect then the stoichiometry will be in error. In order to calibrate and insure the proper functioning of our instrument, a calibration experiment was performed using instructions from GE

Run Parameters for CaCl₂ -EDTA Calibration Experiment	
Total # Injections	29
Cell Temperature	25
Reference Power	10
Initial Delay	60 sec
Syringe Concentration	1mM
Cell Concentration	0.1mM
Stir Speed	310 rev/min
Volume 1 st Injection	2 μL
Duration 1 st Injection	4 μL
Volume after 1 st Injection	10 μL
Duration after 1 st Injection	20 μL
Injection Spacing	210 sec
Filter Period	2 sec
Feedback Mode/Gain	High
ITC Equil. Options	Fast Equil; Auto

Table 2.2.1. Parameters provided by MicroCal for the calibration experiment.

Healthcare–MicroCal.⁷ The calibration titration was performed according to run parameters in **Table 2.2.1**, provided by the manufacturer.

The calibration solutions were provided by the manufacturer in a kit. All solutions were buffered with MES (2-(*N*-morpholino)ethanesulfonic acid) pH 6 buffer. The ligand consisted of 1mM CaCl₂ solution and the binding compound, which binds in a 1:1 ratio was 0.1 mM EDTA solution. The EDTA solution was loaded into the sample cell, buffer in the reference cell and the CaCl₂ titrant was loaded into the syringe. A representative titration curve provided by MicroCal, together with the thermodynamic parameters obtained by fitting the data, is shown in **Fig. 2.2.4**. According to MicroCal, the results obtained from a calibration experiment should be as follows if the instrument is performing properly: $N = 0.964 \pm 5\%$; $K = 2.31 \times 10^6 \pm 20\%$; $\Delta H = -4233 \pm 10\%$.

The raw data shown in **Fig. 2.2.2**, was obtained when the calibration experiment was performed in our laboratory. The raw data points were converted by integration of the area under spikes to give the heat released by the addition of the titrant. This resulted in processed data shown in **Fig. 2.2.3**. The resulting data from the calibration experiment differed slightly from the values provided by the manufacturer probably due to experimental error. When the uncertainty ranges are considered, K_b and ΔH are within experimental error and N differs slightly from the stated ranges of uncertainty are considered.

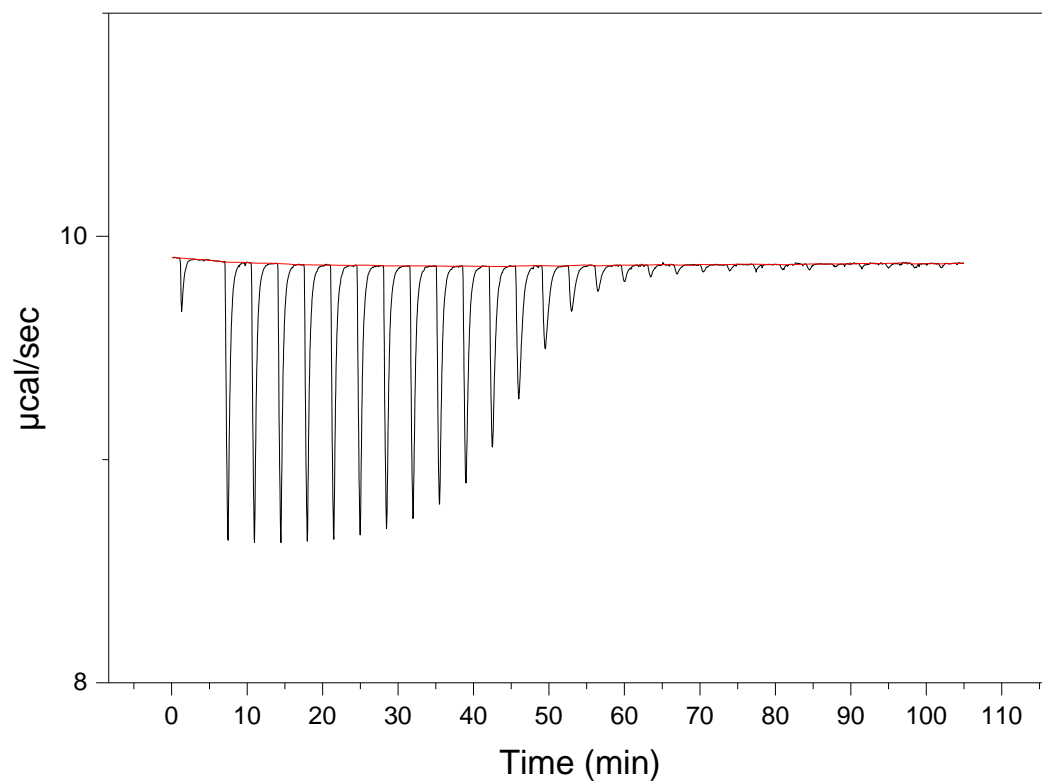


Fig2.2.2 Raw data for the EDTA/CaCl₂ calibration titration. The raw data shown in this image is of an exothermic reaction as can be seen by the downward spikes due to the power compensating for the heat given off by the reaction.

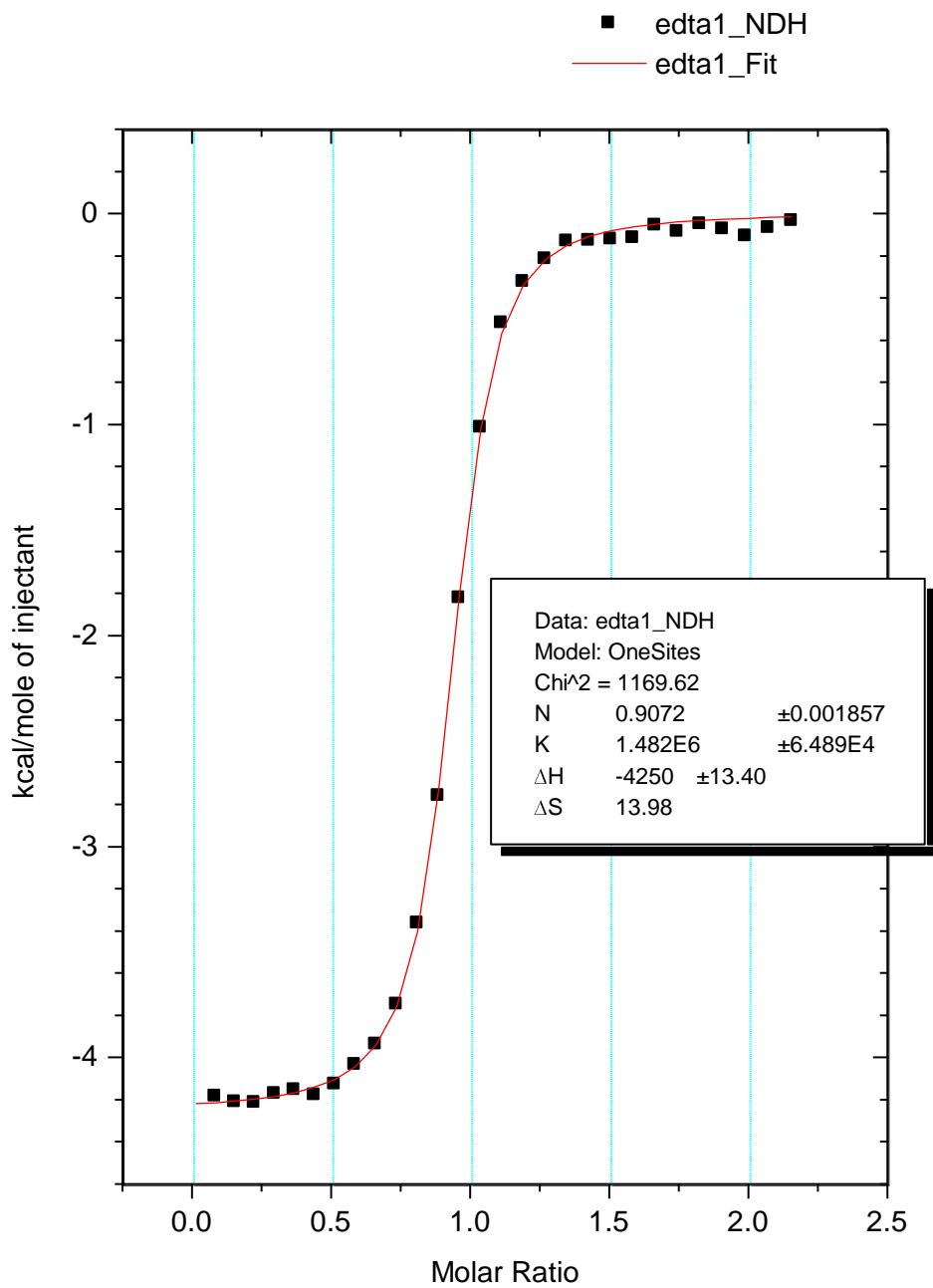


Fig. 2.2.3 Processed data from the titration shown in **Fig. 2.2.2** using Origin 5.0 software with the one-site model.

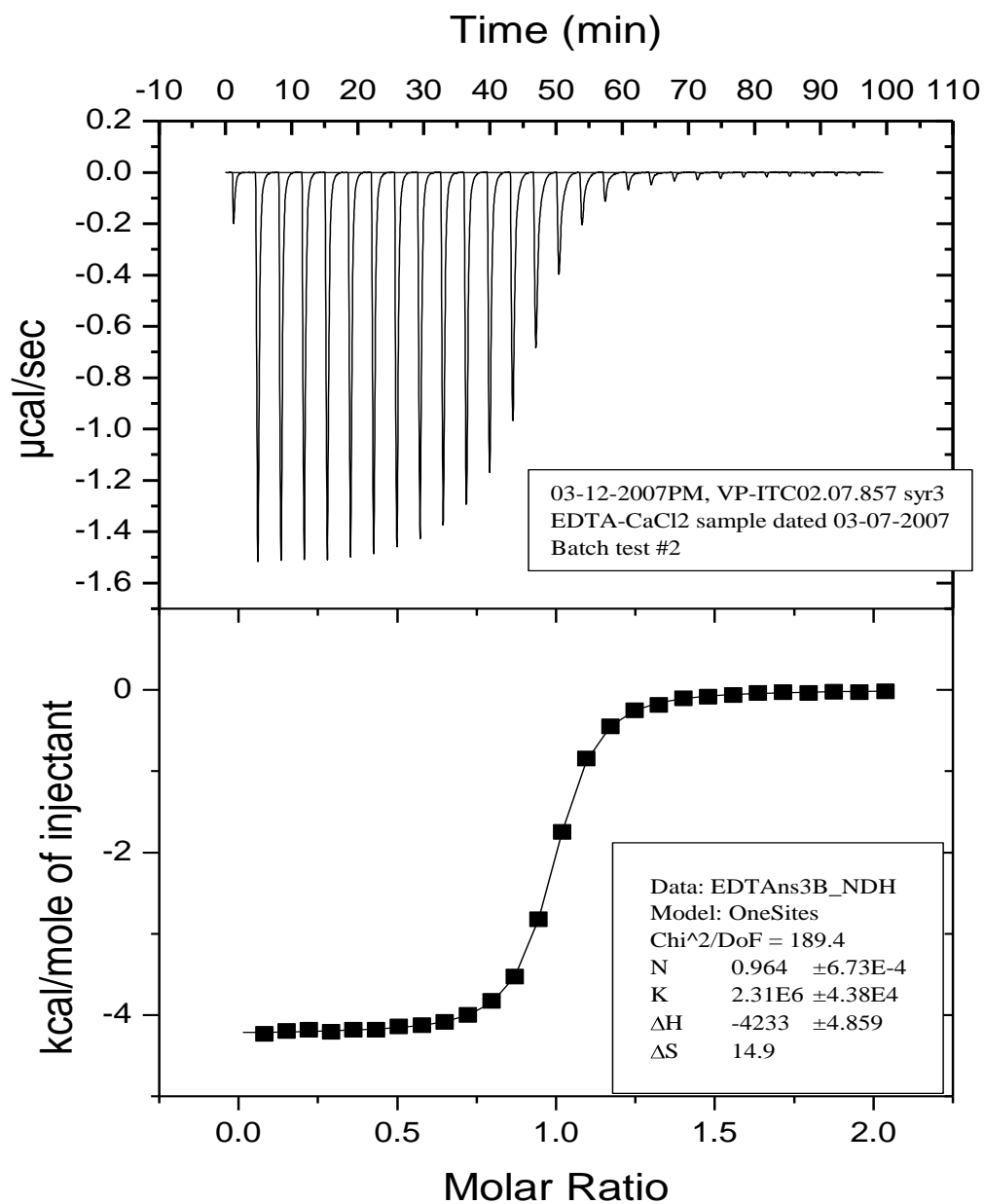


Fig. 2.2.4 Calibration data for E DTA/CaCl₂ provided by MicroCal Inc. along with the parameters obtained and errors.

2.2.3. Example Isothermal Titration Calorimetry experiment.

Before running an experiment, all of the equipment, including the cells, 250 μL titrant syringe and any syringes used to conduct the experiment were thoroughly cleaned with 5% Contrad 70 detergent, followed by deionized water and finally methanol. House vacuum was used to draw the cleaning solutions through the titrant syringe by suction. Reference buffer (in these experiments pH 7.25, 50 mM phosphate buffers were used), peptoid in buffer, and heparin in buffer were placed in three separate plastic 5 mL vials. The peptoid solution was in the micromolar to millimolar concentration range. A typical peptoid solution would be 2.0 mM. This solution was prepared by weight, using the molecular weight of the peptoid as its TFA salt. The volume of the solution was usually 10 mL to allow multiple runs and was prepared using the buffer solution in a 10 mL volumetric flask. The heparin used was porcine heparin with an average molecular weight of 12kD. Concentrations of peptoid and heparin depended upon the binding constant, which was unknown initially but obtained by trial and error. In addition, a systematic mathematical approach based upon the calculation of c , Wisemann's constant was attempted. It was hoped that calculation of Wisemann's constant would lead to an approximation of the correct concentration ratio, but in the end, simple trial and error was used.

Since only 1 mL of heparin solution was needed per run, 5 mL of heparin solution was prepared using a 5 mL volumetric flask and the same buffer. The third solution used was the reference solution, consisting of pure buffer. After placement of the three solutions in the plastic vials, 3 small magnetic stir fleas were inserted in the vials and the

solutions were placed in the degassing/ stirring apparatus that came with the VP ITC, and solutions were degassed at 25°C for no more than 5 minutes under stirring. While this was taking place, the software parameters for the titration were entered into the computer attached to the instrument. Typically, the temperature was set to 25°C, the number of injections was 30 or 40 per run. The injection volume was between 4-10 μ l, with the spacing between injections set at 360 sec., and a stirring speed of 310 revolutions/min was used.

The degassed solutions were placed into the cleaned cells, which the manufacturer recommended washing out with at least 200 mL of deionized water followed by filling each cell twice with buffer using a 2.5 mL glass syringe with a long metal needle with a flat-ended tip while a large 200 mL syringe with a luer lock, long metal, flat-ended syringe tip was used to siphon solutions out from the cells. The magnetic stir fleas were removed from the plastic vials and the heparin containing vial was placed in position with a small inverted beaker to keep the vial in place while filling and purging the heparin solution. Next the 250 μ L titrant syringe was screwed into place and set with the tip at least 0.5 mL beneath the surface of the heparin solution. A special 1 cc plastic syringe with a luer lock, metal flat-ended tip 2 inches long was attached to a 12 inch plastic tube that fits into the side of the titrant syringe below the point where the plunger is set in its upward position. The mouse controls the position on the screen for various operations. When the plastic tube is attached to the automatic syringe, the button is clicked to raise the plunger tip above the point allowing filling of the syringe with heparin solution.

Heparin solution is then partially drawn into the plastic tube, the titrant syringe tip is

closed, and the plastic tube is removed. Then the solution is purged 3X to remove air bubbles. The reference cell is filled with buffer using the 2.5 mL syringe. It is filled to the brim and quickly burped several times to disperse gas bubbles, as is the sample cell after being filled with peptoid solution . In each case after several burps, the level of solution is leveled to the exact top of the cell inlet.

Following purging the titrant syringe, which is now full of 250 μ L of heparin solution, the syringe is wiped with a wet Kimwipe, then a dry Kimwipe and inserted into the sample cell. At this point, all the preparations are in place to run an experiment. The folder and file name is set and the start button is clicked by mouse on the P.C. to begin the experiment. At the end of the run, the instrument and all parts are again cleaned as described above in order to ready the instrument for the next run or at the end of a series of runs.

Analysis of the titration data was performed using the Origin 5.0 software, which uses a Marquardt non-linear least squares algorithm. The one-site model, which assumes N equivalent ligand binding sites per macromolecule, fit the titration data well for the amine-bearing cationic peptoids, but not for the guanidylated peptoids. The titration curve for the guanidylated peptoids contained an anomalous dip in the curve and does not follow the expected S shaped curve. The raw data begins with spikes of power compensating for an endothermic binding event pointing upward, only to cross the baseline and then change direction suggesting an exothermic pattern. For this reason, ITC was used to determine the binding constants for amine-bearing peptoids only while binding constants were estimated for the guanidylated peptoids from a heparin affinity

retention time-binding constant calibration curve obtained for the amine-bearing peptoids.

A titration curve for a 9-mer Cad peptoid, H-[N(Cad)-N(Bu)-N(spe)]₃-NH₂ is shown in **Fig. 2.2.5**. As is typical for peptoids with primary amines as the charge bearing group, the titration results indicate an endothermic binding event. The raw data displays upward spikes produced by the power necessary to compensate for the loss of energy that takes place in an endergonic binding event such as this.

2.3 Heparin Affinity Chromatography

2.3.1. Overview

Heparin Affinity Chromatography (HAC) is a reliable and convenient method to determine the relative binding affinities of the peptoids for heparin, where the peptoids are chromatographed through a column packed with a solid phase consisting of agarose functionalized with heparin. A NaCl gradient from no NaCl in mobile phase A to 1.0 M NaCl in mobile phase B, both of which also contained a pH 7.4 50 mM phosphate buffer, was used to elute the peptoids from the column. The heparin affinity matrix can function in at least two means to bind heparin. The heparin itself can bind the ligand. Also the heparin can act as a strong cation exchanger due to the many Na⁺ ions associated with the anionic sulfated ester and amide sites, all of which are deprotonated at

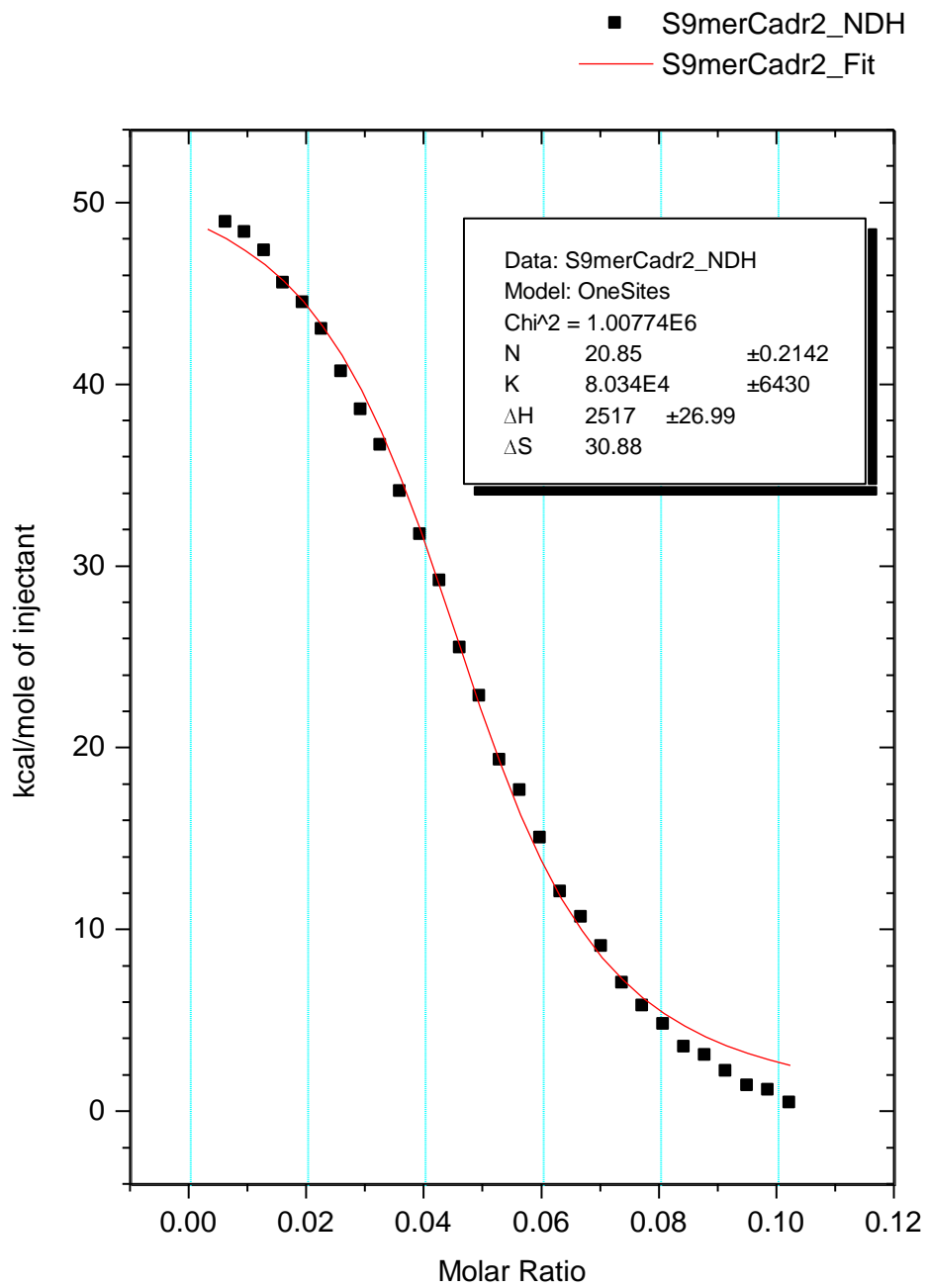


Fig 2.2.5. Titration curve for the titration of 0.164 mM peptoid H-[N(Cad)-N(Bu)-N(spe)]₃-NH₂ with 0.126 mM heparin in pH 7.4 50 mM phosphate buffer.

the buffer. Because of its higher negative charge density, heparin is a polyelectrolyte, i.e., a certain fraction of the negative charge is neutralized by the Na^+ ions associated with the heparin, thus heparin can act as a cationic exchange resin that can also bind the cationic peptoid ligands until the concentration of NaCl present in mobile phase B overcomes the binding of the peptoid and the heparin releases the peptoid in favor of Na^+ ion. According to GE Healthcare, the manufacturers of the Hi Trap Heparin Affinity columns, the agarose matrix is functionalized with porcine heparin using N-hydroxysuccinimide in a reductive amidation process.

For the first library of peptoids with lengths from 3-mer to 12-mer, with both amine side chains and guanidinium side chains, the results of the heparin affinity chromatography study will be shown in the results section of this thesis. This data clearly shows the relationship between relative affinities for the guanidinium peptoids and amine peptoids, with the guanidinium peptoids having a greater affinity. This greater affinity is presumably due to enhanced hydrogen bonding of the guanidinium groups to the anionic sites on heparin, as opposed to ammonium groups.

The results demonstrate that heparin affinity chromatography is very informative in demonstrating the ability of peptoids to bind to heparin, e.g., the results show that the longer the peptoid, the greater the binding affinity. The results also demonstrate the relative affinities of amine side-chain versus guanidinium side-chain bearing peptoids for heparin.

2.3.2. Materials and Instrumentation

Hydrated sodium monobasic and dibasic phosphate was purchased from EMD Chemicals. HiTrap Heparin HP (0.7 × 2.5 cm, 1.0 mL column volume) affinity columns with porcine heparin functionalized on 6% cross-linked agarose (average particle size was 34 μm) were purchased from GE Healthcare Biosciences. Sodium chloride, ACS grade, was purchased from Fisher Scientific. The instrument consisted of a combination of a Dionex AD20 absorbance detector, GP40 gradient pump and Dell optiplex GS system PC. Mobile phase A was pH 7.4 50 mM phosphate buffer and mobile phase B was pH 7.4 50 mM phosphate buffer with the addition of NaCl to provide a concentration of 1 M NaCl. A mobile phase flow rate of 0.65 mL /min was used. The gradient in the method began with 100% mobile phase A and 0% mobile phase B, and at the end of 60 min ended at 0% mobile phase A and 100% B although most of the peptoid runs were complete within 30 min or less.

2.3.3. Experimental Method

The Dionex HPLC was set up with the Hi-Trap heparin affinity chromatography column, a 200 μL sample loop, and prefiltered fresh mobile phases A and B. All peptoid solutions were 0.1 mM in the same buffer as was used in the ITC experiments and mobile phase A. Three runs were conducted and retention values that agreed within 0.5 min. The flow rate and parameters were set as described above in Materials and Instrumentation section 2.3.1. Injections were 200 μL of peptoid solution per run. Following each set of runs, the injection port was rinsed with deionized water. At the end

of a set of experiments, 20% EtOH in deionized water was injected into the column for 5 minutes before storage of the column in the refrigerator at 4 °C.

2.4 Circular Dichroism

2.4.1. Overview of Circular Dichroism

Circular Dichroism⁸ (CD) is defined as the unequal absorption of left-handed and right-handed circularly polarized light by a solution of a compound. CD is a particularly useful technique when the circularly polarized light is passed through a solution of chiral compound, which results in a differential absorption of the right and left polarized light. This differential absorption as a function of wavelength is presented as a CD spectrum, which provides insight into the secondary structure of proteins, peptides and also peptoids. Circular dichroism is a manifestation of optical activity in the vicinity of absorption bands. The amide bonds in the backbone of proteins, peptides, and peptoids absorb circularly polarized light in the region between 180-240 nm. In this range, there are three major absorptions due to transitions in the atomic and molecular orbitals. The longest wavelength absorption at 220 nm is known as the $n - \pi^*$ absorption and is due to the promotion of an electron from an amide oxygen nonbonding orbital to an antibonding orbital involving the oxygen, carbon and nitrogen of the amide bond. Two shorter bands are also seen in CD spectra of peptides and peptoids and are due to the splitting of a single absorption band related to the helical arrangement of the amide backbone. The band at the longer of the two wavelengths, seen at 204 nm, is known as the $\pi - \pi^*$ parallel

transition and is due to the polarized light parallel to the helix axis, and the other at 190 nm is known as the $\pi - \pi^*$ perpendicular transition and is due to the polarized light perpendicular to the helix axis⁹.

The CD instrument measures the difference between absorptions at a range of wavelengths set by the operator. The differential absorption is plotted on the y-axis as molar ellipticity θ_m , in units of degrees - cm²/dmol, defined as the angle, whose tangent is the ratio of the minor to major elliptical axis produced by the division of the two circular polarized components of plane polarized light. The division is accomplished by passage of a monochromatic polarized beam through a birefringent plate, which is a quarter wave plate that has two axis, such that each produces light with a different index of refraction.

This division results in a left (CP_L) and right (CP_R) circularly polarized light being produced. A_L is the absorption of the left and A_R is the absorption of the right circular polarized light.

The difference between the absorption of the two circular polarized lights is given by **Eq. 2.4.1**.

$$\text{Eq. 2.4.1} \quad \Delta A = A_L - A_R$$

Delta A can also be defined using Beers' law as shown in **Eq. 2.4.2**.

$$\text{Eq. 2.4.2} \quad \Delta A = (\epsilon_L - \epsilon_R)cl,$$

where ϵ_L and ϵ_R are the molar extinction coefficients for CP_L and CP_R, c is the concentration, and l is the path length (in cm). The quantity given by $\epsilon_L - \epsilon_R$ is $\Delta\epsilon$, the molar circular dichroism. As mentioned above, circular dichroism is measured in units of

degrees of ellipticity, which can be corrected for concentration by **Eq.2.4.3** to give molar degrees of ellipticity (θ_m).

$$\text{Eq. 2.4.3} \quad \theta_m = 100\Delta\epsilon \left(\frac{1\text{m}10}{4} \right) \left(\frac{180}{\pi} \right) = 3298.2 \Delta\epsilon,$$

In this form, θ_m is converted to degrees and is in the units that appear on the y-axis of a CD spectrum, i.e., degrees-cm²/dmoles, or deg-cm²/dmol.

2.4.2. Materials and Instrumentation

All the circular dichroism experiments were performed on a Jasco J-815 CD spectrometer attached to a Dell Celeron D P.C.. One mm quartz crystal QX cuvettes were purchased from Fisher Scientific Inc and used in the experiments. Nitrogen gas was used to purge the instrument for 5 minutes prior to and during the operation of the instrument to protect the optics and mirrors of the spectrometer

2.4.3. Method of Circular Dichroism

A volume of 2 mL of 200 μ M solutions of peptoids were prepared in deionized water. 300 μ L of solution was placed in the 1 mm cuvette and the CD spectrum was acquired using the following parameters: sensitivity = 100 mdeg; wavelength range was 240 nm – 190 nm; data pitch = 1nm, scanning speed = 100 nm/ min; scanning mode = continuous; response time = 1 sec; accumulations = 3. N₂ was used to purge the instrument at 20 psi for 5 min. before and throughout the operation of the spectrometer.

2.5. Time-of-Flight Matrix Assisted Laser Desorption Ionization Mass Spectrometry

2.5.1. Overview

In MALDI TOF mass spectrometry, the compound is embedded in a matrix, which in this study was α -cyano-4-hydroxycinnamic acid (CHCA), on a stainless steel sample stage. The CHCA and peptoid form a cocrystal mixture. The cocrystal mixture is then irradiated with a nanosecond laser beam pulse in the energy range of 1×10^7 - 5×10^7 W/cm². This causes desorption of the matrix/compound into a cloud, known as the plume and condensation of the compounds in the plume. Ions are extracted from the plume by an electric field. Following acceleration through the electric field, the ions travel through a field free path to a detector. By measuring the time of flight (TOF) of the ions to the detector, typically several milliseconds, the instrument converts this measurement to the ion mass (mass-to-charge ratio [m/z]).

2.5.2. Materials and Instrumentation

The following instrumentation in the UCR Mass Spectrometry facility was used to obtain MALDI-TOF spectra of all peptoids: A Voyager-DE STR Biospectrometry MALDI-TOF-MS Workstation, using a WinNT system, running PerSeptive Biosystems software. The matrix used was α -cyano-4-hydroxycinnamic acid (CHCA), which was obtained from Sigma-Aldrich. A 50:50 acetonitrile: methanol solvent with 0.1%

trifluoroacetic acid (TFA) was prepared. The methanol and acetonitrile were also purchased from Sigma-Aldrich.

2.5.3. Experimental Methods

The peptoid solution can be quite dilute and even as little as 3 μ L of sample collected from HPLC eluent can be sufficient to obtain a good MALDI-TOF mass spectrum. The molecular weight should be at least 350D in order to obtain a well defined signal in the noise resulting from the matrix. An example of a MALDI mass spectrum is shown in **Fig. 2.5.1**. A 200 μ L of a 50:50 mixture of acetonitrile and methanol with 1% TFA was placed in a 0.5 mL Eppendorf vial along with a small amount of CHCA to produce a saturated solution, which was then vortexed briefly before centrifuging. 9.0 μ L of this solution, which contains the excess yellow solid CHCA at the bottom of the vial, was transferred by micropipette to another Eppendorf vial along with 2.0 μ L of the peptoid solution. 1.5 μ L of this mixture was dotted onto the sample stage in three drops, which were allowed to completely dry before measuring the mass spectrum. The mass spectrum was measured by placing the sample stage in the Voyager-DE STR Biospectrometry MALDI-TOF-MS Workstation and the sample was analyzed using PerSeptive Biosystems software running on a WinNT system.

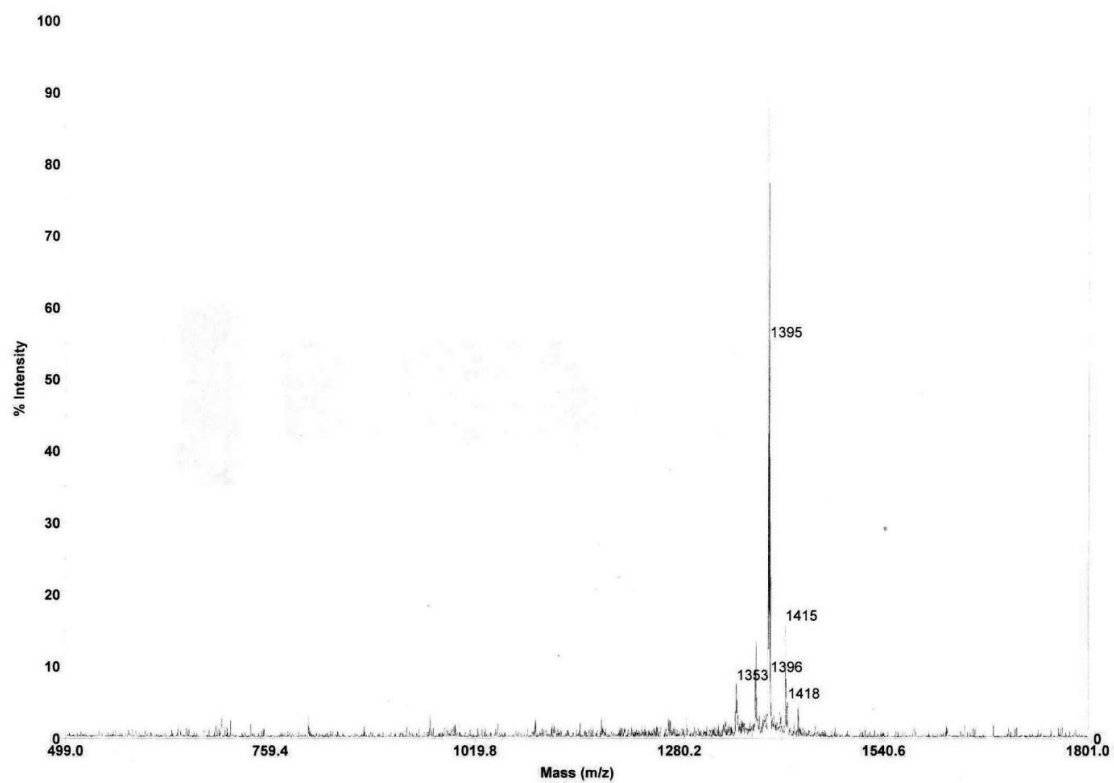


Fig. 2.5.1. MALDI-TOF mass spectrum of the peptoid H-[N(Cad)G-N(Bu)-N(spe)]₃-NH₂. The calculated mass of the peptoid is 1394 m/z. The major peak above is within the error range of +/- 1 m/z.

2.6. High Performance Liquid Chromatography

2.6.1. Overview of HPLC

High Performance Liquid Chromatography (HPLC) is also sometimes known as High Pressure Liquid Chromatography because, unlike manual chromatography, high pressure pumps are used to move the mobile phase through a premanufactured column. In normal phase HPLC, silica of a specific pore size and density is loaded into the column and for many years, this was the standard method used in the industry. In normal phase HPLC, the mobile phases are two organic solvents, one more hydrophobic such as hexanes, and the other somewhat more hydrophilic, typically ethyl acetate much as is used in thin layer chromatography (TLC).

While normal phase HPLC is useful for separations of small organic compounds just as in TLC, larger biological compounds such as peptides and peptoids are more effectively separated and purified using reverse phase HPLC. In reverse phase HPLC, the stationary phase is a hydrophobic material, while the mobile phases consist of very hydrophilic solvents, typically Millipore filtered water with 0.07% TFA added for the extremely hydrophilic phase and acetonitrile also with 0.07% TFA added. The column stationary phase used most often for peptide and peptoid separations is C18, which denotes octadecyl silane which has 3 C₁₈H₃₇ hydrocarbon chains bonded to a central atom of silicon. In reverse phase HPLC, more polar compounds elute first, while the more hydrophobic and also larger compounds elute later in the chromatographic run.

Following elution from the column, the compound, also known as the analyte is detected by a UV detector, which can be programmed to detect specific wavelengths. In the case of peptides and peptoids, the detector is typically set at 215 nm, the chromophore of the backbone amide bond. In the synthesis of peptoids or peptides, there are always deletion sequences present, because each step in the overall synthesis is less than 100% efficient. These deletion sequences should be shorter as will be any small molecule organic compounds, and will elute prior to the target peptoid. In the HPLC separation for a good synthesis, the main peak, which can be easily analyzed off-line by MALDI-TOF mass spectrometry, will be the major peak. In a first run of an unfamiliar compound, it was typical to obtain the mass spectrum of the major peak before continuing a run, however after multiple syntheses of the same compound it was usually reasonable to collect the main peak and analyze it afterwards, if it had the expected retention time and the shape of the peak was sharp.

2.6.2. Materials and Instrumentation

The following materials and their sources were used for purification of crude peptoids by HPLC. All solvents and solutions were HPLC grade or in the case of aqueous solutions were filtered through Millipore filters to eliminate solid particles thus avoiding potentially clogging the column. Peptoid solutions were prefiltered through a Millipore 10 µm pore size syringe filter. The acetonitrile was purchased from Sigma-Aldrich. 2.7 mL of trifluoroacetic acid (TFA) was added for every 4 L of acetonitrile to produce a 0.07% solution for mobile phase B, while the same volume of TFA was added to 4 L of

Millipore filtered water for mobile phase A. The TFA was purchased from Impex International Inc. The TFA is used to control the pH in reverse phase when there are ionizable compounds and impurities present.

The following HPLC instrumentation was used throughout the purification of all peptoids. Varian Prostar model 210 pumps were used with a model 320 uv detector. The column used was a reverse phase Waters sunfire Prep C18, optimum bed density 5 μm 19X250mm length (Model 186004027). A Guard column from Waters (model 186002569 and holder model 186007090) were used to protect the main column from particulate impurities.

2.6.3. Experimental Methods

In the purification of all the peptoids synthesized in this research, following synthesis and cleavage, the solvent was removed under high vacuum at 40 °C and the residue was taken up in Millipore filtered water and a small volume of methanol, which was used to get the last of the residue of the peptoid from the glassware. The solution was typically brought up to a total volume of 6 mL. The addition of the methanol also helped to clear the solution, which was then filtered through a syringe filter in order to protect the guard and main column from particles which would clog the columns. The mobile phases were also prefiltered prior to use for the same reason. Before a run the mobile phase was degassed for 10 minutes and a prerun of 40 minutes was conducted to check for and produce a clean baseline. The gradient was set for a starting point consisting of 100% mobile phase A and mobile phase B was increased at the rate of 2% per minute at a flow

rate of 10 mL/ minute. Depending on the length of the peptoid or if it was guanidylated, the retention time was anywhere from 16 min for a 3-mer to 30 minutes for a 12-merG.

For guanidylated peptoids, there was always a large peak at 8-10 min. corresponding to bi-products of the synthesis such as excess reagents or the pyrazole leaving group produced in the S_N2 reaction after the guanidine portion of the molecule was attached to the primary amines. Since the major peak was always found to be the guanidylated product typically in good yield, no attempt was made to determine the exact identity of the side product. Following separation of each peptoid, the inlet port was injected with 0.5mL of Millipore-filtered water to clean the port and mobile phase B was changed to column wash, which was 50:50 Millipore-filtered water and acetonitrile with no TFA added. The program was set on column wash, which consisted of 100% B for 60 min. at 4 mL/min. before turning off both pumps and the detector.

2.7 Lyophilization

2.7.1. Overview

Lyophilization is the process of freeze drying a compound under high vacuum. The temperature must be low enough, typically below $-55\text{ }^{\circ}\text{C}$, and the vacuum must be without any leaks in order to obtain a properly lyophilized sample. If not, the sample will consist of an oily residue. A properly lyophilized sample will either be crystalline or fluffy in consistency. The sample must also be pre-frozen in aqueous solution in either dry ice or liquid nitrogen.

2.7.2. Materials and Methods for Lyophilization

For lyophilization, the following materials and instrumentation were used: A Labconco Freezone 2.5 attached to a standard high vacuum pump. Since the lyophilizer was designed only for the removal of water but not organic solvents, which require an additional level of refrigeration, no inline Dewar cold trap was necessary between the lyophilizer and the pump. All seals were coated with heavy petroleum grease to prevent leakage and all connecting hoses were sealed with metal screw tighteners. All samples were pre-frozen in dry ice. The Labconco Freezone 2.5 used in this research requires that only aqueous solutions of peptoids be used. This is due to the lack of an extra refrigeration stage. The Labconco Freezone 2.5 would be damaged by the introduction of organic solvents.

2.7.3. Experimental Methods

All peptoid samples were pre-evaporated under high vacuum to remove HPLC solvents. The peptoid TFA salt was evaporated in a small vial with a rubber septum, which fit into a 19/22 adapter on a rotovap, perforated with a syringe needle placed slightly through the septum. This arrangement allows the vial to act as a flask and will rotate while under high vacuum in a hot water bath set to no higher than 40 °C. The residue, now free of HPLC solvents, was taken up in 1 mL of deionized water and the vial was placed in finely shaved dry ice with a parafilm seal and 4 small holes placed by syringe needle. When the solution was completely frozen solid, it was placed on the lyophilizer over night. Typically the peptoid yields were in the range of 50-60mg. Since

the rink amide resin has a loading of 0.56 mmole/g, for a 9mer, starting with 0.200g of resin, 60mg gives a yield of 35%. This is quite acceptable and was sufficient to allow half of the peptoid to be converted to the guanidylated form. The guanidylated peptoids were worked up in the same way as the primary amine-bearing peptoids and ultimately lyophilized in the same way.

2.8. Solvent Evaporation under High Vacuum by Rotovaporation

2.8.1. Overview

The rotovaporator is a simple device in principle but of great value in preparatory scale synthesis, where pure compounds are isolated by HPLC because a complete purification by HPLC can produce sample-containing volumes as high as 200 mL. It is essential when rotovaping solvents such as acetonitrile, methanol and especially water, that a good high vacuum pump is used and that all joints except the last one closest to the adaptor to the round bottom flask or vial, be properly greased with stopcock grease. The coils in the condenser stage are circulated with a submersible pump placed in ice water. In this way even water can be removed from a solution of a peptoid TFA salt at 40 °C.

2.8.2. Materials and Instrumentation

All solvents were evaporated before lyophilization, since the Labconco Freezone 2.5 lyophilizer is designed for aqueous solvent removal only. The following equipment and accessories were used to remove all solvents by rotovaporation prior to lyophilization: A

Buchi model RE 121 rotovaporator with a Buchi 461 waterbath with high vacuum pump, solvent protected by a cold trap filled with acetone and dry ice. The coolant consisted of ice water pumped through the coils by means of a submergible pump.

2.8.3. Experimental Method.

The peptoid TFA salt solutions were evaporated as follows. The HPLC solvents were placed in a round bottom flask with a 14/22 fitting. It is important that the solution to be evaporated is not overfilled in the round bottom flask or bumping may occur. Typically the rule is never fill the flask with more than 1/3 to 1/2 full. The hot water bath is adjusted to 40 °C, to avoid deterioration of the peptoid. The spinning rotor is turned on and adjusted to medium in order to coat the inside surface with solvent, which aids in the evaporation process. The pump is turned on and the inlet valve is set to open atmosphere and the operator places their finger over the opening to control the vacuum entering the system until the round bottom flask is coated with condensation. At this point, the solution is degassed enough to be stable and the valve can be closed to atmosphere and high vacuum is applied.

Normally the process must be halted more than once to refill the round bottom flask until all of the solvent has been evaporated. Following evaporation of most of the solvent, the operator tests the outside surface of the spinning round bottom flask. If it is still cold to the touch, then further evaporation is necessary. Only when the flask is room temperature is the process complete and the system can be shut down after carefully opening the inlet valve to atmospheric pressure. After rotovaporation, lyophilization is

the final step before the samples were weighed, analyzed by MALDI TOF MS and stored in a refrigerator at 4 °C.

2.9. References

1. Zuckermann, R. N., Kerr, J.M., Kent, S.B, Moos, W.H. *J. Am. Chem. Soc.* **1992**, *114*, 10646-10647.
2. AAPPTEC. <http://www.rinkamideresin.com/> **2011**.
3. ChemPep. Inc. <http://www.chempep.com/> **2011**
4. Barron Research Group, Dept.of Chemistry, Stanford University, **2011**
5. Bernatowicz, M. Wu, Y., Matsueda, G. *J. Org. Chem.* **1992**, *57*, 2497-2502.
6. Haines Inc. <http://www.hastalloy.com/> **2011**
7. Microcal:G.E.;Healthcare. <http://www.microcalorimetry.com/> **2011**.
8. Greenfield, N. J. *Nat Protoc.* **2006**, *6*, 2876–2890.
9. Beychok, S. *Science* **1966**, *154*, 1288-1299.

Chapter Three:

The Effect of Chirality and Length of Peptoids on Heparin Binding Affinity

3.1. Introduction

All of the peptoids synthesized in this study were designed with specific considerations, each of which was varied to determine the effect of the design feature on the binding of peptoids to heparin. The general sequence for all peptoids synthesized was based upon a repeating trimer sequence. For the initial phase of the research, this general sequence was $H-[N(R_1) - N(R_2) - N(R_3)]_n-NH_2$, where $n = 1 - 4$, and R_{1-3} were side chains attached to the nitrogens of the amide backbone.

For the results presented in this chapter, R_1 consisted of $CH_2CH_2CH_2NH_3^+$ to mimic the amino acid ornithine. The purpose of the cationic ammonium group of R_1 is to bind to the anionic sulfonic acids and esters of heparin through electrostatic attraction and hydrogen bonding. By locating the ammonium-bearing side chain on every third monomer, the peptoid was designed to align the cationic groups along one face of the peptoid helix, which was expected based upon principles discussed in Chapter One. The central monomer side chain R_2 is $-C_nH_{2n+1}$, which acted as a linking spacer between the monomer unit with the cationic side chain and the monomer with side chain R_3 , which is a chiral side chain consisting of either *spe* or *rpe*, which are expected to cause the peptoids to adopt a right handed or left handed helix, respectively.

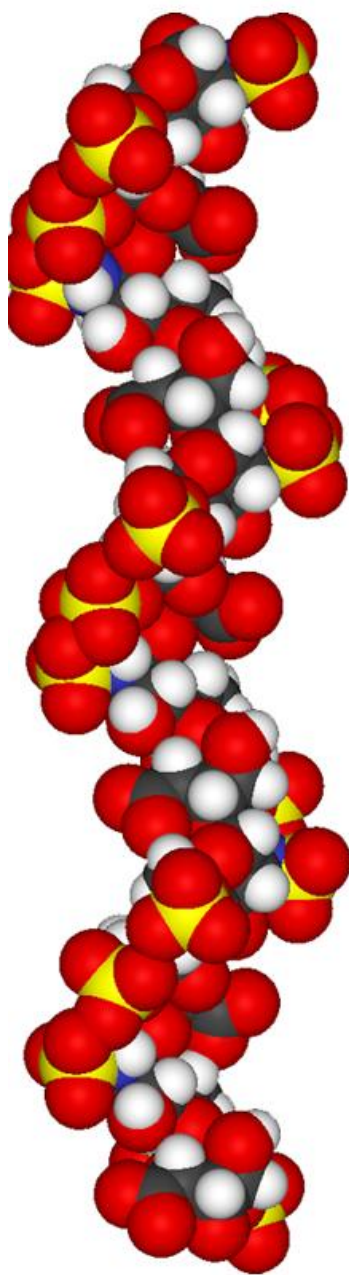


Fig. 3.1.1. Linear helical structure of heparin, where oxygen is shown in red, sulfur is shown in yellow, black is carbon and blue is nitrogen. Molecular surface maps of heparin also show a groove that wraps around the helix of the structure as will be seen in Chapter 6 regarding computer docking studies.

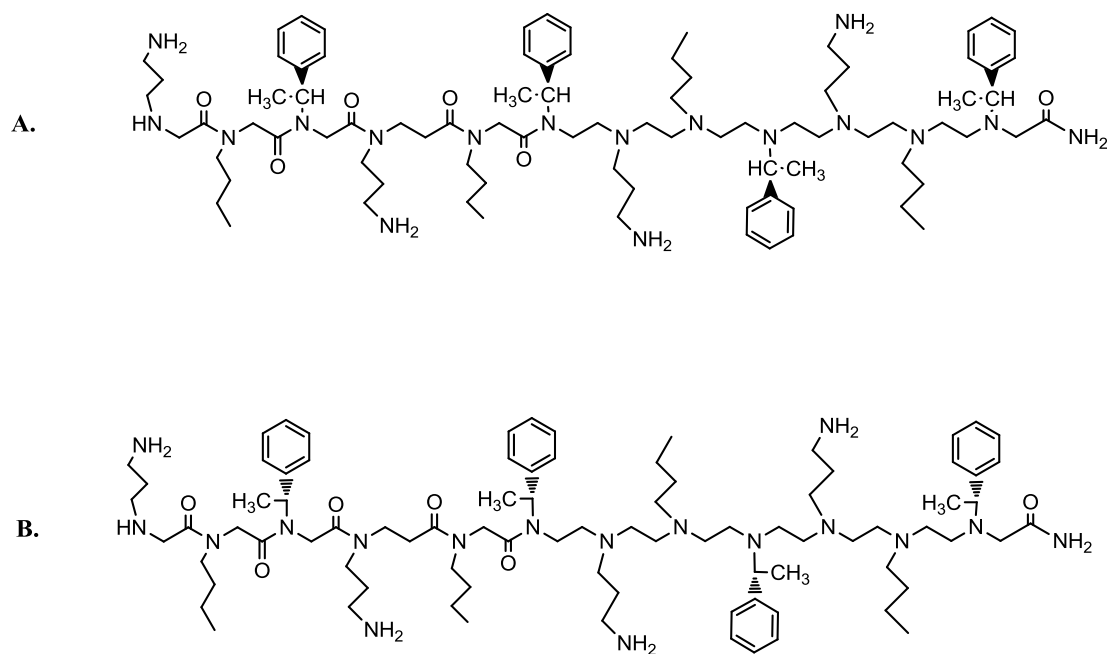


Fig 3.1.2. Structural formulas of the peptoids, **A.** H-[N(Orn)-N(Bu)-N(spe)]₄-NH₂ and **B.** H-[N(Orn)-N(Bu)-N(rpe)]₄-NH₂.

It is possible that the handedness of the peptoid helix, i.e., left-handed helix versus right-handed helix, might affect the binding affinity since heparin has a linear helical structure as can be seen in **Fig. 3.1.1**. The disaccharides can be seen alternating from side-to-side. To determine if the handedness of the peptoids affects the binding affinity for heparin, the two 12-mer peptoids were synthesized and CD spectra were taken. The sequences of the S-12-mer and R-12-mer (shown in **Table 3.1.1** and **Fig. 3.1.2**) are expected to form helices with opposite handedness.

The chiral rpe and spe side chains are expected to cause the peptoids to form helices of opposite handedness, left-handed and right-handed, respectively. The chirality of the peptoids was studied by CD spectroscopy, and their heparin binding affinities were determined by measuring binding constants by ITC. Their relative heparin binding affinities were also studied by heparin affinity chromatography.

In the second phase of the research presented in this Chapter, the effect of peptoid length on the heparin binding affinity for the family of peptoids: H-[N(Orn)-N(Bu)-N(spe)]_n-NH₂, where n = 1-4, was studied. As the length of the peptoid increases, the number of cationic ammonium binding sites increases.

3.2. The Effect of Chirality on Heparin-Binding Affinity

3.2.1. Determination of the Chirality of the Peptoids

To determine if the spe and rpe containing peptoids adopt helical structures of opposite handedness, CD spectra were measured for the two peptoids in **Fig 3.1.2**. The

Peptoid	Sequence
S12-mer	H-[N(Orn)-N(Bu)-N(spe)] ₄ -NH ₂
R12-mer	H-[N(Orn)-N(Bu)-N(rpe)] ₄ -NH ₂

Table 3.1.1. The two chiral 12-mer peptoids used in the initial study on the effect of chirality on handedness and heparin affinity.

CD spectra for the two chiral 12-mers are presented in **Fig 3.2.1**. As can be seen, the spectropolymers containing peptoid displays double minima due to the $n - \pi^*$ and $\pi - \pi^*$ transitions described in Chapter Two.

Also, as can be seen in **Fig 3.2.1**, the two chiral analogs give CD spectra that mirror each other. The spectra indicate that both peptoids possess helical secondary structures. As was mentioned above, any helix, regardless of which type, gives a CD spectrum with absorptions displayed either as a double minimum or a double maximum absorption, depending on the handedness of the helix. As discussed in Chapter 2, these two absorptions are due to electron transitions ($n - \pi^*$ and $\pi - \pi^*$ parallel transitions) both related to backbone-amide bonds that are common to the helices of all peptoids, peptides and proteins.

Secondly, one can derive from **Fig 3.2.1**, the handedness of the two chiral analogs¹. CD spectra for helices that are right-handed display the double minima, while left-handed helices display a double maxima in the same region. From **Fig 3.2.1** it can be seen that the S-analog (shown in blue) is due to a right-handed helix, as the correlation between helix handedness and CD spectra was previously determined by Beychok in the 1966². Right-handed helices for peptides, proteins and peptoids, all display a double minima spectra as does the S-analog shown (in blue) in **Fig 3.2.1**. The CD spectra of the R-analog is consistent with a left-handed helix which is shown in red. It also will be shown to bind through a different binding modality in the computer docking study in Chapter Six.

3.2.2. Determination of the Effect of Chirality on Heparin Binding Affinity

The heparin binding affinity of the S and R 12-mer analogs was obtained through ITC. In section **3.2.2.1**, the ITC data will be presented along with the raw data and integrated titration curves. The two analogs display opposite enthalpy and the entropy of the S analog is higher. This suggests that in the case of the S analog, the reaction is driven by entropy. In the case of the R analog the reaction appears to be driven paradoxically by enthalpy.

3.2.2.1. Determination of Binding Constants by Isothermal Titration Calorimetry

While CD spectra indicate that the chirality of the side chains causes the peptoids to have helical secondary structure of opposite handedness, the most important aspect that chirality had on the peptoids, for the purposes of this research, was binding affinity of chiral peptoids to heparin. The binding affinity was studied by measuring binding constants using isothermal titration calorimetry. The ITC titration data for titration of the S12-mer peptoid with heparin is presented in **Fig. 3.3.2**; the titration curve obtained by integrating the area under each peak is presented in **Fig. 3.2.3**, together with the thermodynamic parameters for S12-mer-heparin binding obtained by fitting the titration with the one binding site model. The analogous titration data and titration curves are presented in **Figs. 3.2.4** and **3.2.5**. It is immediately apparent from the titration data that the binding of the S12-mer is endothermic while the binding of the R12-mer is exothermic.

The binding constants and thermodynamic parameters for the binding of the two 12-mers as determined by ITC are given in **Table 3.2.1**. The data represents the results of three titrations for the S12-mer analog and two titrations for the R12-mer analog. For the S12mer, values are given as the mean \pm mean % st. dev. For the R12-mer the values are given as the mean value and the range. The value of Gibbs free energy, ΔG was calculated from **Eq. 2.2.1**, i.e., $\Delta G = -RT\ln K_b$, using the mean values in the table, and $R = 1.986 \text{ cal}^\circ\text{K}^{-1}\text{mol}^{-1}$, and $T = 298 \text{ }^\circ\text{K}$.

The binding constants presented in **Table 3.2.1**, along with binding constants obtained from previous research in this laboratory³, indicate that peptoids that contain a side chain of S chirality bind more tightly. Thus, all peptoids used in the remainder of this research were then designed using spe in the chiral positions, which resulted in right-handed peptoids.

3.2.2.2. Determination of Relative Affinities by Heparin Affinity Chromatography

In addition to ITC, heparin affinity chromatography (HAC) was also performed on the S and R 12-mers to determine relative heparin binding affinities. The retention times are presented in **Table 3.2.2**. For each of the two analogs, three trials were conducted. The data are given as mean values \pm standard deviations.

As can be seen from the data in **Table 3.2.2**, the S peptoid had a higher retention time which indicates that the S peptoid has a higher heparin affinity than the R peptoid. **Figs. 3.2.6** and **3.2.7** are representative HAC plots for the two chiral peptoids.

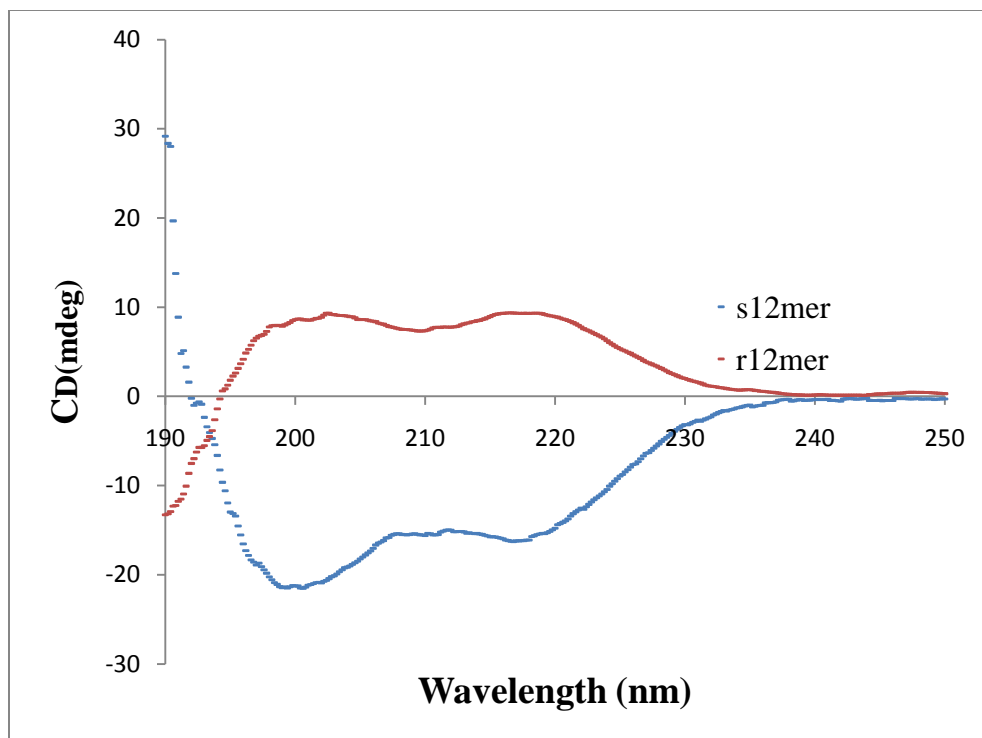


Fig 3.2.1. CD spectra for the S12-mer peptoid analog (shown in blue), and the R12-mer analog (shown in red). The two curves produced by the CD spectra mirror each other and are indicative of a right and left-handed helix respectively.

This data supported the decision to use spe as a chiral side chain in all subsequent peptoids studied in this dissertation research.

3.2.3. Discussion

The ITC and HAC data for the S 12-mer and R 12-mer chiral peptoids indicate that the S 12-mer has a higher heparin binding affinity. Thus spe was used for the chiral side chain in all the other peptoids studied in this dissertation. The results of computational docking studies of the binding of spe-containing and rpe-containing peptoids are presented in Chapter Seven

3.3 Effect of Peptoid Length on Heparin Binding Affinity.

Following the fundamental choice of the chiral side chain to be used in the design and synthesis of the peptoids in this research, the next design variable to be explored was the effect of length of peptoids, and therefore the number of binding sites per peptoid on heparin binding affinity. To investigate the effect of length, and thus the number of cationic side chain binding sites, on heparin binding affinity, the binding of the series of peptoids $H-[N(\text{Orn})-N(\text{Bu})-N(\text{spe})]_n\text{-NH}_2$, where $n = 1-4$, was studied. In this series, the number of ammonium groups varies from one to four. The structures of the peptoids studied in this series is shown in **Fig. 3.3.1.**

Peptoid	N	K _b (M ⁻¹)	ΔH(cal/mole)	ΔS(cal/mole- °C)	ΔG(cal/mole)
S-12-mer	19.48 ± 2.68	2.33X10 ⁵ ± 37950	1733 ± 46.96	30.53 ± 0.31	-6309
R-12-mer	16.26 ± 0.9	1.28X10 ⁵ ± 74410	-1278 ± 379	19.01 ± 2.46	-6956

Table 3.2.1. Binding constants and other thermodynamic parameters determined for the chiral 12-mer analogs by ITC. The S12-mer data represents 3 trials, and the R12-mer represents 2 trials. Values for the parameters K_b, ΔH, and N are obtained by fitting the titration curves. ΔG is calculated from $\Delta G = -RT\ln K_b$ and ΔS is calculated from $\Delta G = \Delta H - \Delta S$.

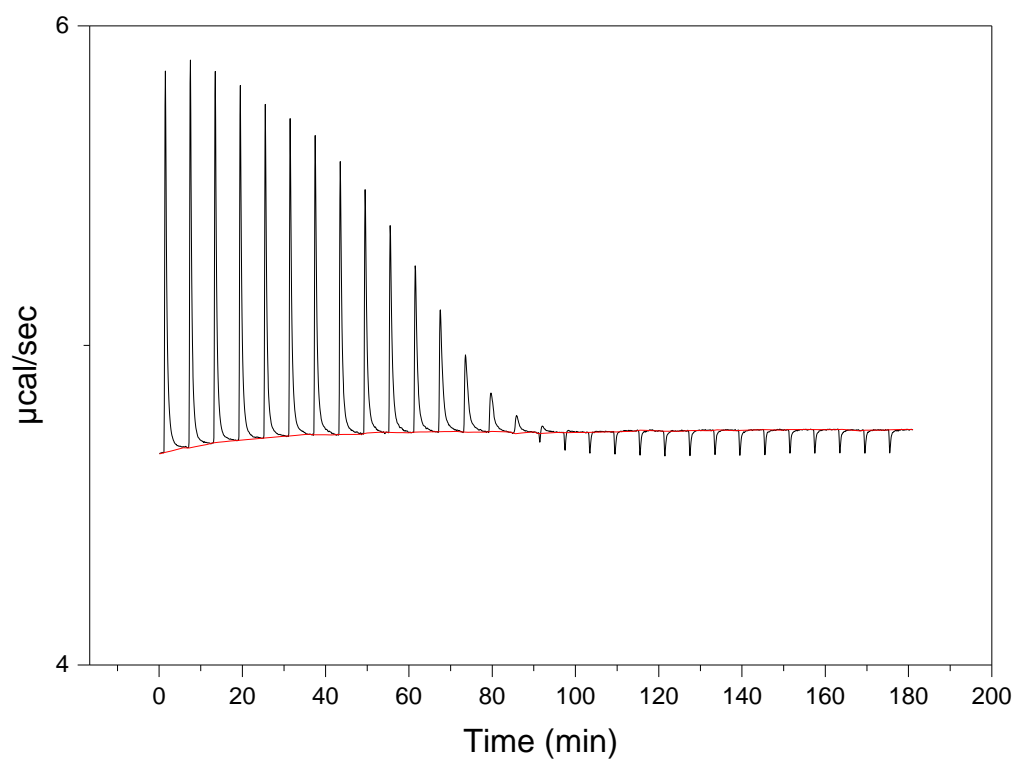


Fig. 3.2.2. Raw ITC titration data for the S-12mer. The spikes point upward after the addition of each aliquot of titrant, indicating an endothermic binding event.

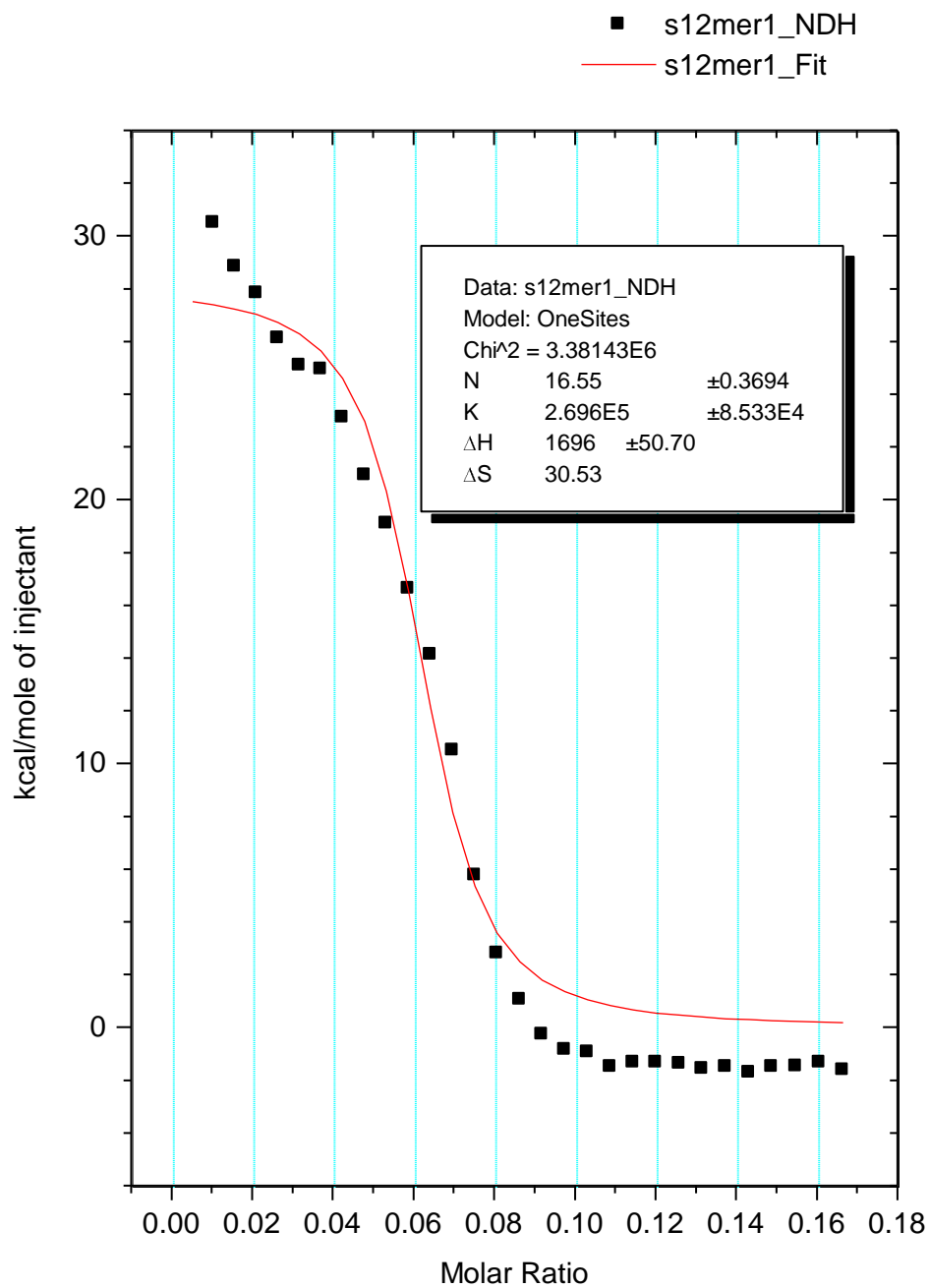


Fig. 3.2.3. Titration curve for the S-12mer, obtained by integrating the area under each peak of the raw data in **Fig. 3.2.2.** As can be seen from the thermodynamic parameters shown in the inset box, the ΔH is positive, which is indicative of an endothermic binding event.

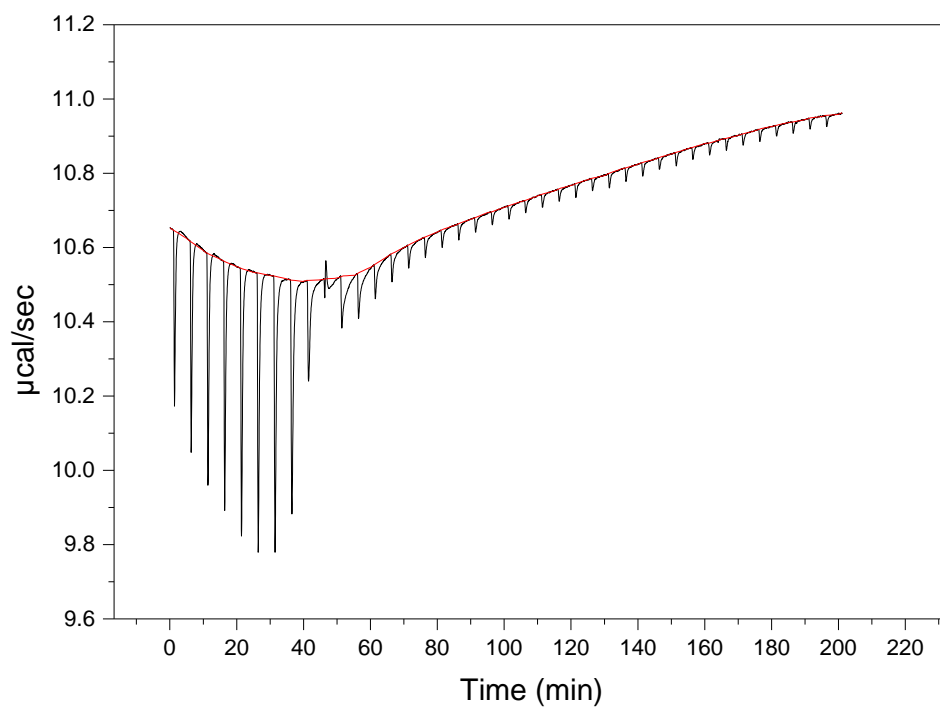


Fig.3.2.4. Raw ITC titration data from the R analog of the 12-mer. The enthalpy is exothermic as can be see by the downward spikes. The baseline drifted during the titration due to an unknown effect.

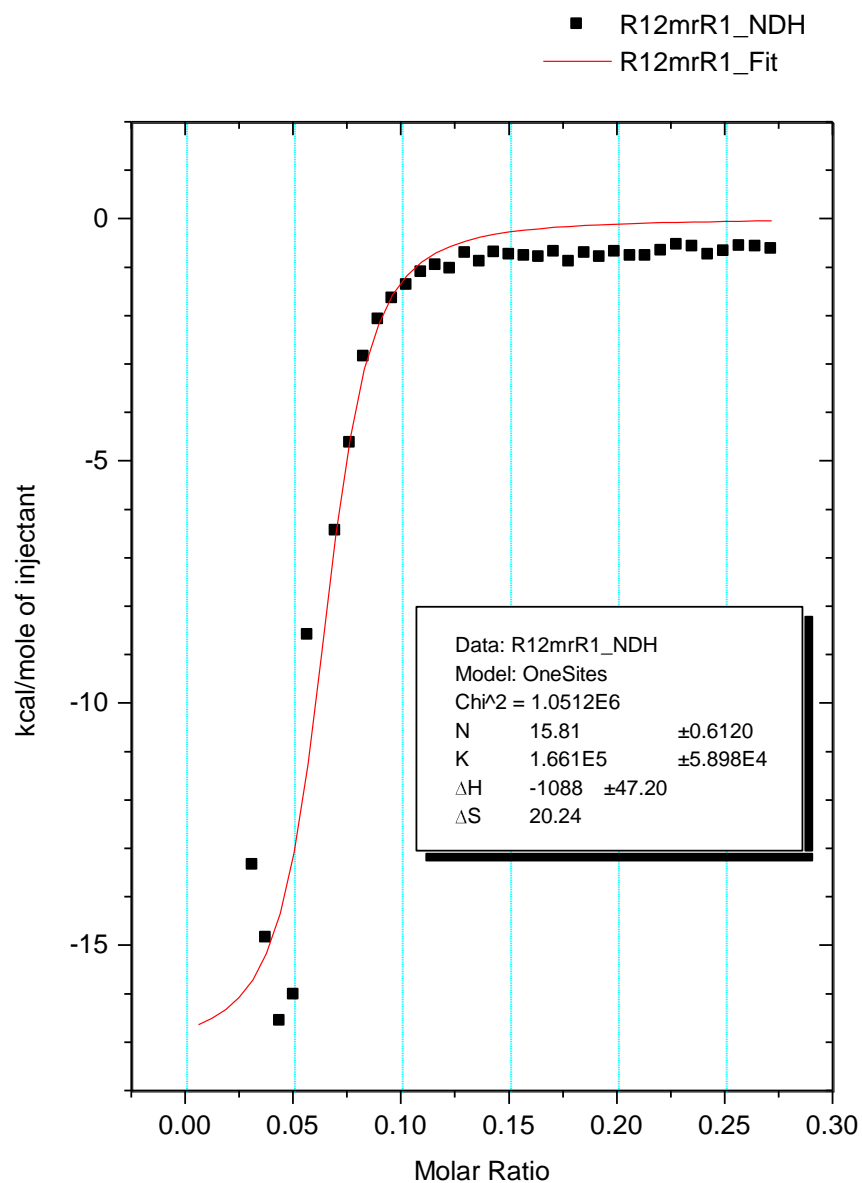


Fig. 3.2.5. Titration curve for the R analog of the 12-mer, obtained by integrating the area under each peak of the raw data in **Fig. 3.2.4.** The negative enthalpy is indicative of an exothermic binding event. The binding constant is also slightly lower than that for the S analog.

Peptoid	mean HAC Ret. Time \pm st. dev.
S12-mer	21.6 min. \pm 0.6
R12-mer	18.5 min. \pm 0.6

Table 3.2.2. Heparin Affinity Chromatography Retention times for the chiral 12-mer analogs. The mean retention times were derived from triplicate runs.

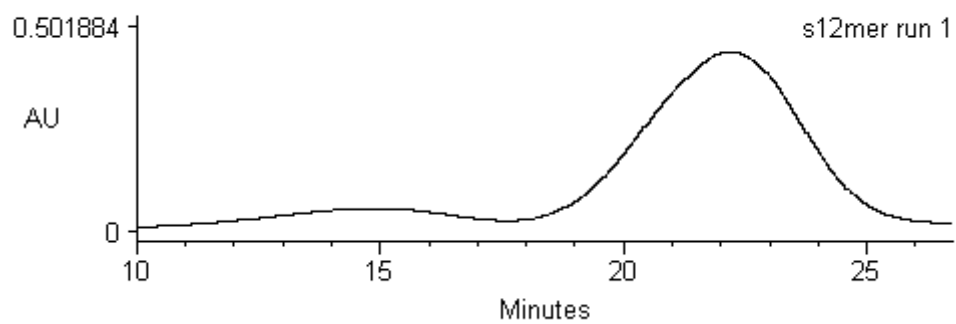


Fig. 3.2.6. Heparin Affinity Chromatogram for the S12-mer analog, i.e., H-[*N*(Orn)-*N*(Bu)-*N*(spe)]₄-NH₂. This one of three trials shows a retention time of 22 minutes, which is approximately 4 minutes greater than that for the R12-mer analog.

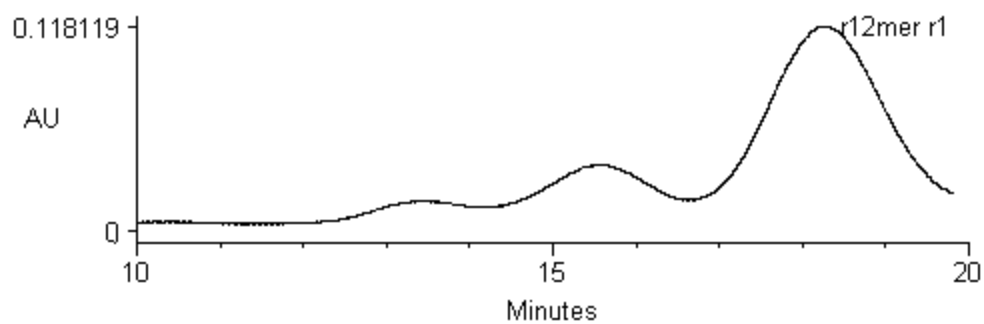


Fig. 3.2.7. Heparin Affinity Chromatogram for the R12-mer analog, i.e., H-[N(Orn)-N(Bu)-N(rpe)]₄-NH₂. This trial shows a retention time of 18.2 minutes. The second smaller peak at 15.5 min. is due to an unknown impurity.

3.3.1. Determination of Binding Constants by ITC

It was not possible to determine binding constants for all four of the peptoids by ITC. Peptoids with less than nine monomer residues, e.g. the s3-mer and s6-mer, did not possess sufficient binding affinity to yield useful data. Examples of the raw data and associated titration curves are presented in **Figs. 3.3.2 – 3.3.9**, but only the data for the peptoids where $n = 3$ and 4 was used. Fortunately this situation did not arise when using heparin affinity chromatography. All peptoids yielded good retention times. The HAC retention times were then converted into estimated binding constants using a calibration curve based upon the natural log of K_b versus HAC retention times for eight peptoids as will be discussed in Chapter Five. This method yielded data used in this Chapter for the four peptoids studied.

The four ammonium-bearing spe-containing peptoids shown in **Fig.3.3.1**, yielded the following four ITC titration curves for each of the peptoids along with the raw data. The first set consists of the raw data and integrated curves for the s3-mer peptoid and is presented in **Figs. 3.3.2 and 3.3.3**.

The binding constants for the two larger peptoids is presented in **Table 3.3**. As can be seen from the table, the s12-mer has a greater binding affinity to heparin in comparison to the s9-mer. This is expected as the longer the peptoid, the greater the number of binding sites.

3.3.2. Determination of Relative Heparin Binding Affinities by Heparin Affinity Chromatography

Heparin affinity chromatograms for the ammonium-bearing peptoids from 3 to 12 monomer units in length is shown in **Fig 3.3.10**. The mean retention times from three trials for each peptoid, in **Table 3.4**, are presented along with standard deviations. **Fig 3.3.11** presents the data in graphical format. The plot is HAC mean retention times on the vertical axis versus the number of monomer units on the horizontal axis in units of 3. The linear relationship between length of peptoid and HAC retention times is evidenced by the coefficient of determination, $R^2 = 0.98$. The coefficient is very close to unity, which is a good indication of linearity. This correlation is logical since the greater the length of the peptoid, the greater the number of binding sites.

The last important issue to consider is the endothermic nature of the S-analog compared to the exothermic nature of the R-analog. When one considers that the entropy of the S peptoid-heparin interaction is higher than the R form, it becomes apparent that this binding event is entropically driven while the R peptoid-heparin interaction is enthalpically driven. The larger positive enthalpy of the S form and larger entropy changes in this case are hypothesized by this researcher to be due to the possible release of ordered water molecules or Na^+ ions and the associated entropy gain is due the difference in secondary helical structure. The computational study of these two chiral peptoids do not bind in quite the same way. The R form is loosely bound with a different set of dihedral cis and trans amide bonds.

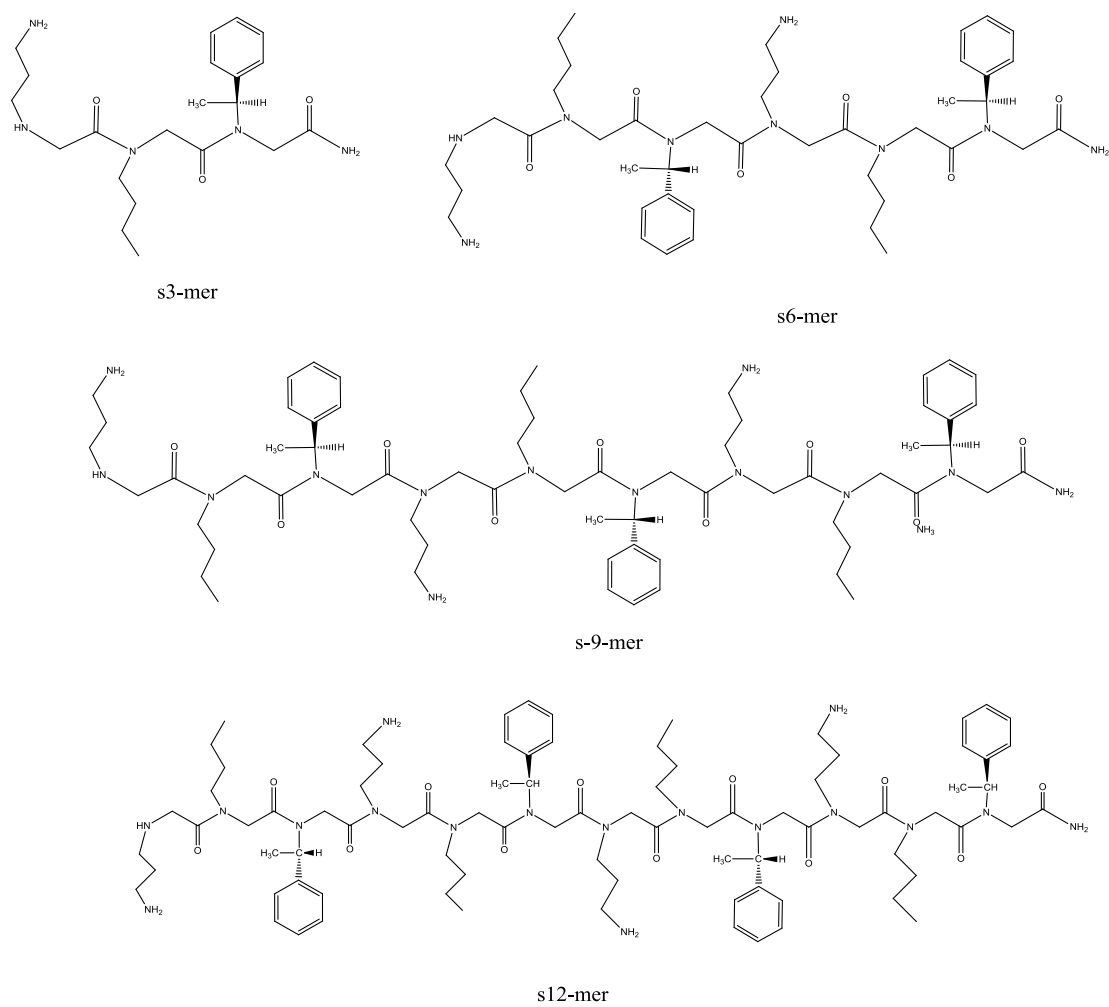


Fig.3.3.1 Structures of the peptoids $H-[N(\text{Orn})-N(\text{Bu})-N(\text{spe})]_n-\text{NH}_2$ where $n=1-4$.

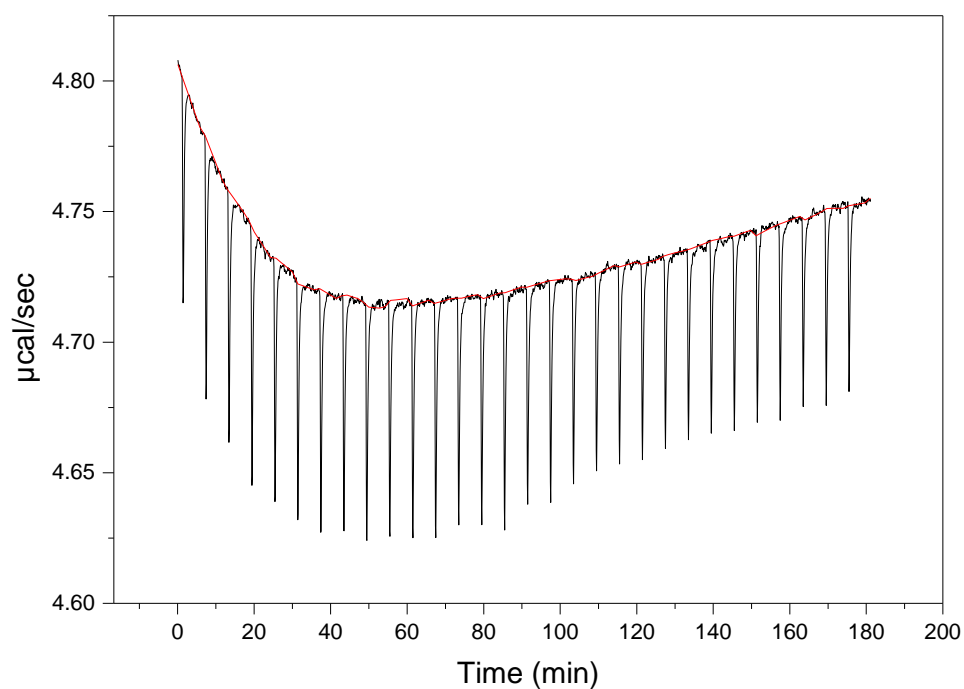


Fig. 3.3.2. Raw ITC titration data for the s3-mer analog. One of the problems that plagued the ITC data too often was uneven baselines. The reason behind this anomaly was never determined. One possible hypothesis was that uneven air flow caused by the air conditioner might contribute to the problem. To combat this potential problem, a cardboard box was placed over the ITC instrument during titrations. Some improvement in the results of the titration curves was observed, but the difference was slight at best.

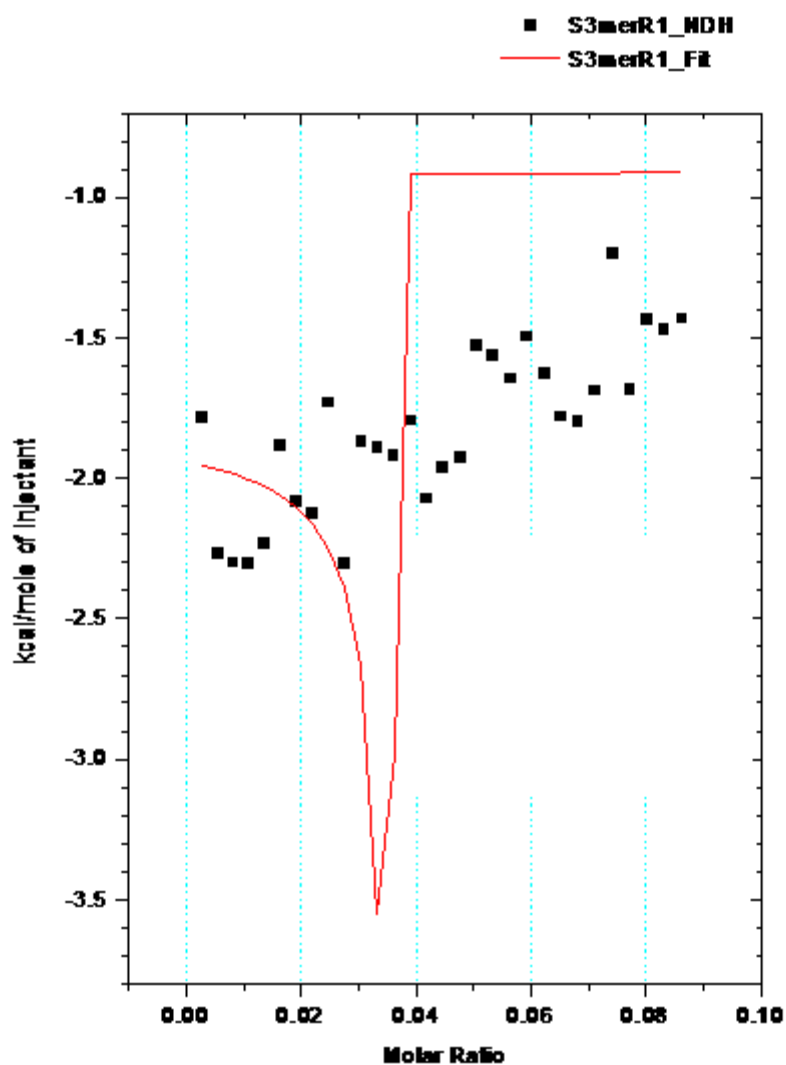


Fig. 3.3.3. The titration curve obtained by integration of the raw data presented in the preceding figure for the s3-mer peptoid. The data do not give an S-shaped titration curve for a binding interaction of sufficiently large K_b to be quantitatively characterized by ITC. The concentration for the peptoid in this run was 0.363 mM and the heparin concentration was 0.235 mM.

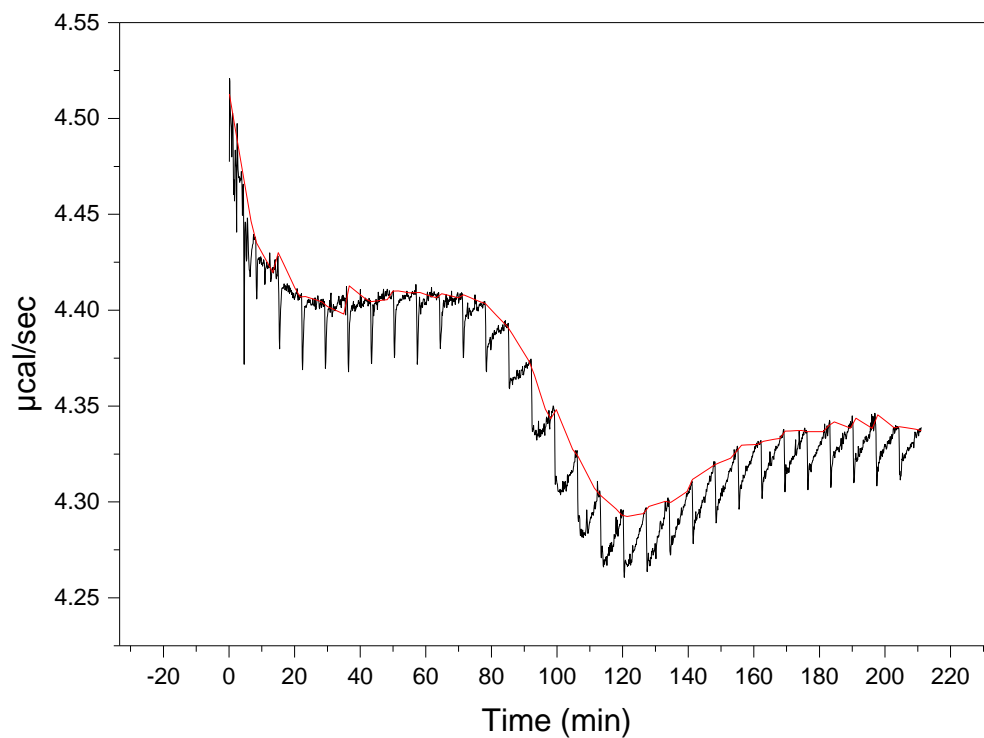


Fig. 3.3.4. Raw ITC titration data for an s6-mer, H-[N(Orn)-N(Bu)-N(spe)]₂-NH₂ displaying a drifting baseline. The concentrations were peptoid = 0.1 mM and heparin = 0.125 mM. Following integration, the titration curve shown in **Fig. 3.2.5.** resulted.

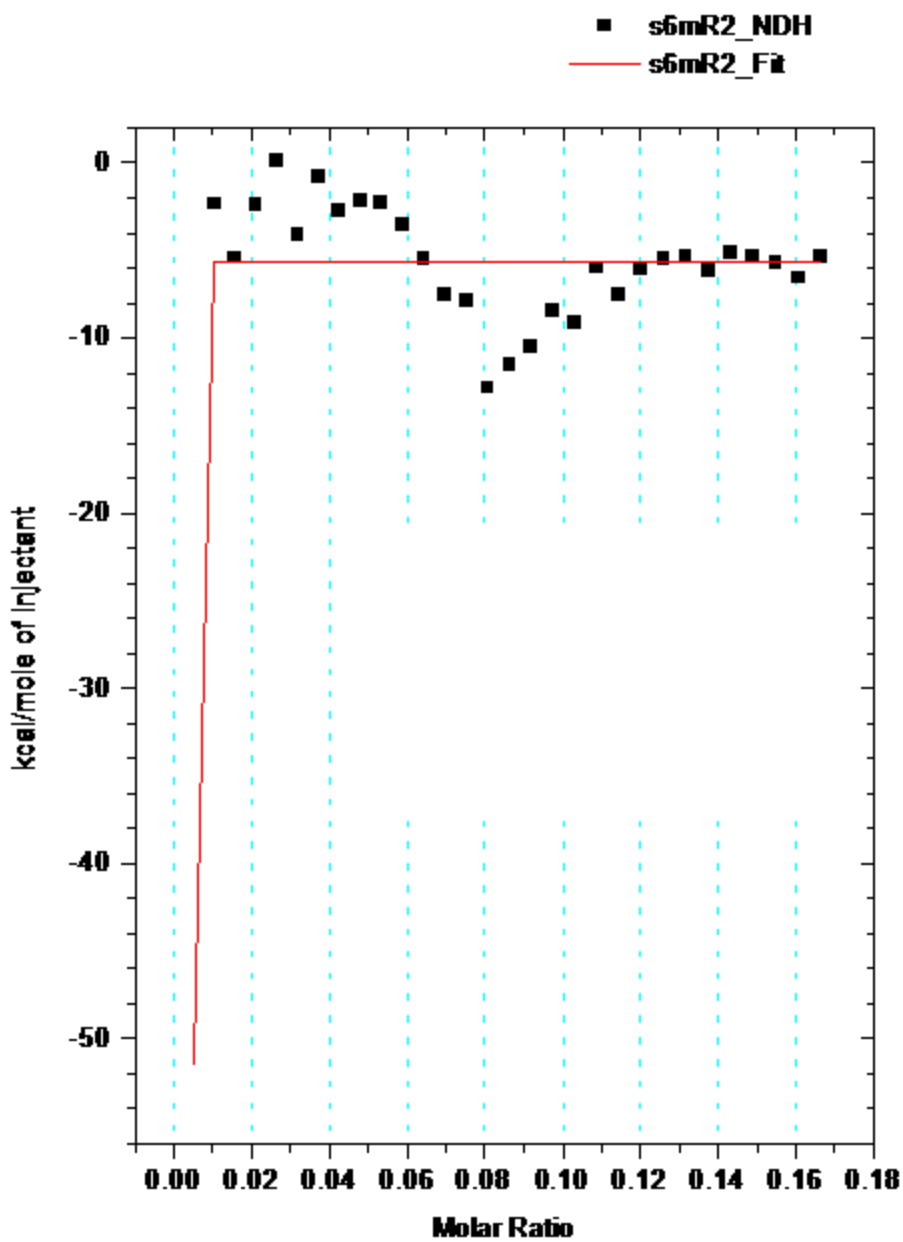


Fig. 3.3.5. The titration curve obtained by integration of the raw data in **Fig. 3.2.4**. As can be seen, the binding is too weak to resolve the titration data into a set of thermodynamic parameters and binding constant.

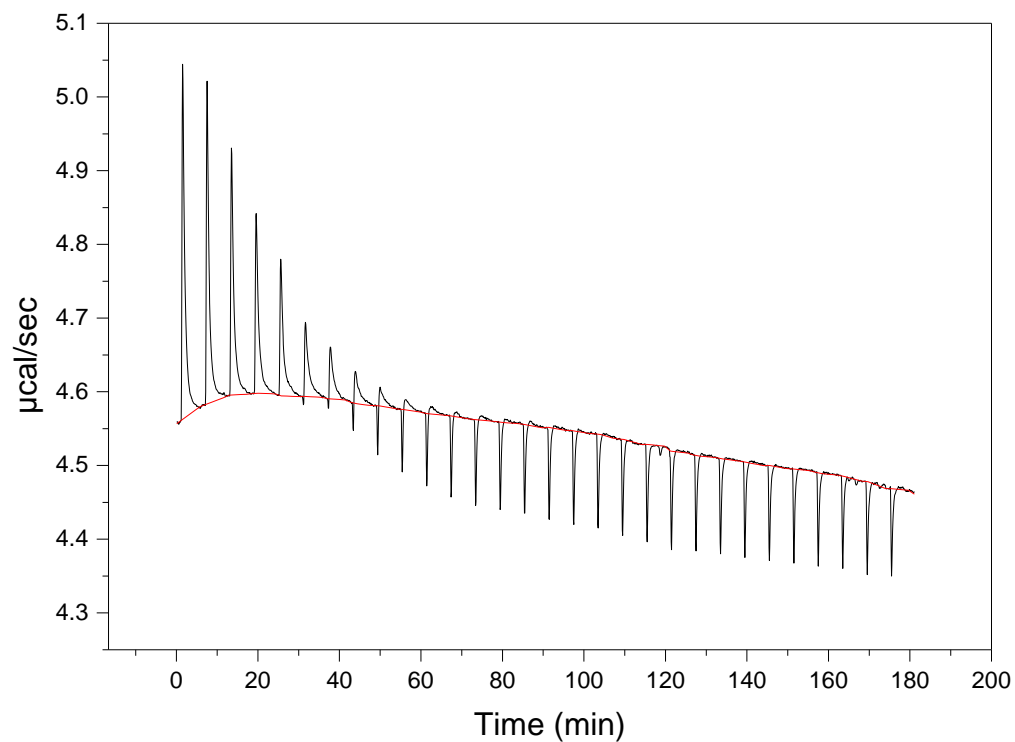


Fig. 3.3.6. The raw data for a s9mer, $\text{H-[N(Orn)-N(Bu)-N(spe)]}_3\text{-NH}_2$. The direction of the spikes are pointing up, which is indicative of an endothermic reaction. The baseline is an improvement over the shorter peptoids, although subsequent peptoids yielded superior data, since practice in experimental procedures, like most other activities, tends to yield improved results, i.e., ‘practice makes perfect’.

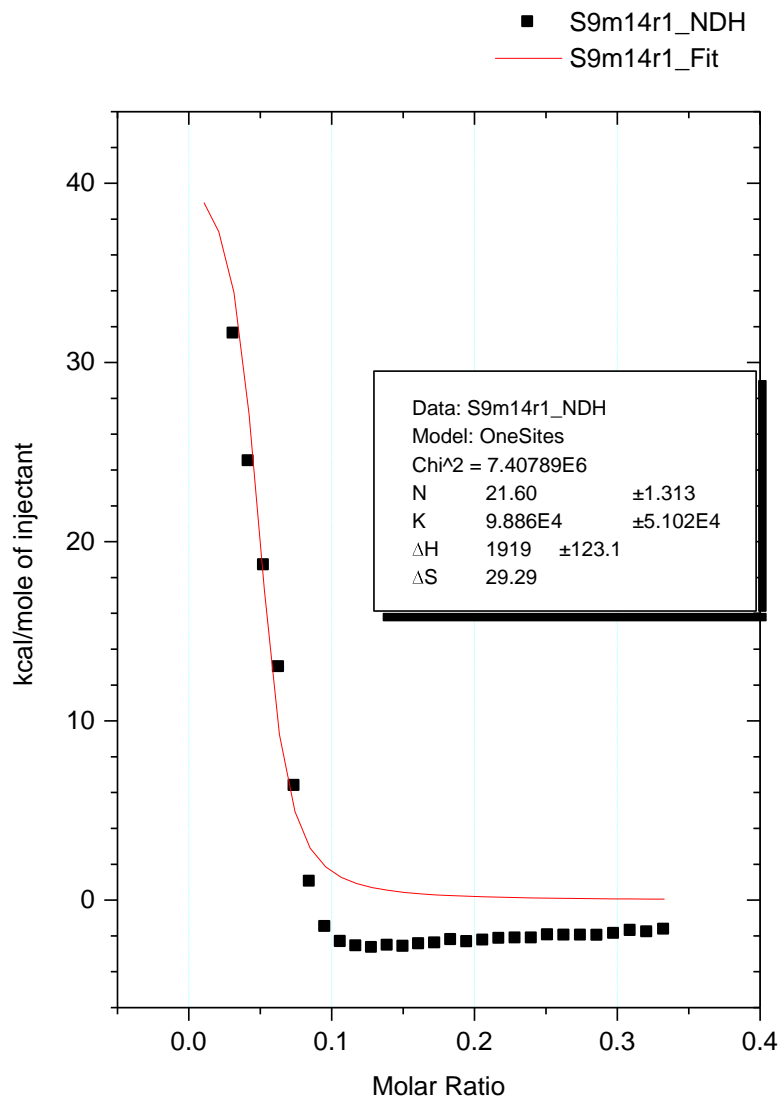


Fig. 3.3.7. The titration curve for s9-mer peptoid integrated from the raw data shown in Fig.3.2.6.

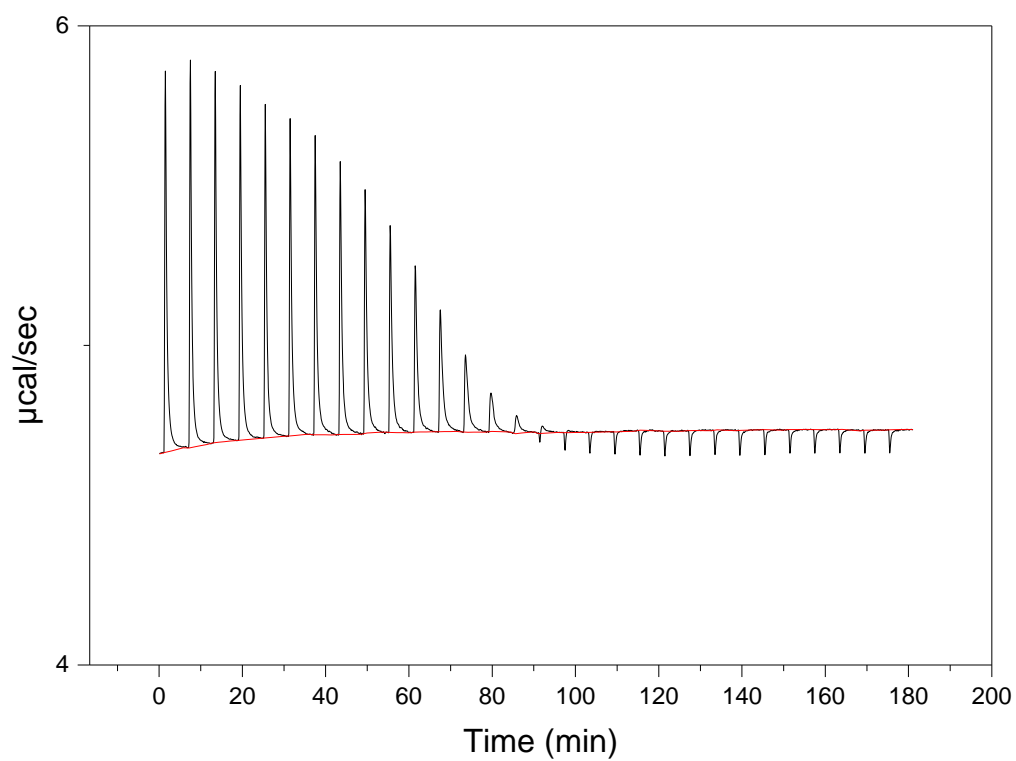


Fig. 3.3.8. Raw ITC titration data for an s12-mer, H-[*N*(Orn)-*N*(Bu)-*N*(spe)]₄-NH₂. The base line for this peptoid was quite even, which possibly could be related to length, but this is only hypothesis.

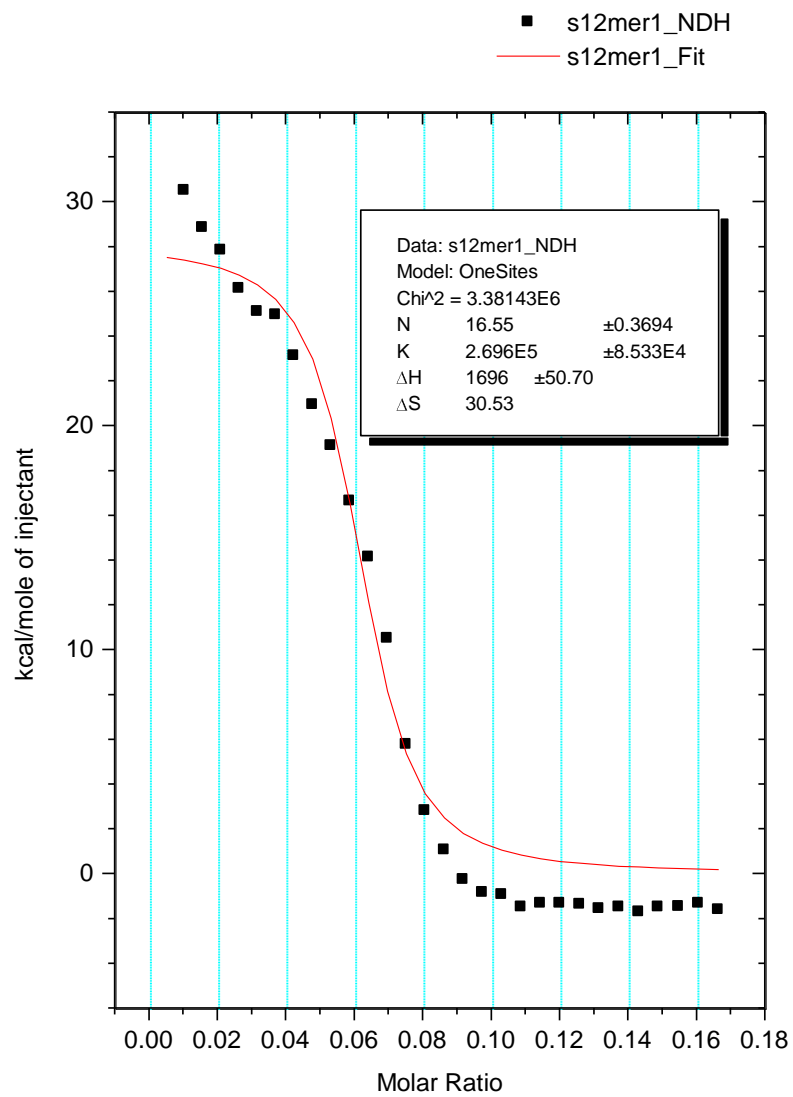


Fig. 3.3.9. The titration curve produced by integration of the raw data shown in **Fig. 3.2.8**. As can be seen, the last two (larger) peptoids with $n = 3$ and 4 produced reasonable data.

Peptoids	$K_b(M^{-1})$	N	$\Delta H(\text{cal/mole})$	$\Delta S(\text{cal/mole})$	$\Delta G(\text{cal/mole})$
s9-mer	$5.394 \times 10^4 \pm 9386$	17.45 ± 1.9	732 ± 89	26.84 ± 0.8	-6448 ± 2.5
s12-mer	$2.324 \times 10^5 \pm 43620$	16.55 ± 0.36	1696 ± 51	30.53 ± 0.5	-7311 ± 4.7

Table 3.3.1. Binding constants and thermodynamic parameters determined from ITC data for the peptoids H-[N(Orn)-N(Bu)-N(spe)]_n-NH₂, where n = 3 and 4. ΔG was calculated from $-RT \ln K_b$, and ΔS was calculated from $\Delta G = \Delta H - T\Delta S$.

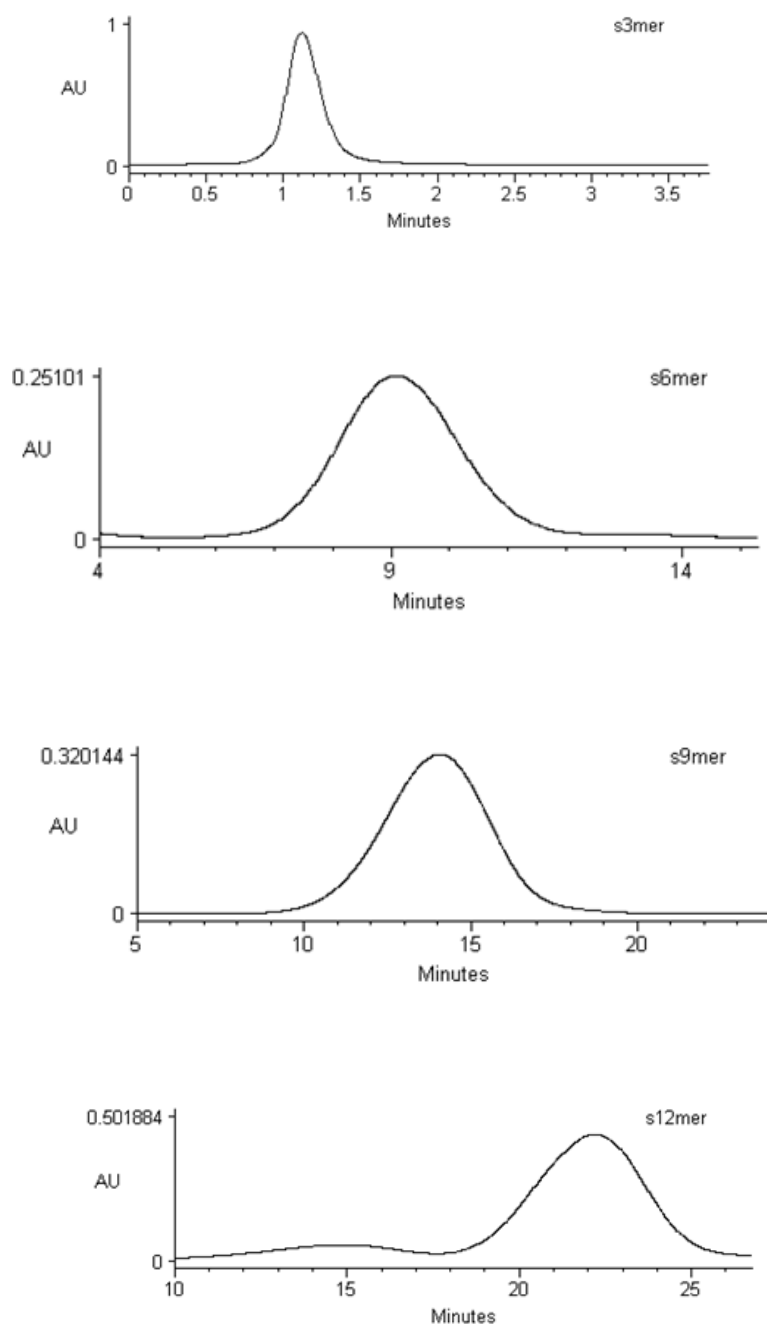


Fig. 3.3.10. HAC retention times from ammonium-bearing peptoids from 3 to 12 monomers in length.

peptoid	Mean Ret. Time (min)	st. dev.
3mer	1.22	0.1
6mer	9.2	0.4
9mer	14.2	0.25
12mer	22.3	0.45

Table 3.3.2. Heparin affinity chromatography mean retention times and standard deviations from 3 trials for each peptoid.

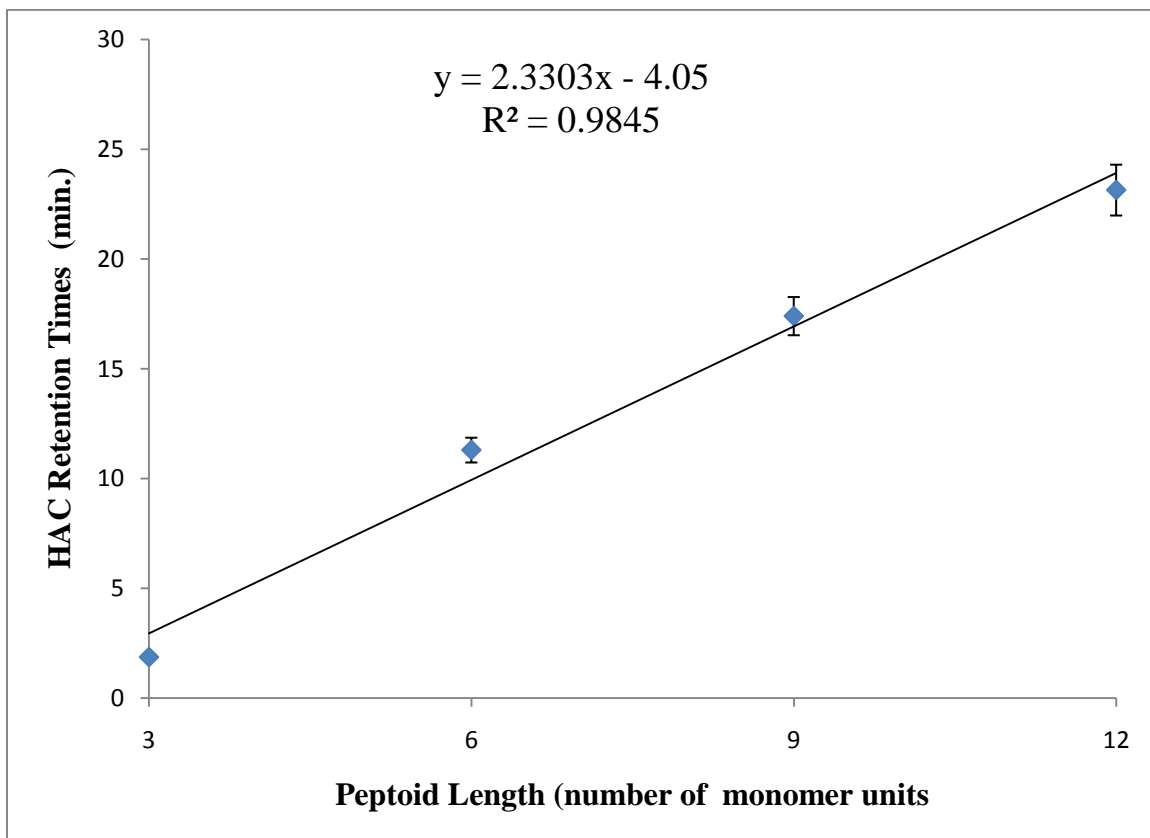


Fig. 3.3.11. Heparin affinity chromatography retention times vs. peptoid length for the family of peptoids H-[N(Orn)-N(Bu)-N(spe)]_n-NH₂, where n = 1- 4.

3.4. Summary and Conclusions

A series of peptoids was synthesized based upon a trimer sequence that included, starting from the C-terminal end, a chiral side chain (R_3) bearing-monomer, followed by a butyl side chain (R_2) bearing-monomer, and finally a charged ornithine side chain (R_1) bearing-monomer. The formula for the trimer is $H-[N(R_1) - N(R_2) - N(R_3)]_n-NH_2$, where $n = 1 - 4$. The effect of the chirality of R_3 was studied to determine the effect of chirality on the relative heparin binding affinities, using the chiral *spe* or *rpe* monomer side chains. Based upon ITC data of two identical peptoids with opposite chirality, as well as prior data from this laboratory, it was determined that the *S*-analogs have a relative higher heparin binding affinity over the *R*-analogs. Therefore all subsequent peptoids were synthesized using (*S*)-1-phenylethylamine to yield *spe*-bearing peptoids.

Following this initial design consideration, the effect of length of the peptoids, and thus the number of cationic binding sites on the peptoid was investigated using ITC heparin affinity chromatography. The mean HAC retention times for the ammonium-bearing peptoids from $n = 1 - 4$ were plotted against length of peptoids, where length was expressed in terms of the number of monomers. The results showed that there is a direct linear correlation between peptoid length (i.e., number of cationic binding sites) and HAC retention times. This meets the expectation that increasing the number of binding sites results in increased heparin binding affinity.

3.5 References

1. Zuckermann, R. N., Kirshenbaum, K., Barron, A. E., Goldsmith, R.A., Armand, P., Bradley, E.K., Truong, K.T.V., Dill, K A., Cohen, F.E. *Proc. Natl. Acad. Sci. USA* **1998**, *95*, 4303–4308.
2. Beychok, S. *Science* **1966**, *154*, 1288-1299.
3. Hamza, M., PhD. Thesis University of California at Riverside, **2010**.

Chapter Four:

The Relative Heparin Binding Affinities of Peptoids Containing Ammonium and Guanidinium Side Chains

4.1. Introduction

Heparin-binding peptides are found throughout nature and have also been designed. The sequences of heparin binding peptides often contain multiple lysines and arginines.^{1,2} The peptoids designed and synthesized in this study also have multiple side chains that contain ammonium and guanidinium groups. The goal of the research discussed in this chapter is to compare relative binding affinities for ammonium-containing and guanidinium-containing peptoids and the effect of length of guanidinium-containing peptoids on heparin affinity. The general sequence of peptoids studied in this chapter is based upon the same repeating trimer sequence $H-[N(R_1)-N(R_2)-N(R_3)]_n-NH_2$, where $n = 1 - 4$, as in Chapter 3. To make the comparison between heparin binding affinity of ammonium-containing and guanidinium-containing peptoids, the R_1 side chain contained either an ammonium group ($CH_2CH_2CH_2NH_3^+$) or a guanidinium group which was obtained from the same three carbon chain. The ammonium group terminating the three carbon chain is the mimic of the amino acid ornithine. R_2 was N(Bu) and R_3 was N(spe), as in Chapter 3, which yielded peptoids that adopted a right handed helix, that was shown in Chapter 3 to bind with slightly higher affinity to heparin than a left-handed helix.

The design rationale behind converting R_1 into a guanidinium group was to enhance the binding to the anionic sulfonic acids, esters, and amides of heparin discussed in Chapter Three, through electrostatic attraction and hydrogen bonding. **Fig. 1.6.3** in Chapter One showed the probable hydrogen bonding of the ammonium group and the guanidinium group to deprotonated sulfonic acid groups of heparin.

The peptoids studied in this chapter therefore had the sequence $H-[N(R_1)-N(Bu)-N(spe)]_n-NH_2$, $n = 1-4$ and R_1 is either Orn or Arg. The structures of the ammonium-containing peptoids are shown in **Fig. 3.2.2**. The structures of the guanidinium-containing peptoids are shown in **Fig. 4.1.1**.

4.2. Measurement of Binding Constants by Isothermal Titration Calorimetry

Isothermal titration calorimetry, while a valuable tool in the study of ammonium-bearing peptoids of sufficient length, was found to not be useful for all of the guanidinium-bearing peptoids synthesized in this study. The problem with the guanidylated peptoids was that the ITC data plots resulted in an anomalous dip that the Origin 5 software was unable to resolve and it was not possible to fit a model to the data. An example of an ITC titration curve for a guanidinium-bearing peptoid is shown in **Fig. 4.2.1**. In the example shown, the guanidinium-containing S9-mer peptoid has the sequence: $H-[N(Cad)G-N(Bu)-N(spe)]_3-NH_2$. It was not possible to fit a titration binding curve to the data points. This suggests that there are several binding events that take place during the titration of guanidinium-bearing peptoids with heparin, as compared to

ammonium-containing peptoids, whose titration data can be fit to a one-binding-site model.

As discussed in Chapter 3, ammonium-bearing peptoids under nine monomer units in length did not possess sufficient binding affinity to obtain reasonable ITC titration data. There were two classes of peptoids that produced anomalous data. For peptoids, it was still possible to estimate binding constants using the heparin affinity chromatography data and the binding constants obtained from ITC data for the ammonium bearing –peptoids that were nine monomer units or twelve monomer units in length. Using HAC data and the binding constants, a calibration curve was constructed, with which binding constants could be estimated for the guanidylated peptoids and the 3-mer and 6-mer ammonium-bearing peptoids.

4.3. Heparin Affinity Chromatography

Although it was not possible to characterize the binding of the guanidinylated peptoids with heparin by ITC, relative binding affinities could be determined by heparin affinity chromatography. Representative HAC chromatograms for the guanidinium-bearing peptoids of three to twelve monomer units in length are shown in **Fig. 4.3.1**. Mean values of the retention times obtained from triplicate runs are listed in **Table 4.3.1**. Retention time data for the peptoids and the data are presented in graphical format, along with the ammonium-bearing peptoids in **Fig. 4.3.2**.

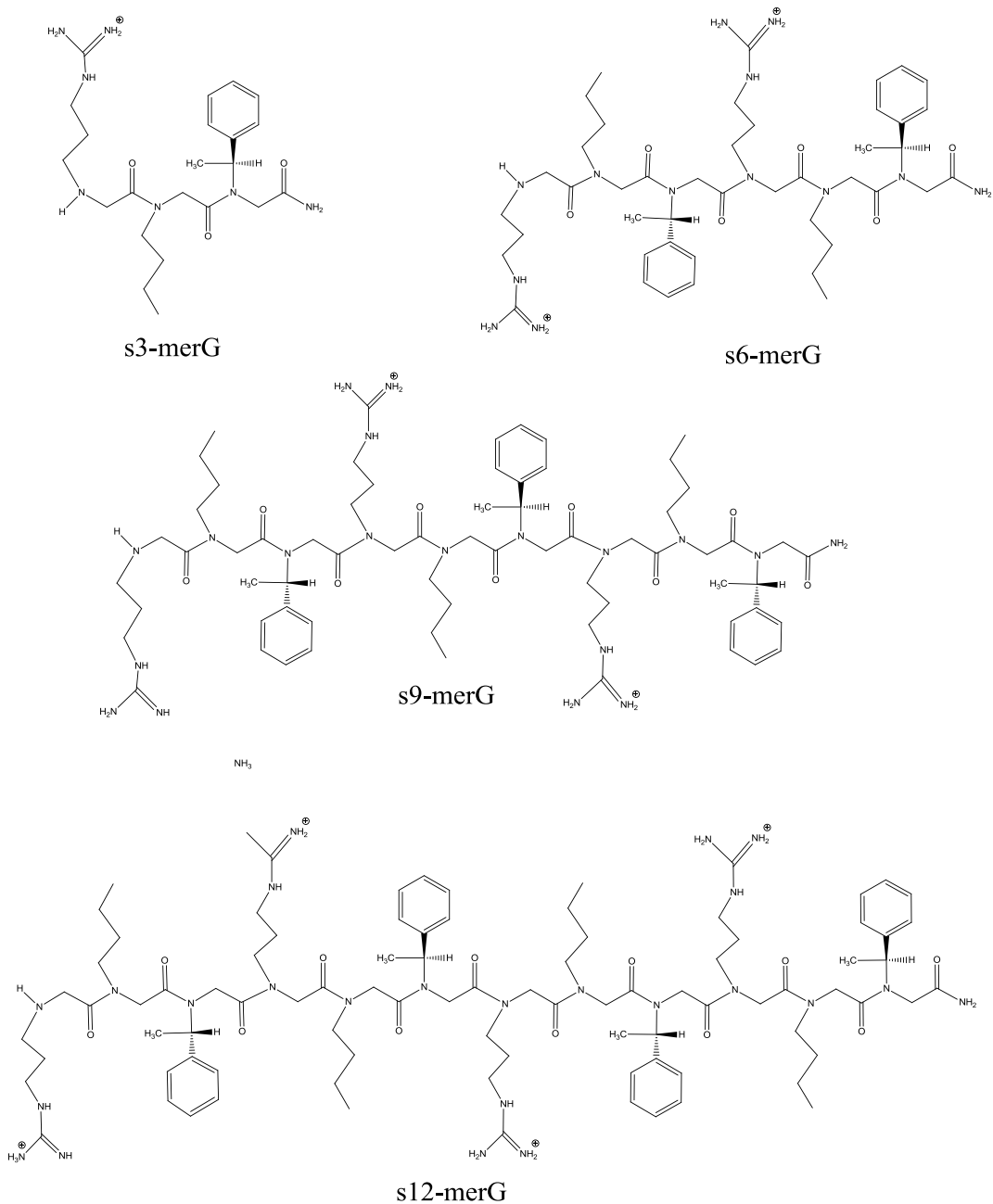


Fig.4.1.1. Guanidinium-bearing peptoids studied in this chapter. The structures of the analogous ammonium-bearing peptoids are shown in **Fig. 3.3.1**.

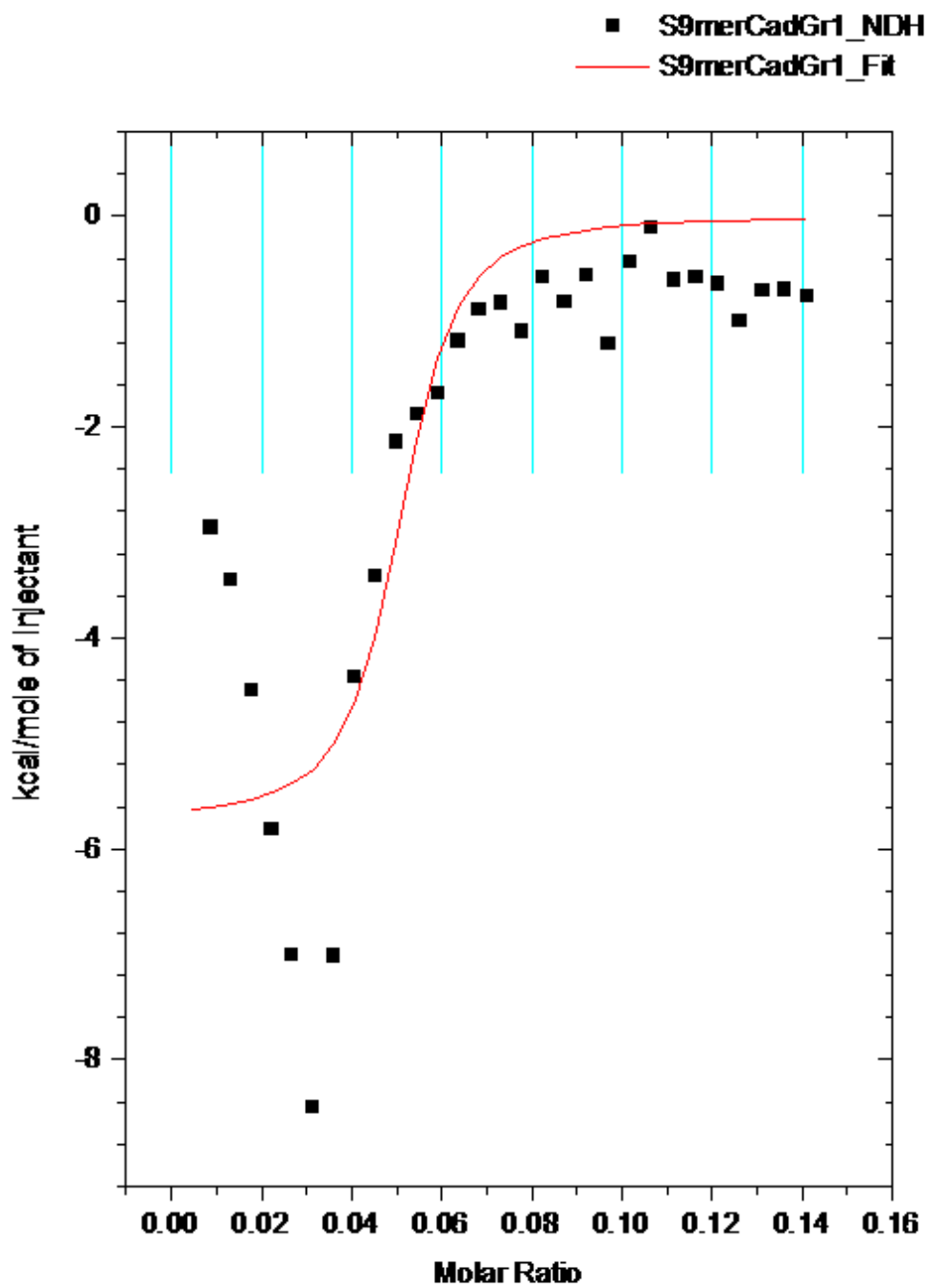


Fig. 4.2.1 ITC titration curve for the titration of 0.20 mM S9merCadG peptoid, i.e. H-[N(Cad)G-N(Bu)-N(spe)]₃-NH₂ with 0.25 mM heparin. The model does not fit the data.

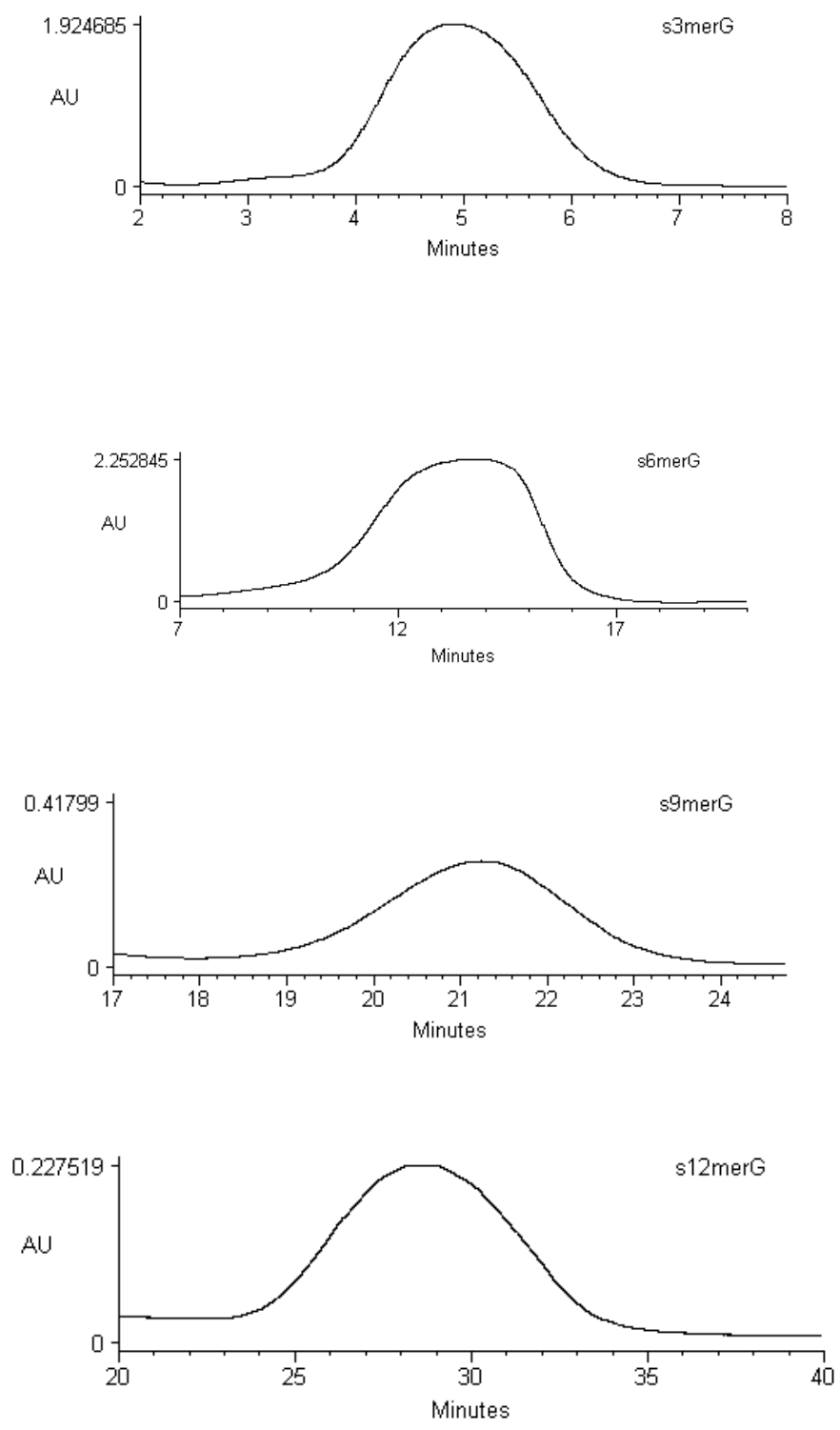


Fig. 4.3.1. HAC retention times for four guanidinium-containing peptoids.

peptoid	mean	st. dev.
3merG	5.1	0.3
6merG	13.8	0.5
9merG	21.3	0.7
12merG	29.2	0.4

Table 4.3.1. HAC mean retention times for guanidinium-bearing peptoids from 3 to 12 monomer units in length. The retention times for the ammonium-bearing peptoids are presented in **Table 3.3.2.**

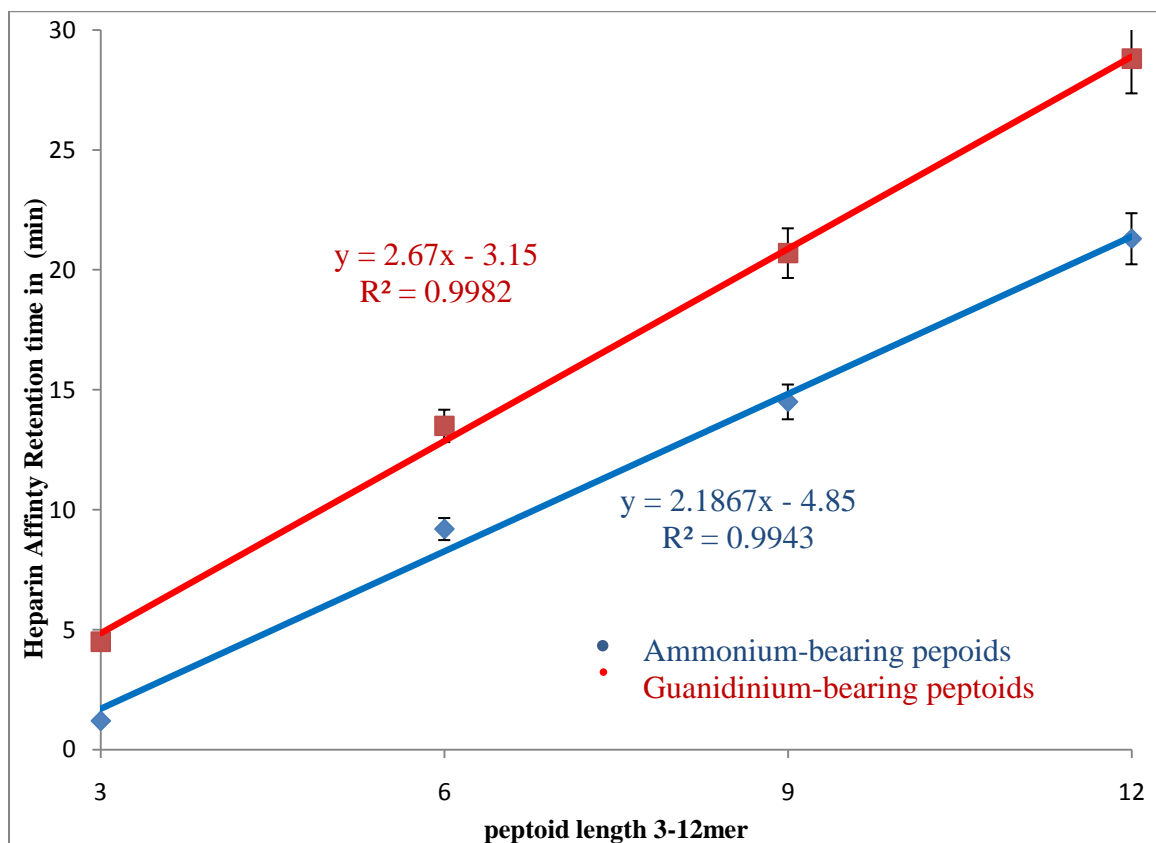


Fig. 4.3.2. HAC retention times versus peptoid length. Both ammonium and guanidinium-bearing peptoids are plotted together for comparison. In this plot, the length is the number of monomer units, shown on the horizontal axis, while the mean retention time in minutes is shown on the vertical axis.

4.4. Circular Dichroism Studies on the Ammonium and Guanidinium-Bearing Peptoids with and without Heparin Present

Circular dichroism studies were conducted on both the ammonium and guanidinium-bearing peptoids studied based upon length of peptoids from three to twelve monomer units in length. The CD spectra all displayed the classical helical absorptions expected from right-handed S analogs.

In addition to the above CD spectra, which were conducted with 0.2 mM peptoid solutions in deionized water, solutions of 0.2 mM peptoid were made with 0.25 mM of porcine heparin added. These solutions were prepared in 5 mL volumetric flasks prior to adding them to the cuvettes for CD analysis. The purpose of the addition of the heparin was to investigate the secondary helical structure of the peptoids while in the presence of heparin. If the absorptions associated with helical structures changed or diminished to a significant degree, it would suggest that the binding event of peptoid to heparin involved loss of secondary helical structure.

Since this clearly did not occur, the binding of the peptoids to heparin does not alter the secondary structure in such a way that the helices are lost. This binding phenomenon will be investigated further using molecular docking as a tool in order to attempt to visualize the binding of peptoids to heparin. In all molecular modeling and docking, a perfect helix is never seen. It is usually a percentage of helicity that is seen due to cis/trans isomerism. This causes the overall secondary structure to twist and curve while still maintaining some helical structure.

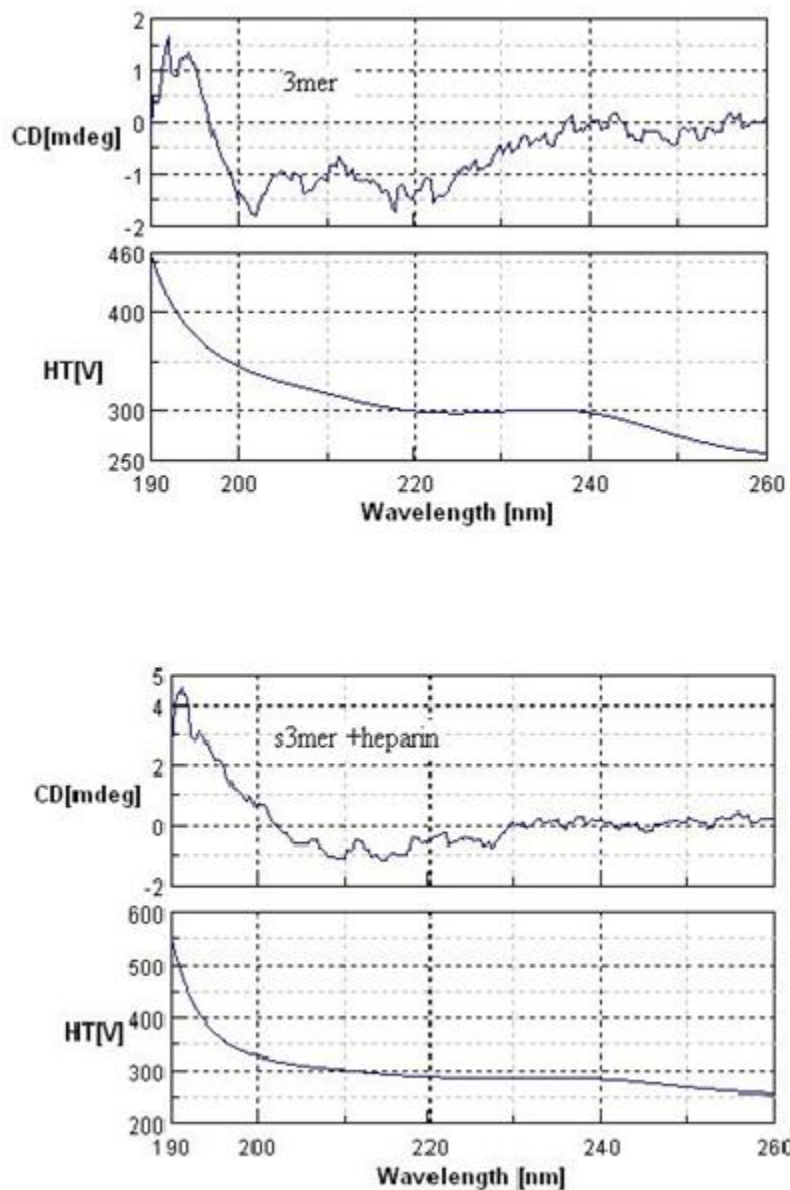


Fig. 4.4.1. CD spectra of S3-mer and S3-mer with heparin. All peptoid/ heparn solutions are are 0.2 mM peptoid /0.25 mM heparin. Solutions of peptoid only are 0.2 mM in concentration.

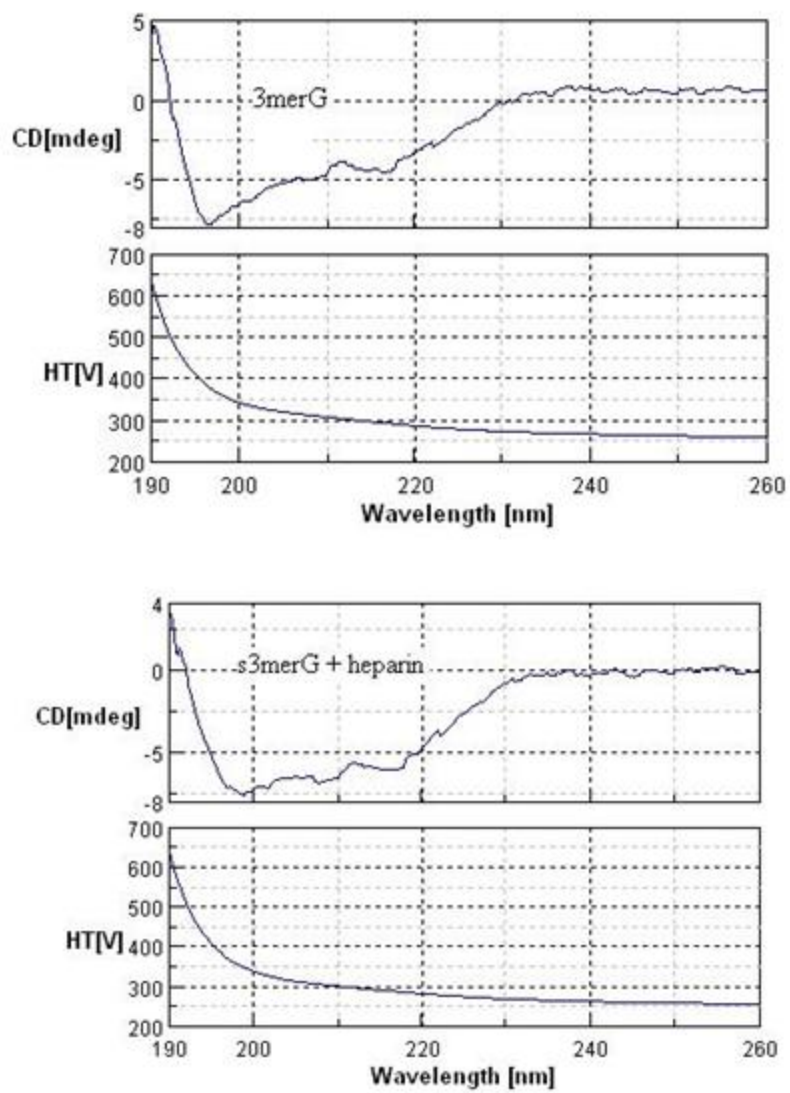


Fig. 4.4.2. CD spectra of S3-merG and S3-merG with heparin.

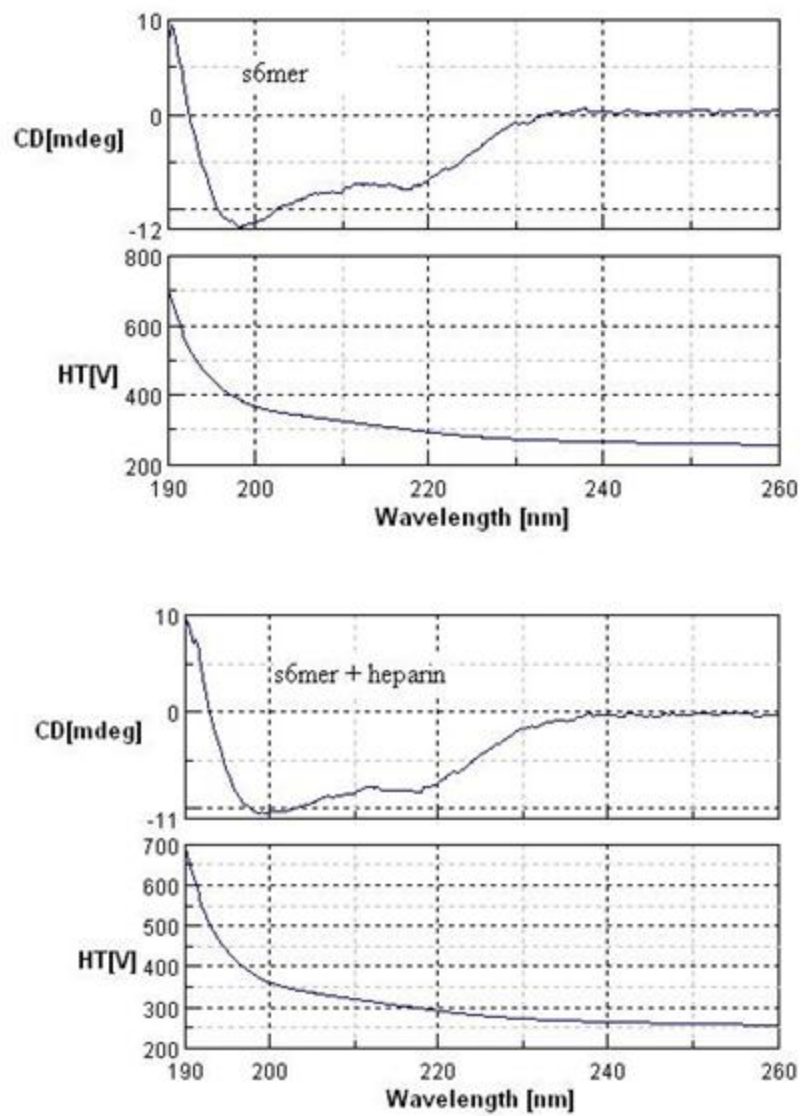


Fig. 4.4.3. CD spectra of S6-mer and S6-mer with heparin.

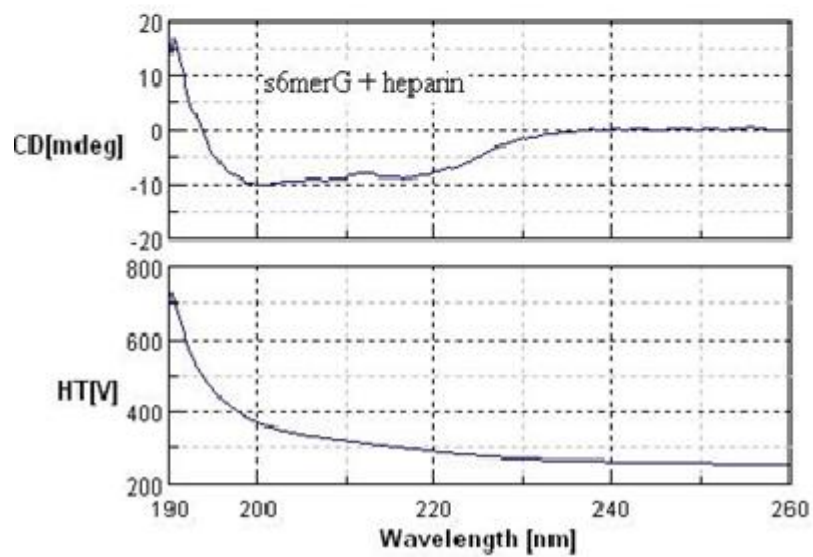
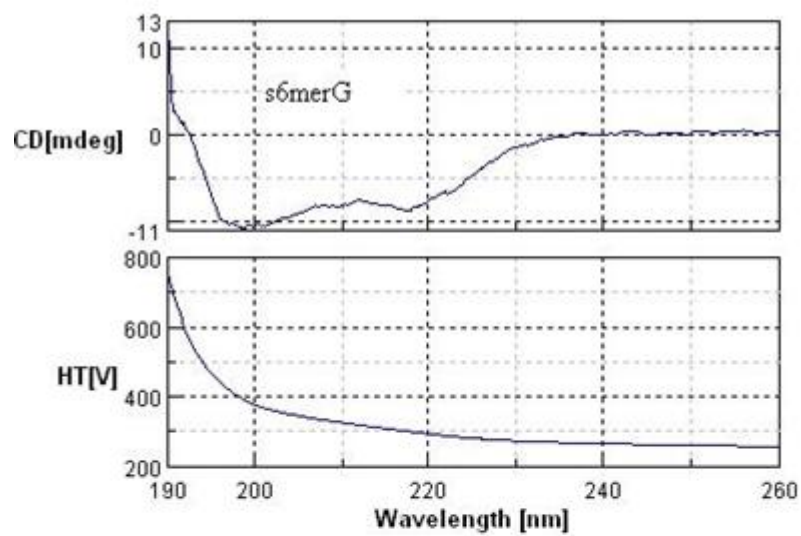


Fig. 4.4.4. CD spectra of S6-merG and S6-merG with heparin.

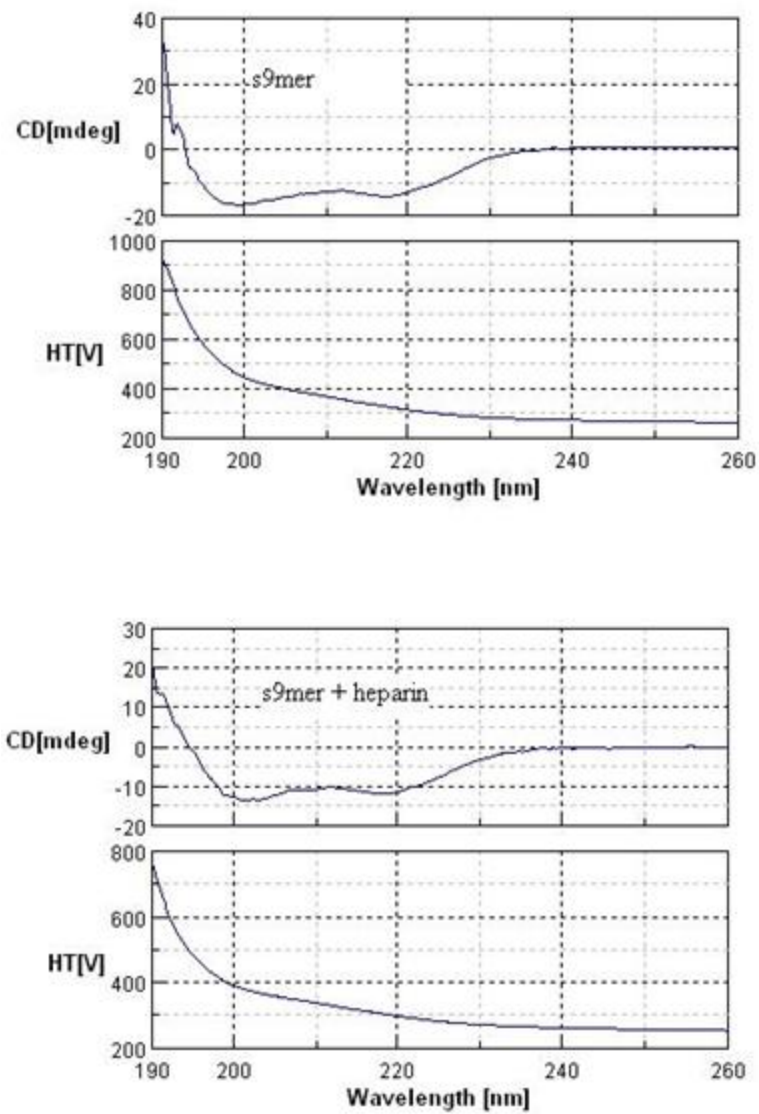


Fig. 4.4.5. CD spectra of S9-mer and S9-mer with heparin.

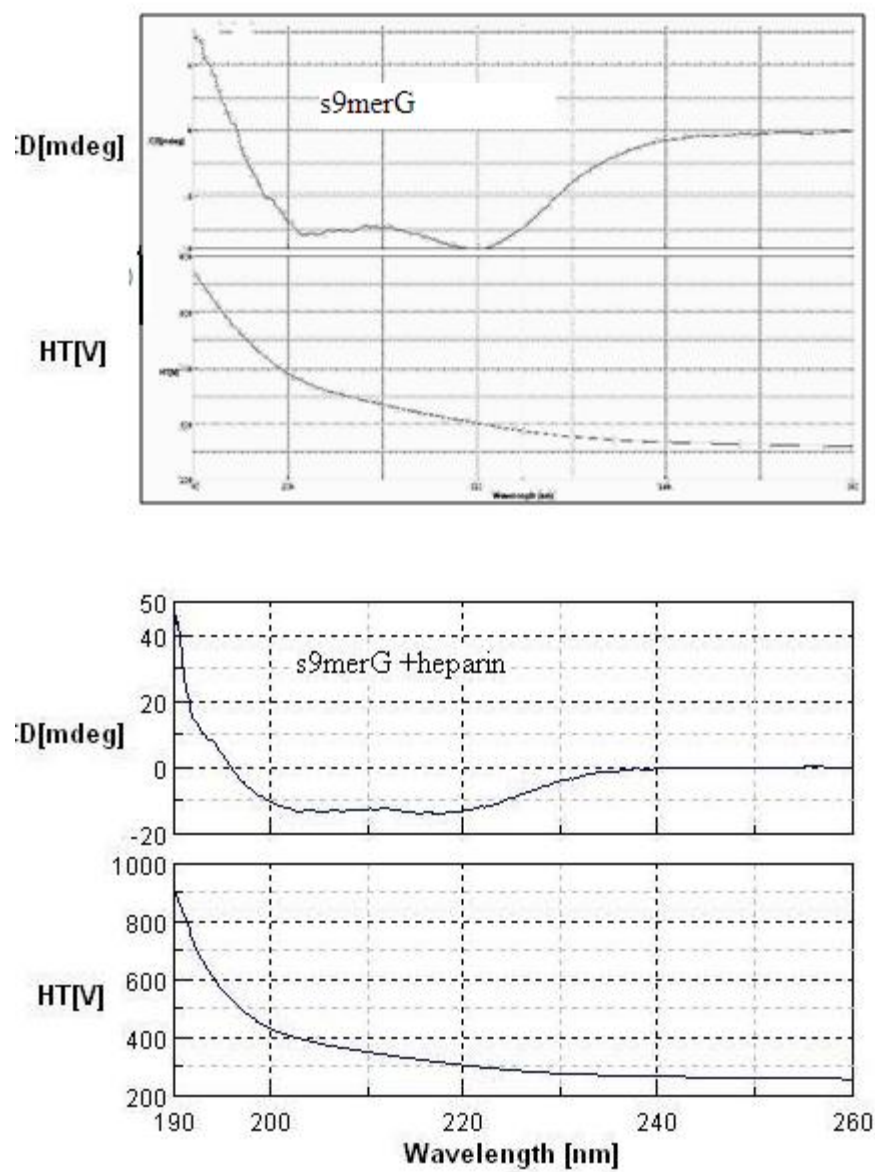


Fig. 4.4.6. CD spectra of S9-merG and S9-merG with heparin.

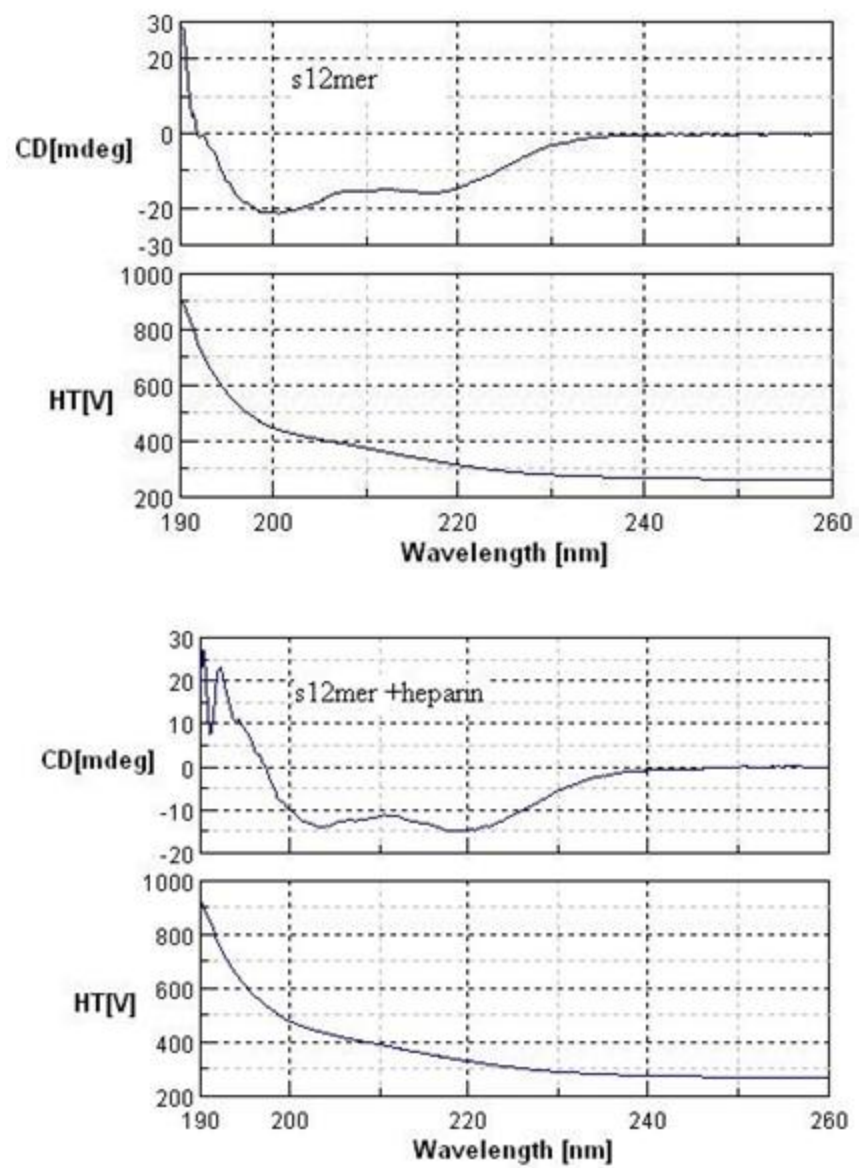


Fig. 4.4.7. CD spectra of S12-mer and S12-mer with heparin.

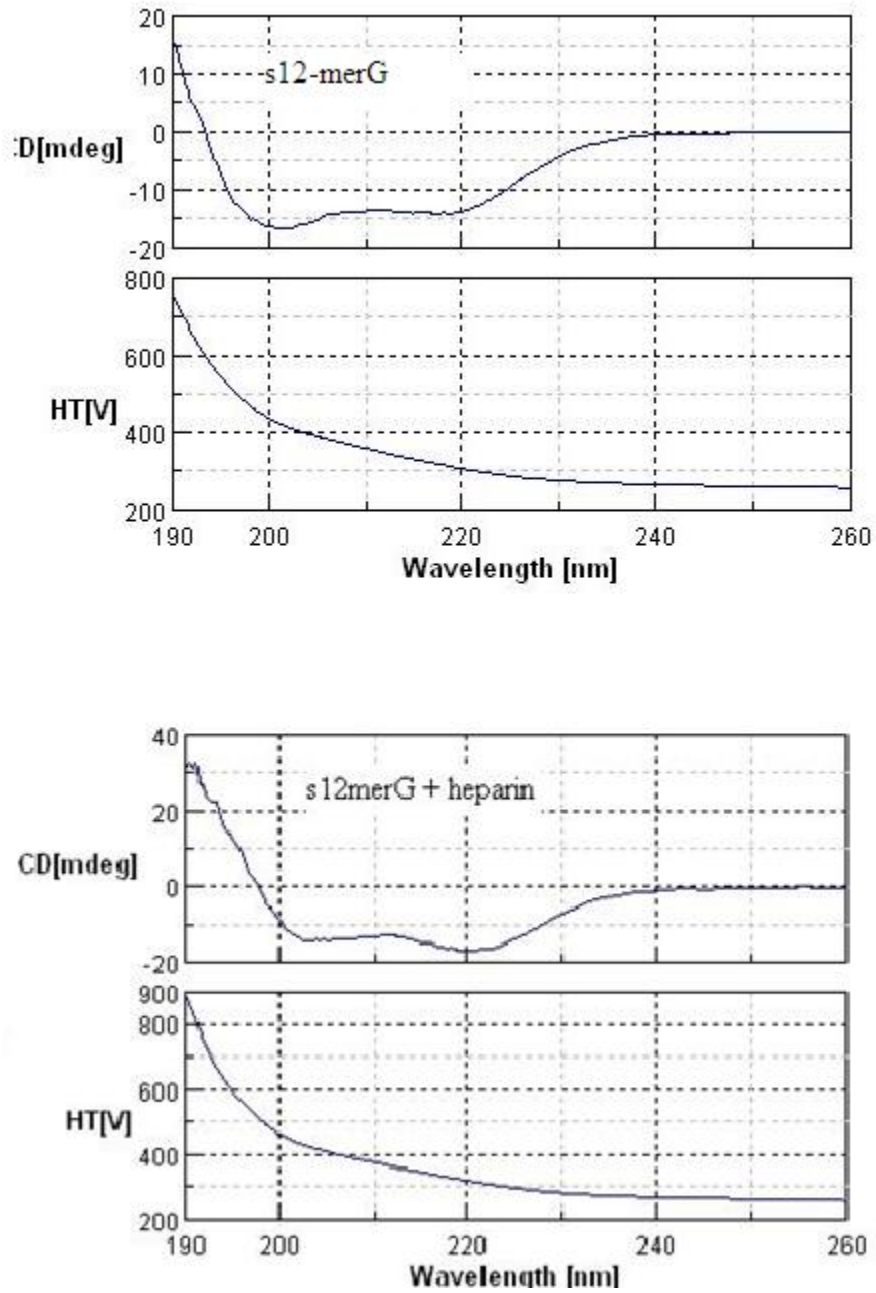


Fig. 4.4.8. CD spectra of S12-merG and S12-merG with heparin.

4.5 Discussion Regarding CD Measurements

When solutions of peptoids are mixed with heparin, there is a noticeable change in the intensity of the two major absorptions at 204 nm and 220 nm. An additional absorption at 190 nm did not appear to change. All three are chromophoric for the back bone amide bonds of both peptides and peptoids. It will be recalled from Chapter Two, that the absorption at 220 nm is known as the $n - \pi^*$ absorption and is known to be due to the promotion of an electron from an amide oxygen nonbonding orbital, i.e., a lone pair to an antibonding orbital involving the oxygen, carbon and nitrogen of the amide bond. The other two bonds are split from a single absorption related to the amide helix and the longer of the two at 204 nm is known as the $\pi - \pi^*$ parallel transition, due to the polarized light parallel to the helical axis, and the other at 190 nm is known as the $\pi - \pi^*$ perpendicular transition, due to the polarized light perpendicular to the helical axis of the amide bond.

Any noticeable change related to bending or twisting in the conformation of the amide bond should be observable in one or more of these three chromophores involving the amide bond. This is in fact the case, to some degree. While the observable change is mild, it does appear but only in two; the longer wavelength absorptions react either by decreasing in intensity or by increasing in intensity and the change may only involve one of the two absorptions. This is evidence of some change in binding conformation, but since it is inconsistent, it is difficult to say with any confidence that the same change is taking place. It could be that it simply shows that conformational changes are taking

place upon binding of the peptoids with heparin. This binding interaction will be explored in greater detail using computer docking with Autodoc Vina in Chapter Six.

What is very clear from the CD spectra is that in almost all cases, the spectra were consistent with helical secondary structures, both with and without the addition of heparin. With the possible exception of the S3-mer itself, even the smallest peptoids showed the classic helical CD signature. Also the helices studied in this chapter were right-handed helices. This is evidenced by the double minima at 204 and 220 nm. The R12-mer studied in Chapter Two, demonstrated the mirror image of this signature, demonstrating a double maxima at the assigned chromophoric absorptions mentioned above.

4.6. Summary and Conclusions

Two factors become apparent from **Fig. 4.3.2**. First, it is clear that there is a direct linear correlation between the number of peptoid monomers (peptoid length) and retention time, which suggests that longer peptoids, i.e., peptoids with more cationic sites, possess greater heparin affinity, as was found in Chapter Three. Additionally, there is a direct correlation between guanidylation of peptoids and increased heparin affinity. While ITC gives quantitative data, it was not always possible to use it with this set of peptoids, in particular with the guanidylated or ammonium-bearing peptoids less than nine monomers in length. This is not the case with heparin affinity chromatography. As can be seen from **Fig. 4.3.2** and **Tables 3.4** and **4.1**, guanidinium-bearing peptoids

show a retention time between 3-5 minutes longer than ammonium-bearing peptoids of the same length.

The inability to fit ITC titration data for the guanidylated peptoids is due to either multiple binding events or the nature of the binding is different than for the ammonium-bearing peptoids. The technical support at GE Healthcare/ Microcal³ also found the data impossible to fit using the tools at their disposal and came to the same conclusion. A hypothesis that may explain this binding difference will be presented in Chapter Six under computational studies. The docking studies with Autodoc Vina demonstrate an alternative binding modality for guanidinium-bearing peptoids, as well as S and R peptoid analogs and for benzyl-bearing peptoids.

Circular dichroism spectra were measured for the eight ammonium and guanidinium-containing peptoids studied in this chapter, both with and without heparin, added to explore the effect of heparin on secondary structure. The CD data indicated a helical secondary structure for the peptoids, both in the absence and presence of heparin.

4.7 References

1. Crim, R. L., Auget, S.A., Feldman, S.A., Mostowski, H.S., Beeler, J.A. *Journal of Virology* **2007**, *81*, 261–271.
2. Harris, R. B., Sobel, M. patent *Commonwealth Biotechnologies Inc.*, U.S.A., **1996**, 660,592
3. MicroCal /G.E.Healthcare. www.microcal.com **2011**.

Chapter 5: A Study of the Effect of Length of Peptoid Side Chains on Heparin Affinity

5.1. Introduction

Following the study on the effects of the length and the chirality of peptoid on their heparin binding affinity, and the study of the relative binding affinities of ammonium and guanidinium groups, it seemed desirable to explore the effect of the length of the carbon side chain-bearing cationic sites. The general formula for the series of compounds studied is $\text{H-[N(cationic side chain)-N(Bu)-N(spe)]}_3\text{-NH}_2$, where the cationic side chain consisted of an ammonium or guanidinium group on the end of a carbon chain from 3 to 5 carbons in length. The design consideration being studied was that longer carbon chains may allow the cationic groups to reach their anionic counterparts on the heparin molecule with greater efficiency resulting in enhanced binding affinity. To study the effect of the length of the cation-bearing side chains, the series of six 9-mer peptoids shown in **Fig. 5.1.1** was synthesized and their binding by heparin was studied.

It also seemed desirable to study the effect of different side chains on the central monomer unit of the trimer sequence. A second series of 9-mer peptoids was synthesized in which the length of the alkyl chain of the central unit on the trimer sequence was varied. The general sequence was $\text{H-[N(Orn)-N(Alkyl)-N(spe)]}_3\text{-NH}_2$, where the alkyl side chain was a butyl, propyl, ethyl or methyl group. The resulting series of four 9-mers is shown in **Fig. 5.1.2**. The design consideration was that shorter alkyl chains in the central monomer of the trimer sequence would result in

diminished steric hindrance yielding peptoids with enhanced binding affinity to heparin. In addition, peptoids with allyl and benzyl side chains on the central monomer unit, were also studied. The structures of these two peptoids are shown in **Fig. 5.1.3.**

5.2. The Effect of Length and the Carbon Chain-Bearing the Cationic Binding Site on Heparin Affinity

5.2.1. Determination of Binding constants for ammonium-Containing Peptoids by ITC

Binding constants were determined for the ammonium-containing peptoids with varying lengths of the ammonium-bearing side chains by ITC. The ITC titration curves are presented in Figures **5.2.1** to **5.2.3**. The binding constants and other thermodynamic parameters obtained from the titration curves are presented in **Table 5.1**. The binding constant data is plotted in bar graph format in **Fig. 5.2.4**. In this format, the trend is well defined: the longer the cation-bearing side chain, the greater the binding affinity. The thermodynamic parameters in **Table 5.1** also show an increase in enthalpy and entropy with increasing carbon chain length for the ammonium-bearing peptoids.

The binding constants for the ammonium-bearing peptoids with carbon chains from 3 to 5 carbons in length are from triplicate runs. In each case, the mean values of the triplicate runs were used \pm mean % standard deviation. For the S9-mer peptoid, the concentrations were 0.2 mM peptoid with 0.25 mM heparin in pH 7.2 50 mM phosphate buffer

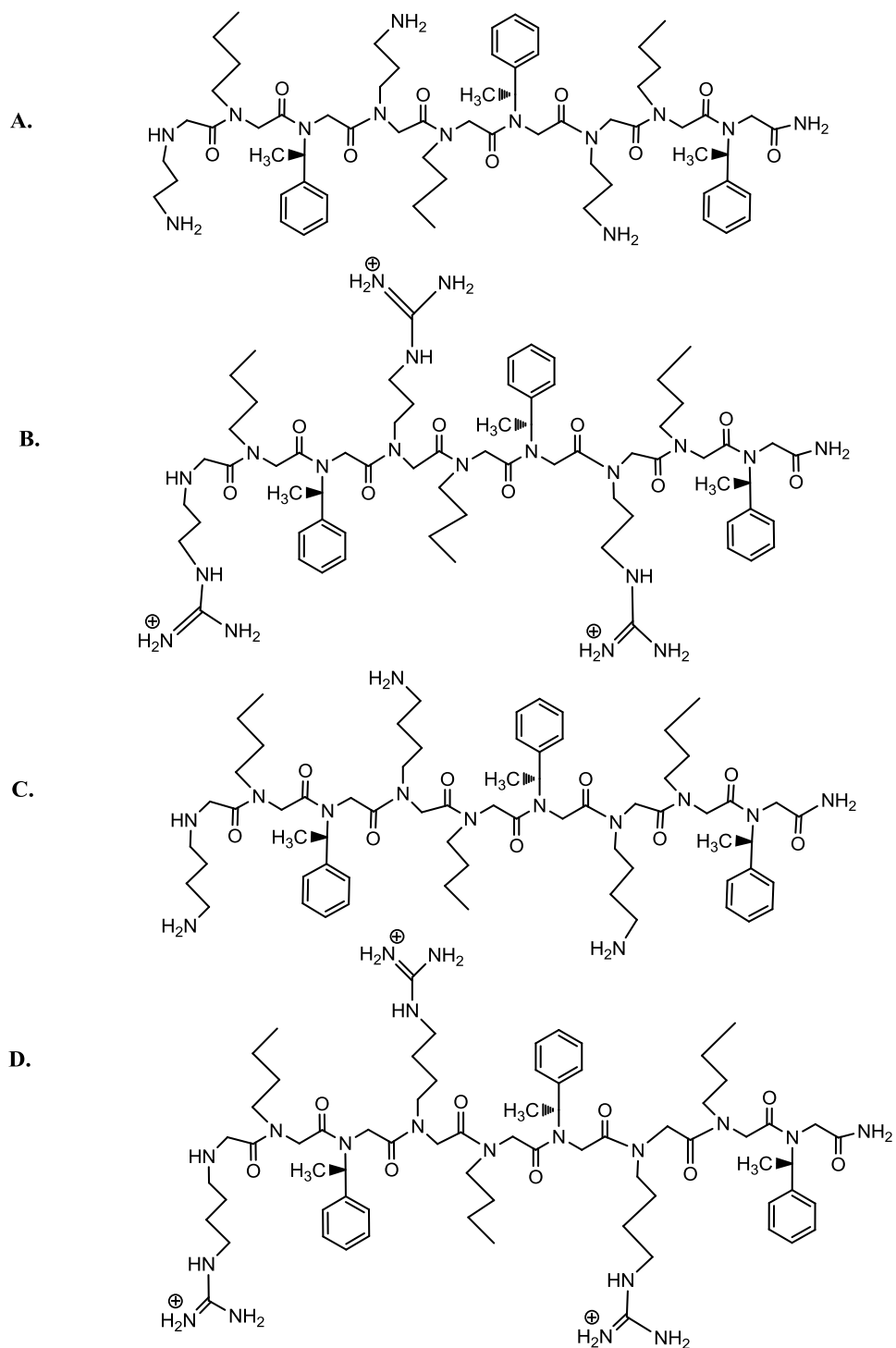


Fig. 5.1.1. Peptoids with cation-bearing side chains of 3 to 5 carbons in length, including both ammonium and guanidinium groups. **A.** s9-mer, **B.** s9-merG, **C.** s9merLys, **D.** s9-merLysG, **E.** s9-merCad, **F.** s9-merCadG.

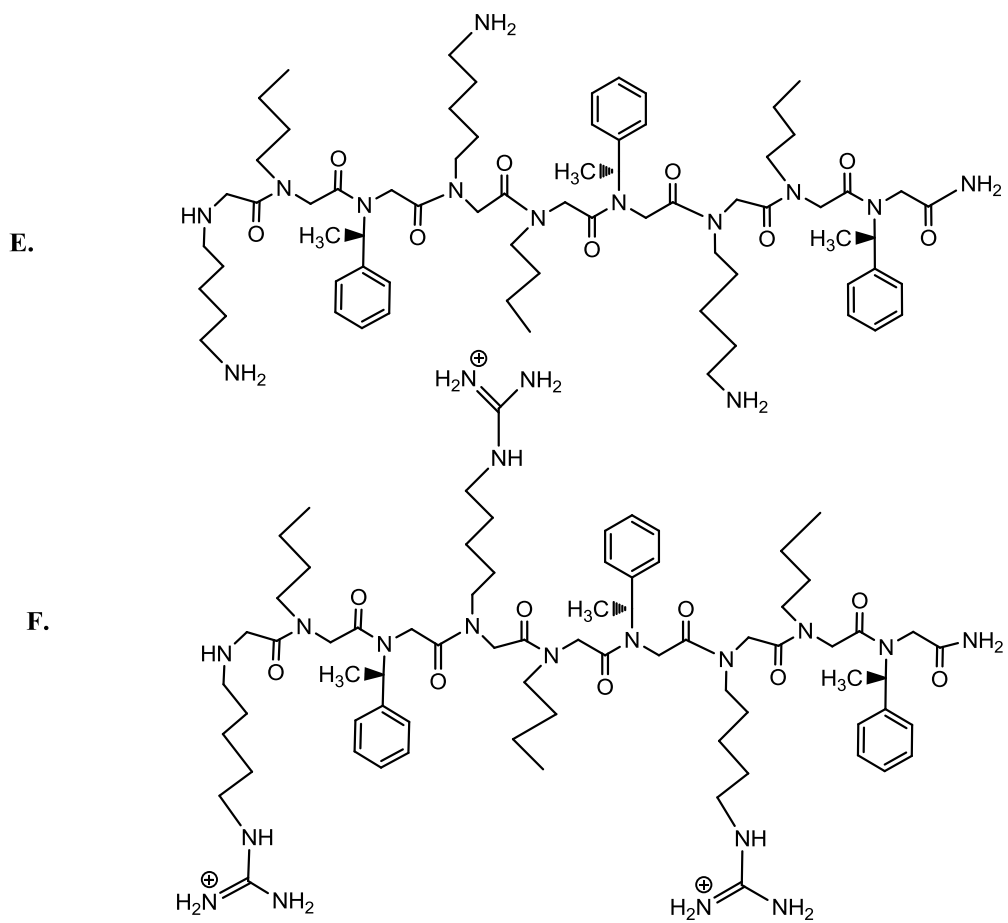


Fig. 5.1.1. Continued.

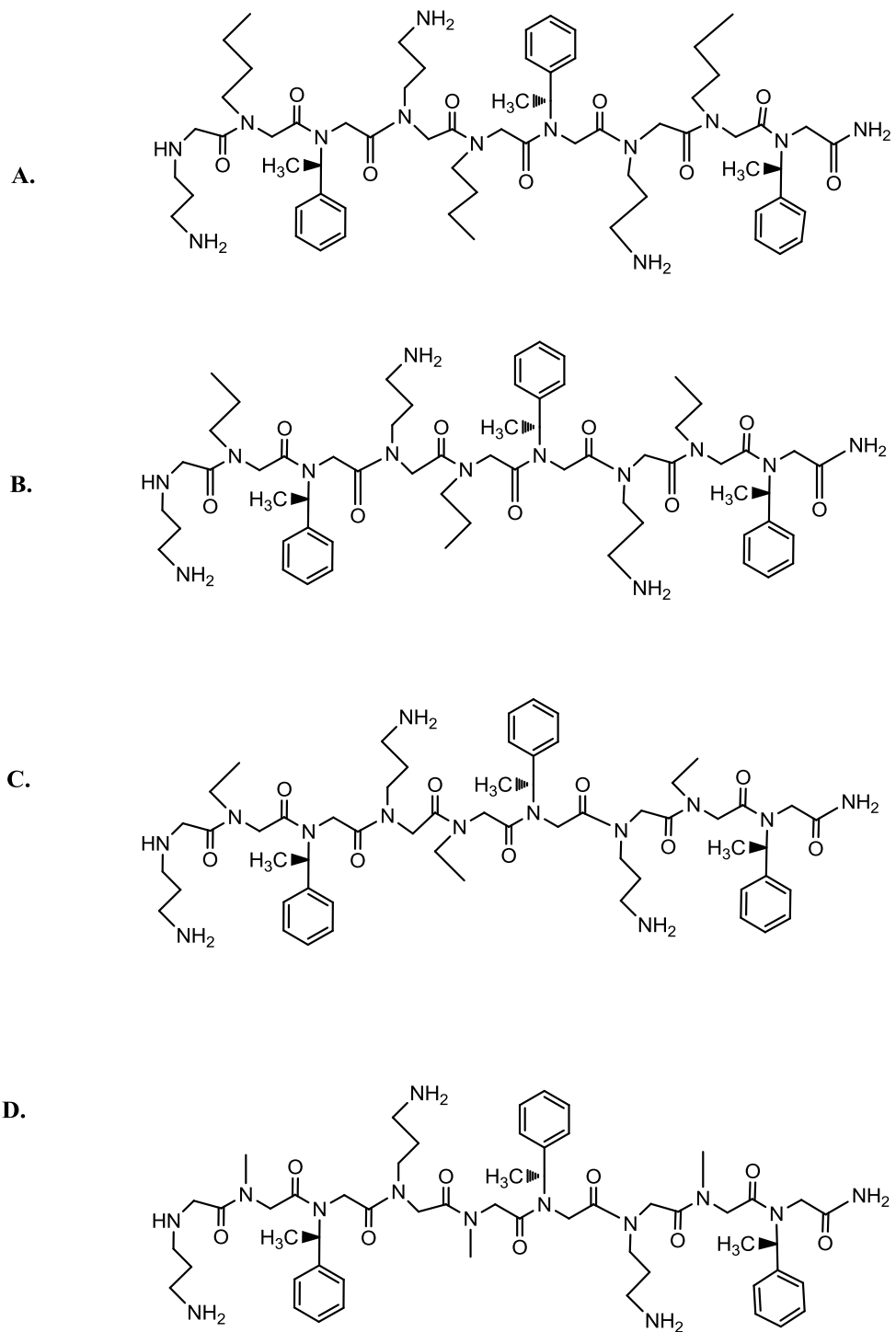


Fig. 5.1.2. Peptoid analogs with alkyl side chains of different lengths on the central monomer of the repeating trimer. **A.** s9-mer, **B.** s9-mer(Pr), **C.** s9-mer(Et), **D.** s9-mer(Me).

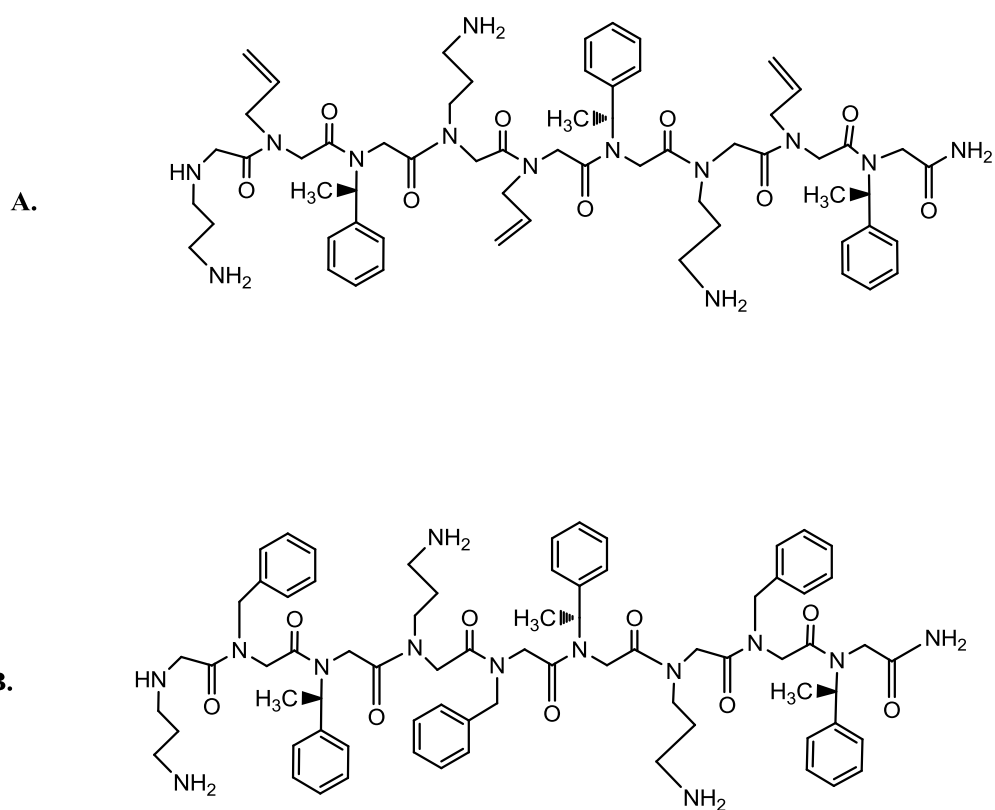


Fig. 5.1.3. Peptoid analogs with allyl and benzyl side chains on the central monomer of the repeating trimer. **A.** s9-merAll, **B.** s9-merBz.

Peptoid	N	$K_b(M^{-1})$	$\Delta H(\text{cal/mole})$	$\Delta S(\text{cal/mole})$	$\Delta G(\text{cal/mole})$
9-mer	17.86 \pm 2.65	5.39E4 \pm 9386	814 \pm 89	24.36 \pm 1.2	-6447 \pm 2.98
s9merLys	16 \pm 1.20	6.11E4 \pm 4.22E4	3305 \pm 119	32.85 \pm 4.6	-6522 \pm 5.45
s9merCad	21.5 \pm 3.34	8.34E4 \pm 8430	2317 \pm 26	30.88 \pm 3.8	-6706 \pm 2.78

Table 5.2.1. Binding constants and other thermodynamic parameters determined from ITC titration data for peptoids with ammonium-bearing side chains of three to five carbons in length. ΔG was calculated from $-RT\ln K_b$ and ΔS from $\Delta G = \Delta H - T\Delta S$. The values reported are mean values \pm mean % standard deviations from triplicate runs.

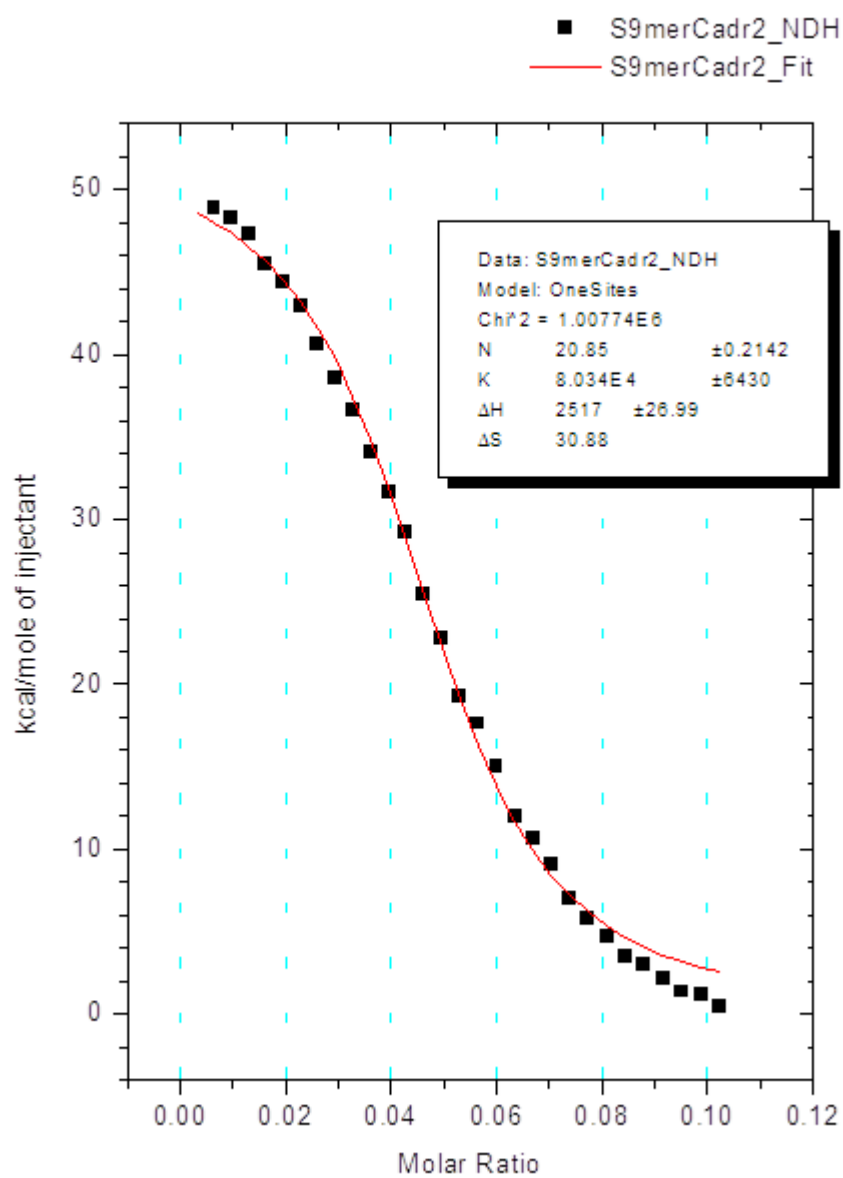


Fig. 5.2.1. ITC titration curve for titration of a 0.164mM solution of the S9-merCad peptoid with 0.126 mM heparin.

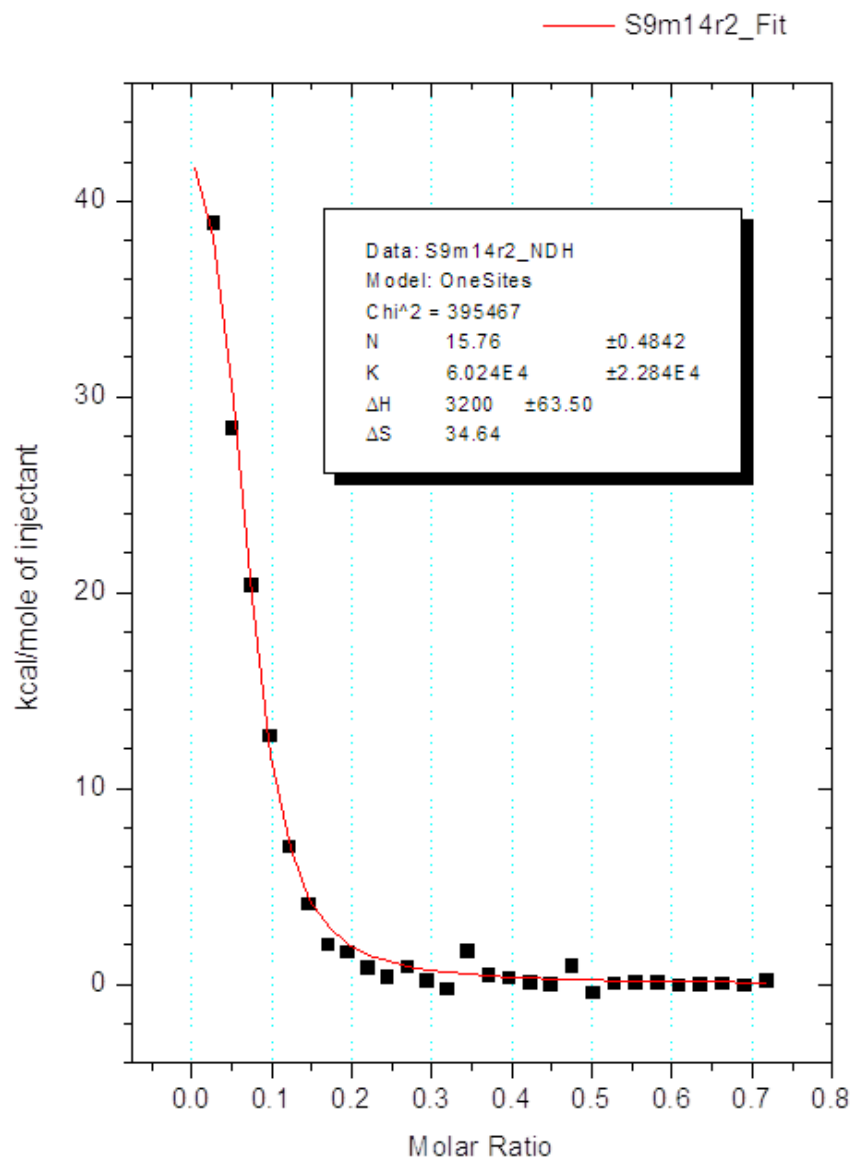


Fig. 5.2.2. ITC titration curve for titration of a 0.15 mM solution of the S9-merLys peptoid with 0.20 mM heparin.

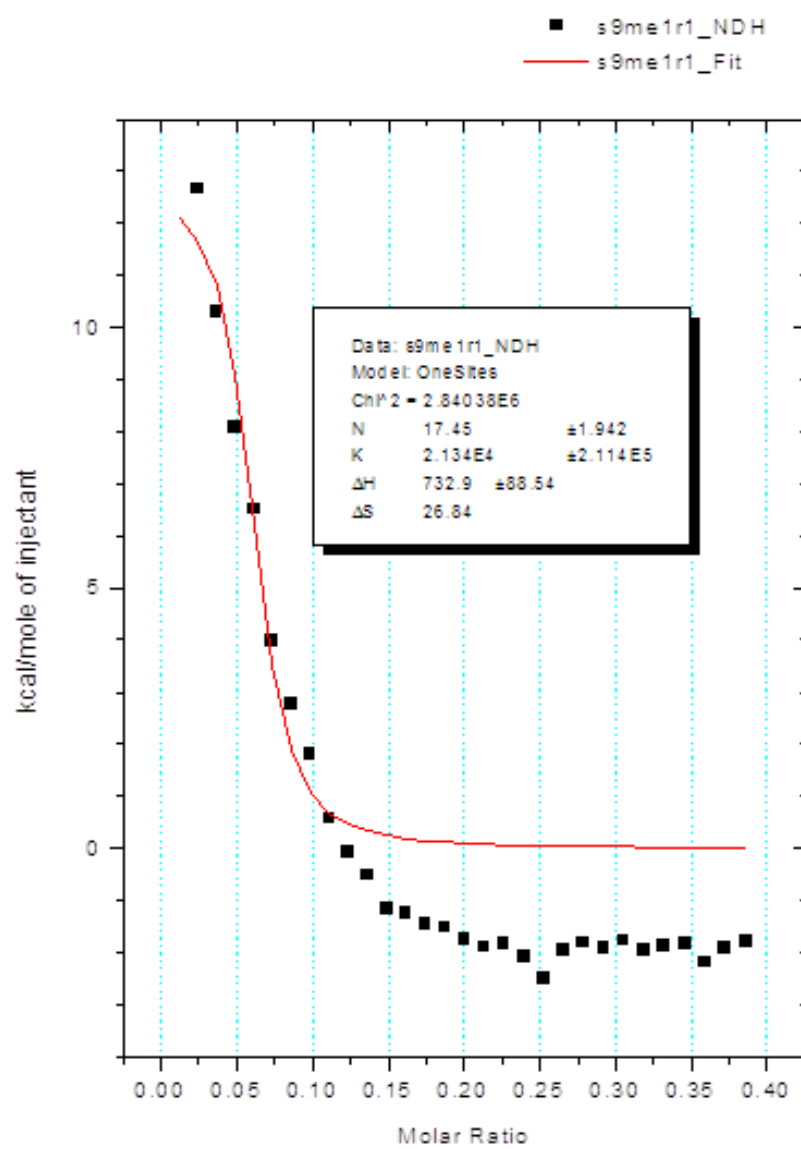


Fig. 5.2.3. ITC titration curve for titration of a 0.2 mM solution of the S9-mer peptoid, H-[N(Orn)-N(Bu)-N(spe)]₃-NH₂ with 0.25 mM heparin.

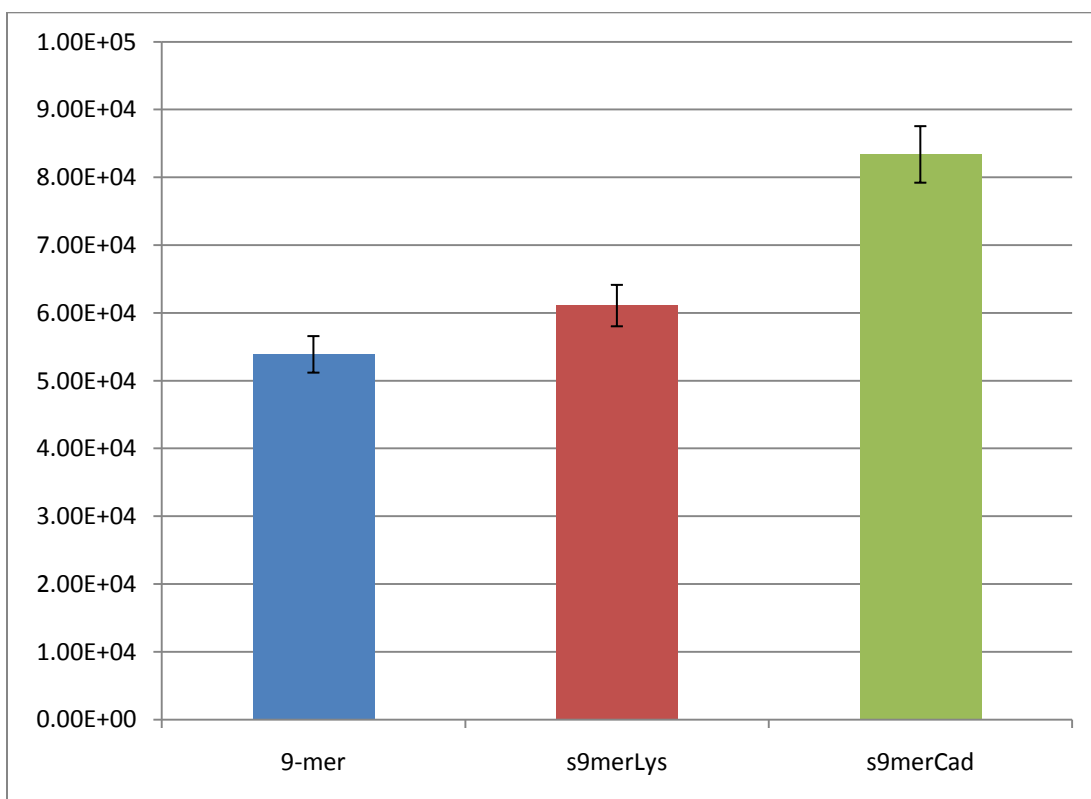


Fig. 5.2.4. Bar graph of binding constants determined by ITC for peptoids with increasing chain length for the ammonium-containing side chains.

5.2.2. Relative Heparin Binding Affinities as Determined by Heparin Affinity Chromatography.

The effect of length of the side chain bearing the cation groups on heparin binding affinity was also studied by heparin affinity chromatography (HAC) to determine relative affinities. The retention times are presented in **Table 5.2.1.** and in the bar graph shown in **Fig 5.2.5.** The bar graph displays two trends. For the ammonium – bearing peptoids, the HAC retention times increase with increasing carbon chain length, while for the guanidinium-bearing peptoids, there is little to no dependence on side chain lengths. However, the results show that, in all cases, the peptoids containing the guanidinium group bind to heparin with a greater affinity.

The retention times for the guanidinium-bearing peptoids are all close to 20 minutes (**Table 5.2.1.**). This suggests that the binding of ammonium-bearing peptoids to heparin is different in some significant way from that of the guanidinium-bearing peptoids. A potential hypothesis for this phenomena will be presented in Chapter 6 where the results of computational studies of heparin-peptoid binding are presented. The ITC data from the calibration curve presented below shows possible evidence of an increasing trend of carbon chain length to binding affinity, but only three data points were available due to the lack of guanidylated 9merMe. The synthesis of this peptoid was repeated several times but the yield was never enough to carry out the guanidinylation reaction.

Peptoid	HAC retention time \pm st. dev. (min)
s9mer	14.0 \pm 0.3
s9merLys	14.6 \pm 0.2
s9merCad	16.3 \pm 0.6
s9merG	20.6 \pm 0.2
s9merLysG	20.6 \pm 0.3
s9merCadG	20.1 \pm 0.5

Table 5.2.2. Mean HAC retention times and standard deviations for ammonium and guanidinium-bearing peptoids with cation-bearing side chains of different lengths. The reported values are mean values for three trial each.

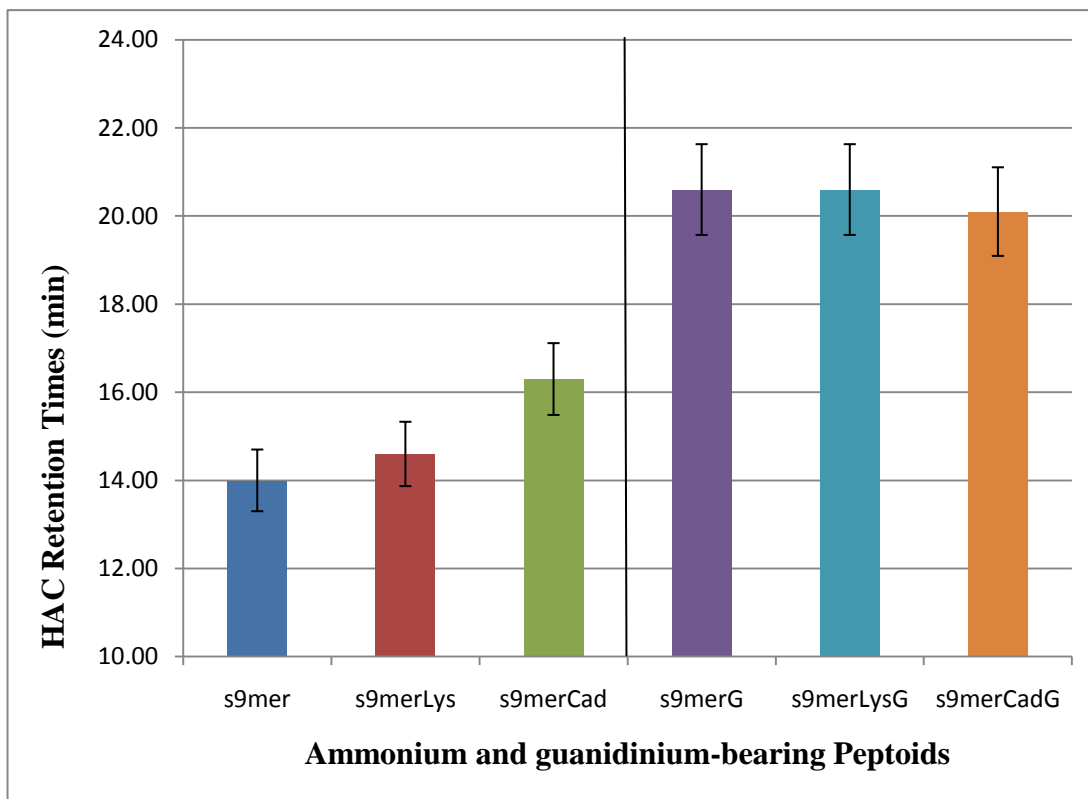


Fig. 5.2.5. Bar graph of heparin affinity retention times for cationic peptoids with different side chain lengths for the ammonium and guanidinium-bearing side chains.

5.3. The Effect of Length of the Alkyl Side Chains on Heparin-Binding Affinity

The design consideration for a study of the length of the side chain of the central monomer of the repeating trimer was that shortening the alkyl side chain could potentially enhance the binding affinity to heparin by decreasing steric hindrance between the alkyl groups and the charge-bearing side chains. To study this potential effect, binding constants were determined by ITC and relative binding affinities were determined by HAC.

5.3.1. Binding Constants

Binding constants were determined for the ammonium-bearing peptoids by ITC. The binding constants and associated thermodynamic parameters are reported in **Table 5.3.1**. Binding constants for the guanidinium-bearing peptoids were unable to be determined by ITC, but were estimated using the calibration curve, which is a plot of the ITC-derived binding constants for the ammonium-bearing peptoids versus the HAC retention times in **Fig. 5.3.1**. The resulting curve was exponential in shape, but became linear when the vertical axis, which is the binding constant axis was converted to exponential form. As can be seen, the coefficient of determination, R^2 (0.99) was quite close to unity.

The estimated values are reported in **Table 5.3.2**. The binding constants for the ammonium-bearing and guanidinium-bearing peptoids are plotted in the bar graph shown in **Fig. 5.3.2**, which is a plot of the ITC-derived binding constants for the ammonium-bearing peptoids versus the HAC retention times .in **Fig. 5.3.1**.

Peptoid	N	$K_b (M^{-1})$	ΔH (cal/mole)	ΔS (cal/mole)	ΔG (cal/mole)
s9merMe	23.55 ± 0.72	$1.1923 \text{ E}5 \pm 376.2$	1967 ± 37	29.81 ± 1.3	-6917 ± 5.6
s9merEth	16.14 ± 0.93	$8.8439 \text{ E}4 \pm 6277$	2357 ± 35	30.52 ± 5.8	-6738 ± 6.9
s9merProp	6.008 ± 0.45	$8.8662\text{E}4 \pm 985.4$	2361 ± 63	30.54 ± 4.2	-6742 ± 7.4
s9mer	17.87 ± 2.65	$5.39\text{E}4 \pm 9386$	814 ± 89	24.36 ± 1.2	-6447 ± 2.9

Table 5.3.1. ITC data for ammonium analogs with varied central side chain. ΔG was calculated from $-RT \ln K_b$. All are mean values \pm mean % st. dev. from triplicate runs.

peptoid	K_b (M^{-1})	ret. time (min)
9-merG	2.00E+05	20.6 ± 0.5
s9merPropG	1.89E+05	20.3 ± 0.6
s9merEthG	2.39E+05	21.5 ± 0.5

Table 5.3.2. Mean HAC retention times for triplicate runs ± standard deviation. K_b was estimated from the calibration curve shown in **Fig. 5.3.1.**

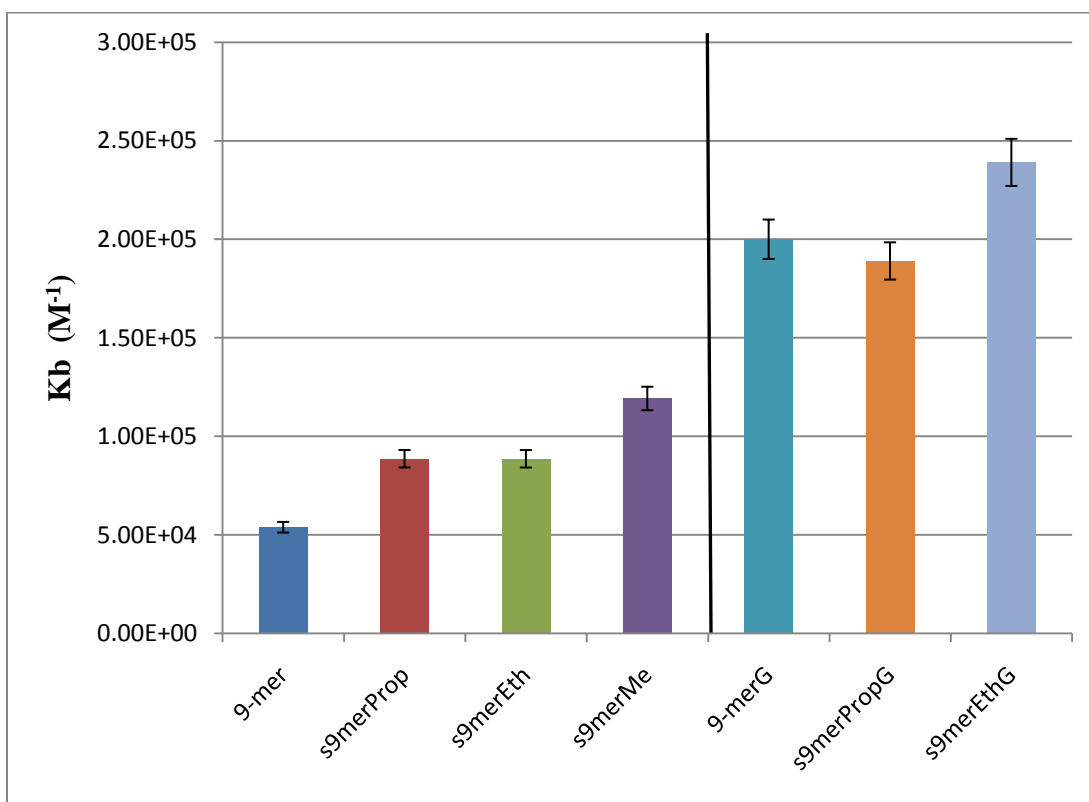


Fig. 5.3.1. Bar graph of estimated binding constants determined by ITC for ammonium-bearing peptoids and binding constants estimated for guanidinium-bearing peptoids from the plot of binding constant vs. HAC retention time in **Fig. 5.3.2**. The peptoids have alkyl side chains from butyl to methyl groups.

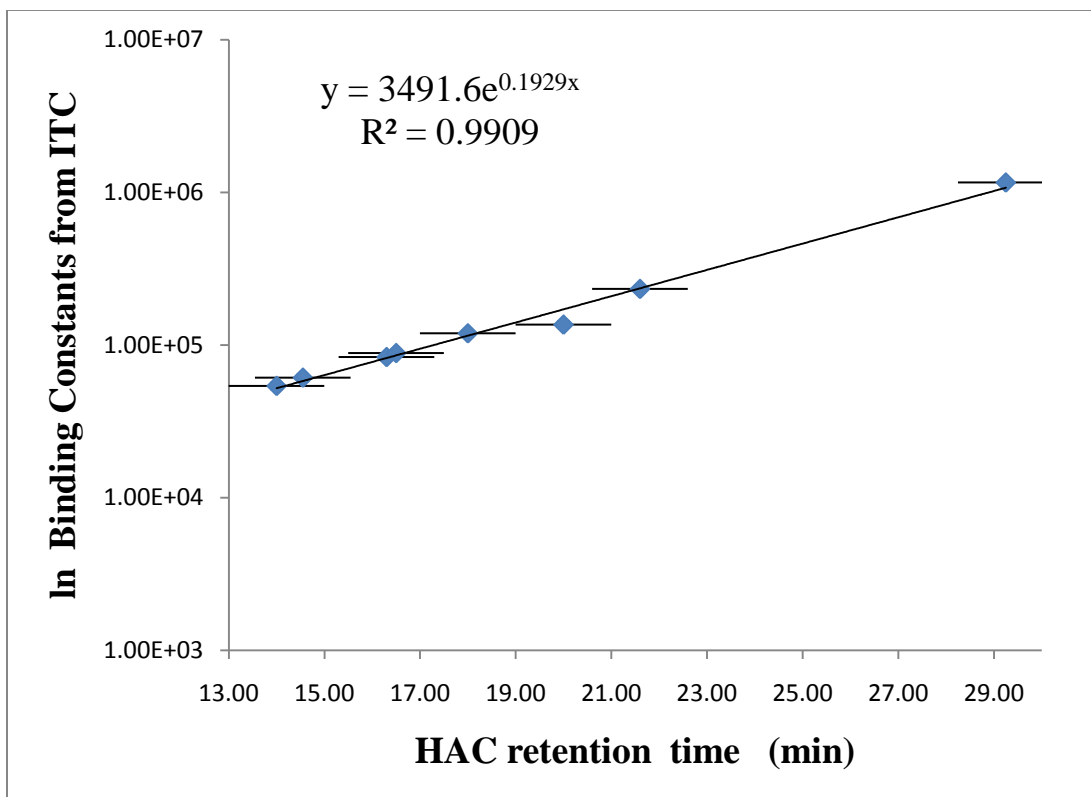


Fig. 5.3.2. Calibration curve obtained from the natural log of the ITC binding constants and the HAC retention times for peptoids with ammonium side chains. The mean values and standard deviations from triplicate runs for the ITC binding constants and HAC retention times are reported in **Table 5.3.3.**

Peptoid	HAC retention times (min)	ITC K_b (M^{-1})
s9mer	14 ± 0.4	5.39E4 ± 9386
s9merLys	14.55 ± 0.2	6.11E4 ± 4.22E4
s9mercad	16.3 ± 0.6	8.34E4 ± 8430
s9merEth	16.5 ± 0.5	8.8439 E4 ± 6277
s9merMe	18 ± 0.5	1.1923 E5 ± 376.2
s9mAll	20 ± 02	1.364E5 ± 4.22E5
12mer	21.6 ± 0.6	2.33E5 ± 37950
9mBz	29.25 ± 0.5	1.16E6 ± 3.7E4

Table 5.3.3. The peptoids, their mean values and standard deviations from triplicate runs for ITC binding constants and HAC retention times that were used to construct the calibration curve shown in **Fig.5.3.2**.

5.3.2. Heparin Affinity Chromatography Results

The mean heparin affinity chromatography retention times for ammonium and guanidinium-bearing peptoids are presented in **Table 5.4.1.** and in bar graph form in **Fig.5.3.3.** The mean retention times were obtained from triplicate runs. The ammonium-bearing peptoids are on the left and the guanidinium-bearing peptoids are on the right of the vertical dividing line in **Fig.5.3.3.**

5.4. Heparin Affinity for Peptoids Containing Other Side Chains

5.4.1. Introduction

Two additional analogs were designed by substituting an allyl group and benzyl group for the alkyl group on the central monomer unit. The design consideration was to see if changing a nonreactive alkyl group for a reactive group such as an allylic or benzylic group, would enhance binding to heparin. Positions adjacent to the π system in both allylic and benzylic groups possess enhanced reactivity in comparison to simple alkyl positions due to the proximity of the adjacent π system. This position, which in this case would be alpha to the backbone nitrogen of the peptoid amide, could be subjected to allylic or benzylic bromination by use of NBS (N-bromo-succinimide), which would then create a good leaving group, thus allowing further functionalization by substitution reactions. Another possibility would be to use the allyl group as a protecting group that could then be selectively removed through use of a ruthenium catalyst¹ (RuCl_3), which would allow the production of peptoids with hydrogen in the position that normally is filled by a side chain, thus producing a mixed hybrid with glycines in selected positions.

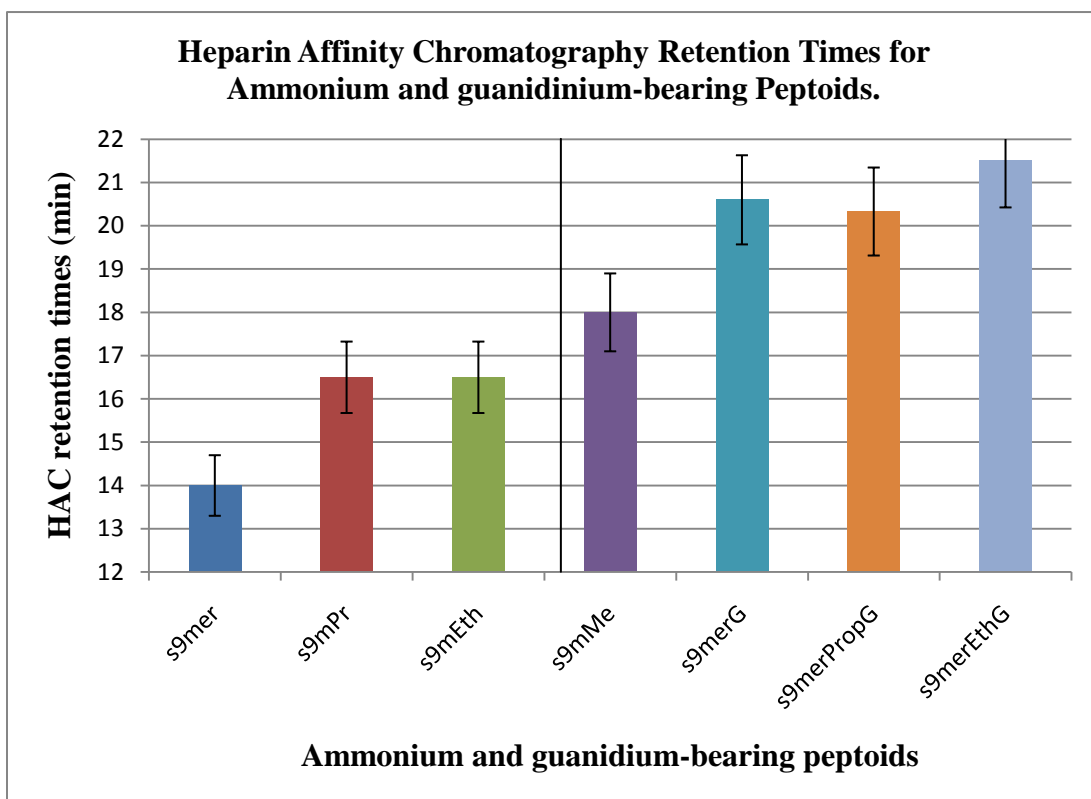


Fig.5.3.3. Bar graph of HAC retention times for ammonium and guanidinium-bearing peptoids.

Peptoid	HAC ret. times (min) \pm st. dev.
S9-mer	14 \pm 0.4
S9-merPr	16.5 \pm 0.7
S9-merEt	16.5 \pm 0.5
S9-merMe	18 \pm 0.5
S9-merG	20.6 \pm 0.5
S9-merPrG	20.3 \pm 0.6
S9-merEtG	21.5 \pm 0.5

Table 5.4.1. Mean values for Heparin Affinity Chromatography retention times \pm standard deviations for triplicate runs. The data is also presented in the bar graph shown in **Fig.5.4.1**.

If one wanted to produce a peptoid with a smaller side chain than methyl in the alkyl series, then hydrogen could be used by this method, enhancing the binding trend produced by shorter alkyl side chains with less steric hindrance. Of course an alternative method to accomplish this same goal is to construct a hybrid using glycine in the desired position. The feasibility of this method would depend upon the viability of the deprotection step using ruthenium chloride.

Regarding the use of a benzyl side chain, the design consideration was that the secondary helical structure could be affected by inclusion of a second benzene ring that could interact with the chiral *spe* group by $\pi - \pi$ stacking or by steric repulsion between large aromatic systems in close proximity. The question remained as to would the interaction result in enhanced or decreased heparin binding affinity.

The structures of the peptoids with the allyl and benzyl groups are shown in **Fig. 5.4.1**.

5.4.2. ITC Results for Other Side Chain-Bearing Peptoids.

Binding constants were measured by ITC and the results are presented in **Table 5.4.2**. As can be seen, the binding data for the benzyl analog is exothermic. Because binding the benzyl analog was exothermic, raw ITC titration data and the titration curve for one of the runs is presented in **Fig. 5.4.2** and **Fig. 5.4.3**. The binding constants are also presented in bar graph format in **Fig. 5.4.4**. The greater

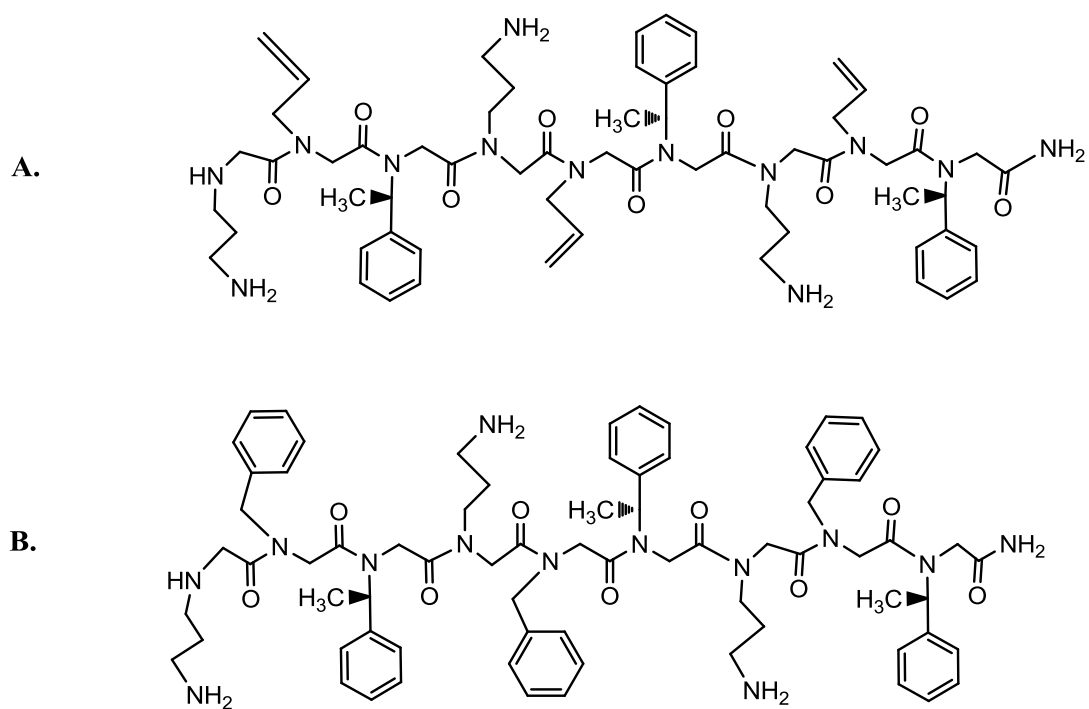


Fig. 5.4.1. The structures for the peptoids studied in this section. **A.** is the allyl-bearing peptoid designated as s9merAll, while **B.** is the benzyl-bearing peptoid designated as s9merBz.

Peptoid	N	$K_b(M^{-1})$	$\Delta H(\text{cal/mole})$	$\Delta S(\text{cal/mole})$	$\Delta G(\text{cal/mole})$
s9-mer	17.86 \pm 2.65	5.39E4 \pm 9386	814 \pm 89	24.36 \pm 1.2	-6447 \pm 2.9
s9-merAllyl	11 \pm 1.20	1.364E5 \pm 4.22E5	2794 \pm 119	32.85 \pm 4.6	-6995 \pm 5.5
s9-merBz	13.87 \pm 0.12	1.16E6 \pm 3.7E4	-5421 \pm 21	9.6 \pm 0.05	-8308 \pm 8.8

Table 5.4.2. ITC data for ammonium analogs. ΔG was calculated from $-RT\ln K_b$ and ΔS from $\Delta G = \Delta H - T\Delta S$. The S9-mer is included as a reference. Data represents mean values \pm standard deviation.

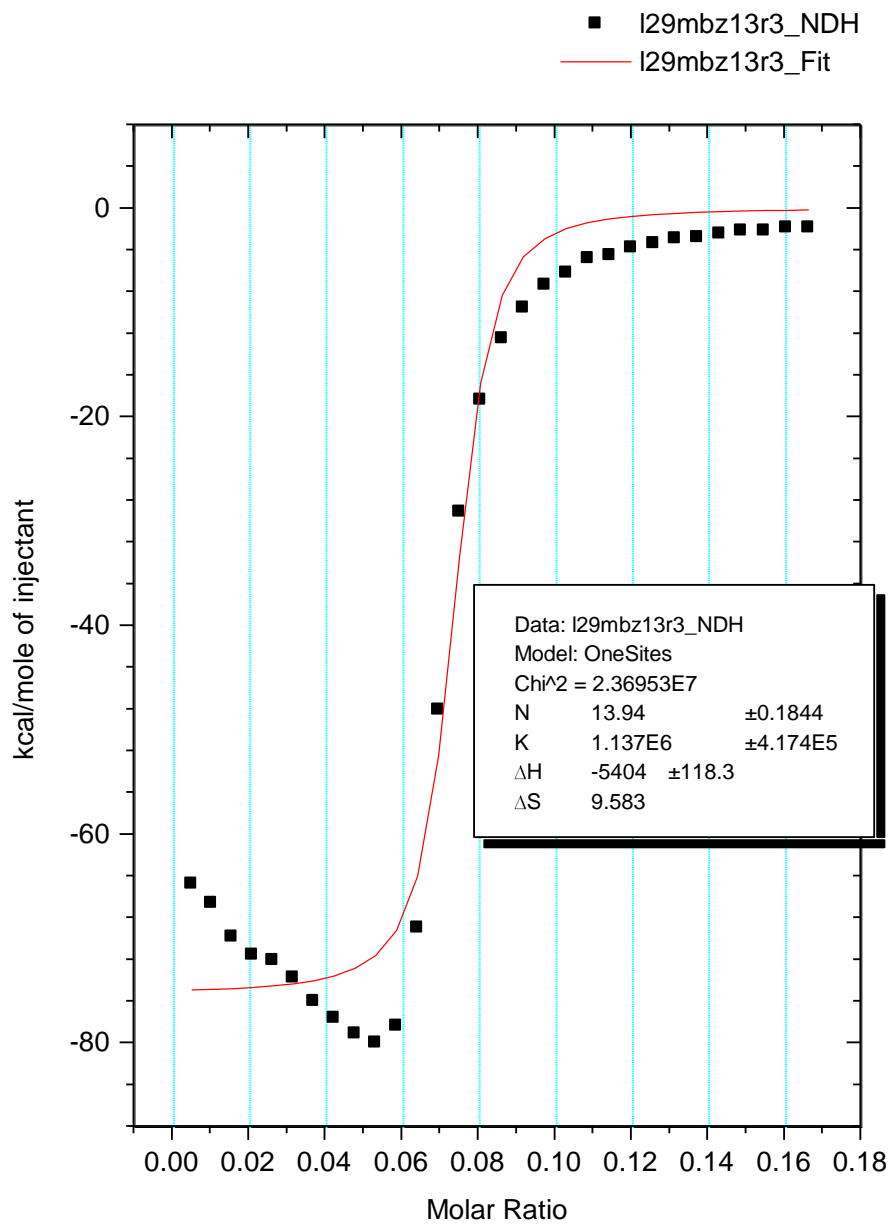


Fig. 5.4.2. Titration curve for the S9-merBz peptoid showing the exothermic nature of the binding.

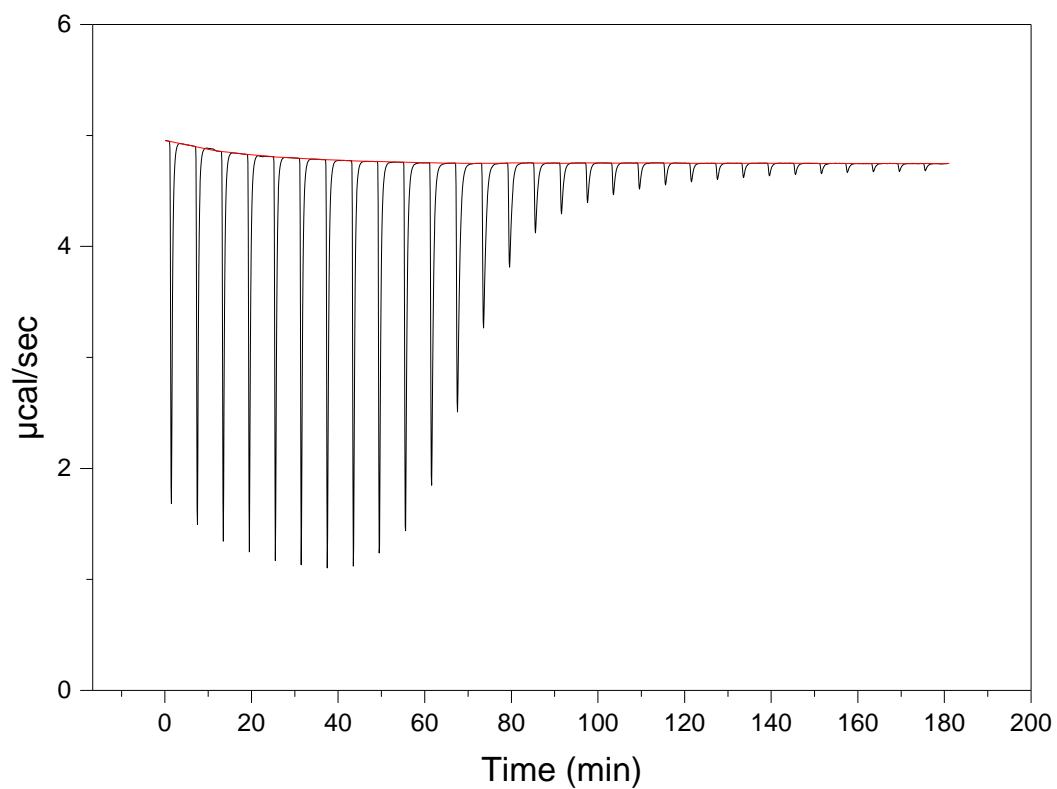


Fig. 5.4.3. Raw ITC titration data for the titration of 0.2mM S9-merBz with 0.25 mM heparin. The downward spikes are indicative of an exothermic reaction as the system reduces its power to compensate for the heat given off by the reaction.

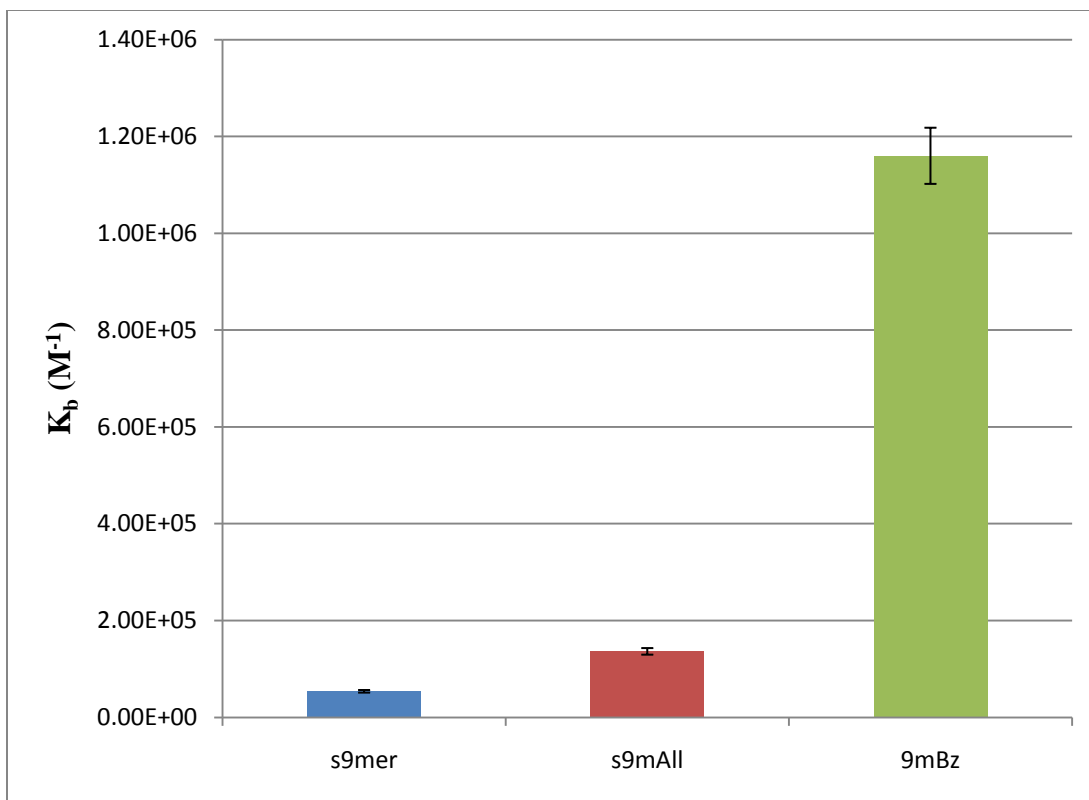


Fig. 5.4.4. Bar graph of ITC binding constants presented in **Table 5.4.2.** The difference in magnitude of the binding constant for the benzyl analog can be clearly seen in this plot.

magnitude of the binding constant of the benzyl analog compared to the S9-mer for reference and the allyl analog is made clear by the bar graph.

5.4.3. Heparin Affinity Chromatography Retention Times for Other Side Chain-Bearing Peptoids.

The HAC retention times are presented in **Table 5.4.3.** and in bar graph form in **Fig. 5.4.5.** Data is the mean values and standard deviations for triplicate runs. The retention time for the S9-merBz is significantly larger than for the other two peptoids, consistent with the finding that its binding constant is significantly larger (**Table 5.4.2.**)

5.5. Discussion

The design considerations explored in this chapter were the effects on heparin binding affinity resulting from changing the carbon chain lengths of two monomer units, i.e., the first one was the carbon chain connecting the backbone nitrogen to the cationic group terminating the chain and interacting with the anionic sulfonic acids and esters on heparin, the second was the length of the alkyl chain on the center monomer unit in the repeating trimer sequence, and the third was substitution of the central monomer unit with two other side chains, i.e., with allyl and benzyl groups.

It was hypothesized that longer carbon chains on the charge-bearing ammonium and guanidinium groups would more effectively bind to their anionic counterparts on the heparin molecule. This was possible to investigate due to the commercial availability of monoBoc protected diamines from 3 to 5 carbons in length.

Peptoid	HAC ret. times (min)
S9-mer	14 ± 0.4
S9-merAll	20.14 ± 0.2
S9-merBz	29.25 ± 0.5

Table 5.4.3. Heparin Affinity Chromatography mean retention times ± standard deviations for triplicate runs. The data is also presented in the bar graph shown in **Fig.5.4.5.**

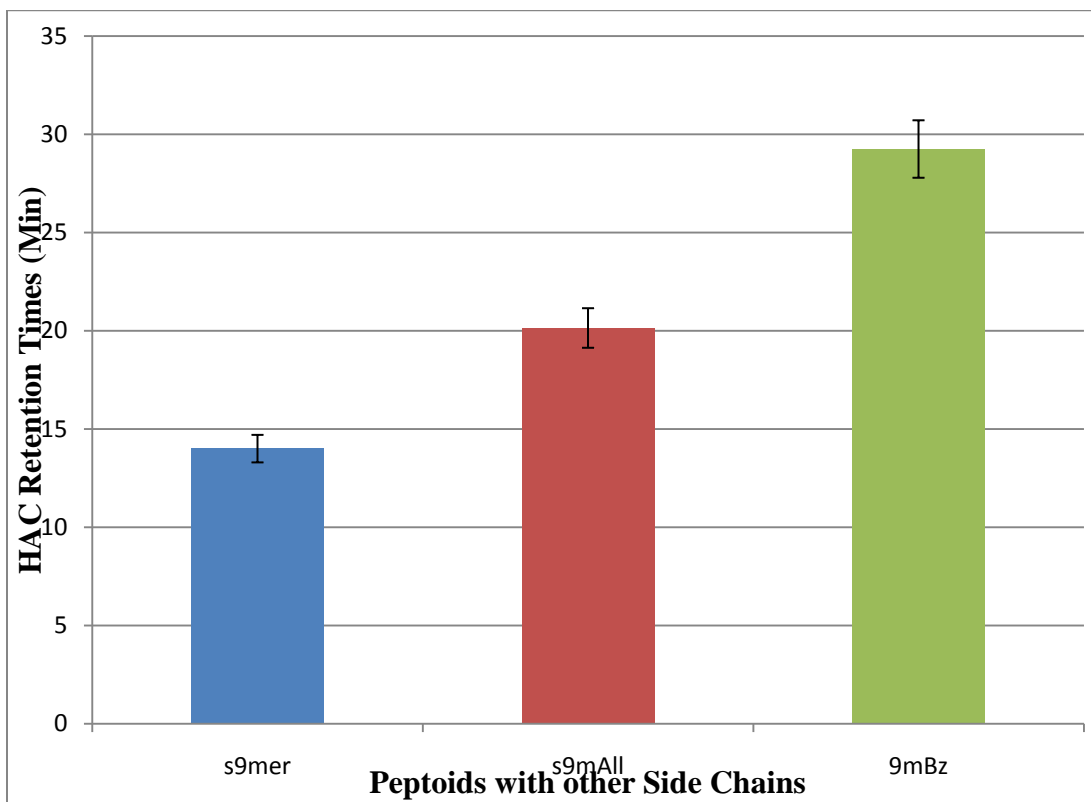


Fig. 5.4.5. HAC retention times from the data presented in **Table 5.7.**,

By using monoBoc protected diamino-propanes, butanes and pentanes in the synthesis, it was possible to increase the length from three to five carbon units in length. The ammonium groups were also converted to guanidinium groups to study the effect of extended carbon chains on the heparin affinity for guanidinylated peptoids as compared to ammonium-bearing peptoids. Both binding constants and HAC retention times demonstrated a trend for the ammonium-bearing carbon chains. In this case, extending the carbon chain did result in enhanced binding to heparin. The effect was quite clear in the bar graphs of the ITC-obtained binding constants and the HAC retention times, which are exponentially correlated with binding constants as demonstrated in a calibration curve produced from HAC retention times and the natural logs of the ITC binding constants, as shown in **Fig. 5.3.2**.

For the case of the extended carbon chains connecting the guanidinium groups, there was insufficient data to demonstrate the same trend as there was insufficient 9merMe available to synthesize the guanidinylated peptoid. For all the peptoids, the HAC retention times and the estimated binding constants obtained from the calibration curve, indicate greater binding affinity for the guanidinium-bearing peptoids compared to ammonium-bearing peptoids. The HAC retention times for guanidinium-bearing peptoids with increasing chain length were all close to 20 minutes. It is possible that the effect of guanidylation overshadows the trend toward increasing binding efficiency due to extending carbon chain length as in the case of the ammonium-bearing peptoids.

The second design consideration investigated was the effect of the alkyl chain length of the central monomer unit on heparin binding affinity. A clear trend emerged from this study that was predicted by the hypothesis that a shorter alkyl chain length would result in enhanced heparin affinity due to decreasing the effect of steric hindrance between neighboring groups and the alkyl chain, especially regarding the charged side chain. The data supports the hypothesis, as both the binding constants and the HAC-derived heparin binding affinity was enhanced by shorter alkyl chains. The effect may also apply to the case of guanidinium-bearing peptoids as well, as the estimated binding constants derived from the calibration curve show a possible trend as can be seen in **Fig. 5.3.3**.

The results in the third section , which was to determine the effect on heparin affinity of the substitution of the central monomer unit in the trimer sequence with a more reactive side chain or a bulkier side chain. The ITC results indicate that the inclusion of an allyl group in the center position of the repeating trimer resulted in some enhancement in heparin affinity, while the benzyl group added to the same position resulted in a great enhancement in heparin binding affinity. In fact when comparing the allyl ITC binding data to the alkyl chain-bearing ITC binding data, the allyl group scored higher than a methyl group.

The reason for this phenomena is unknown. Since it produced larger binding constants than any ammonium-bearing peptoids with alkyl side chains on the central monomer unit, there may be either a direct effect on binding related to interactions

between side chains on the same peptoid, or an indirect effect on secondary structure, resulting in enhanced heparin binding affinity. The greatly enhanced binding affinity for the benzyl-containing peptoid, which can be seen in the bar graph in **Fig.5.4.4**, was the highest of any of the peptoids studied. This will be investigated in Chapter Seven, where results of a computational study of heparin-peptoid binding are presented. The HAC retention times show the same trends, with the benzyl side chain-bearing peptoid displaying retention times similar to those of guanidinium-bearing peptoids with highest heparin affinity.

The results obtained in this section was a shot in the dark, and done out of scientific curiosity, and provided some serendipitous and surprising data. It is for this reason that counterintuitive approaches to rational drug design should not be left out of experimental studies. As it turns out, the benzyl group in the center position provided very scientifically intriguing results that could not be predicted. The main reason it was tried was availability of starting materials, which were on the shelf.

5.5. Summary

A series of analogs of heparin binding peptoids were synthesized based upon two design considerations. The length of the carbon chain connecting the backbone nitrogen to the charged ammonium and guanidinium groups was lengthened and found in the case of the ammonium-bearing side chain to be positively correlated with heparin binding affinity. The same effect was not clear regarding the guanidinium-bearing side chains. This could either be due to insufficient data or it is

quite possible that the effect was overshadowed by the strong binding affinity of the guanidinium group in comparison to the ammonium group.

The length of the central alkyl chain of the repeating trimer was decreased in order to limit the effects of steric hindrance on heparin binding affinity. This resulted in data that supported the hypothesis that shorter alkyl chains in this position enhance heparin binding affinity for both ammonium and guanidinium-bearing peptoids.

Additionally, the same central position on the repeating trimer sequence was substituted with an allyl and a benzyl group. The results of the allyl substitution indicate that there is potential for further study as the heparin binding affinity was higher than expected and may be of use in post peptoid synthesis side chain functionalization, or as an alternative means of introducing a glycine monomer in a sequence without chaining the submonomer methodology. The allyl group is a commonly used means of protecting an amide nitrogen¹. Its removal under aqueous conditions at room temperature using ruthenium chloride makes this a potentially useful means of protection of a peptoid amide nitrogen position, followed by removal to produce a peptoid-peptide hybrid without deviating from Zuckermann's submonomer approach to peptoid synthesis. An example reaction scheme for the deprotection of an amide using ruthenium chloride as a catalyst is shown in **Fig. 5.4.6.**

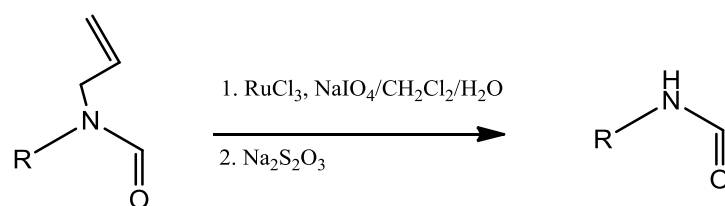


Fig. 5.4.6. Reaction scheme for the removal of an allyl amide protecting group using ruthenium (III) chloride with sodium thiosulfate, used to quench the reaction. The reaction takes place at room temperature and is monitored by TLC for completion.

The most significant data from this last series of substitutions came from the placement of a benzyl group in the central position of the repeating trimer sequence. The enhanced binding affinity was comparable to the guanidinium-bearing peptoids and was completely unexpected. The binding of benzyl-bearing peptoids to heparin will be discussed in Chapter Six where the results of computational studies are presented.

5.6. References

1. Alcaide, B. A., Almendros, P., Alonso, J.M. . *Chemistry-A European Journal* **2006**, *12*, 2874-2879.

Chapter 6: Computational Results

6.1 Introduction

Throughout the course of the dissertation research, one of the aspects that caused much curiosity was the nature of the interaction between the peptoids and heparin. While ITC can provide some information about the binding process such as the thermodynamic parameters and the binding constant, what it can't do is to visualize the docking of the peptoids to the macromolecule, i.e., heparin. To explore the nature of this interaction, a program known as 'AutoDoc Vina', designed by the Molecular Graphics Lab at The Scripps Research Institute¹ was used. The peptoids were constructed and minimized using Spartan '08² before saving them as pdb files.

Spartan 08 was also used to investigate the global minima of several ammonium-bearing peptoids using molecular mechanics level of theory MMFF. In this way the user can input or draw a target molecule and select a set of the lowest energy level conformers for viewing. Higher levels of theory were also investigated but it was found that the investment in computation time was too high to be of much use, and it wasn't until AutoDoc Vina was discovered on the Scripps Molecular Graphics Lab website, that a valuable *ab initio* methodology was found that could be applied resulting in useful information regarding the interaction between peptoids and heparin.

The computations were carried out on an ASUS model G73, with an Intel i7 core processor, which the program recognizes as 8 CPUs. This allowed AutoDoc Vina to

carry out a docking computation in 1.2 hours for a 9-mer binding to a fragment of heparin obtained from the RCSB Protein Data Bank³. The heparin fragment has six disaccharide units and is designated as 1HNP. AutoDoc Vina and its associated software run in a Microsoft Windows environment.

The docking of various peptoids to the heparin fragment were conducted and the results are presented in this chapter. Some were peptoids actually synthesized in this research, and a few were constructed based upon the resulting trends discovered by trial and error and rational drug design methodologies explored in this research.

Image files were produced for several peptoids docked to heparin to observe the potential docking that takes place. The target ligands were constructed and briefly minimized in Spartan '08 before inputting them into AutoDoc Tools v.1.5.4., a program written in Python by the Molecular Graphics Lab at Scripps. It comes as part of a software package called MGL Tools. This software is open sourced and is free of charge by noncommercial users along with AutoDoc Vina, providing that the user credits the manufacturers at Scripps (see reference 1.) .

Before the target ligand was added to AutoDoc Tools, the macromolecule was first saved in pdb format. The program requires that hydrogens occupy all of their normal positions, so as one of the first steps undertaken, hydrogens are added. When the ligand is added, the program has settings for flexibility of each or all of the bonds under the heading 'tortion tree'. The backbone amides were all allowed complete freedom of rotation to allow the highest level of accuracy, as it is known that

peptoids can undergo cis/ trans isomerism. To choose the search space, which is the part of 3D-space that the program explores to investigate the interaction between the ligand and the macromolecule, a grid is selected and adjusted by the user. The macromolecule is saved as a pdbqt file along with the ligand, also as a pdbqt file. AutoDoc Tools is then closed and a command window (also known as a Dos box) is opened, from which Vina is actually run. The easiest way to locate the folder locations used in the command window is to open the folder in Windows first and then copy and paste its location into the command window. The complete command set can be observed by selecting `-help` after selecting the appropriate path tree followed by the program name `vina.exe`. The program is very location specific and as in computer language coding, is very specific regarding the command chain. The information previously selected by the user in the grid box is placed in a txt file that is named `conf.txt`, which is called upon in the command chain following `-config`. The final command chain will look similar to the following command line: `"c:/path/The Scripps Research Institute/ vina/ vina.exe" -config conf.txt -log log.txt .` At this point 'enter' is pressed and AutoDoc Vina starts its computations.

To read the output file, Pymol v. 1.5.4 can be used, and is contained in the MGL Tools software package. Pymol is short for Python Molecular Viewer, since it too is written in Python computer language. The file will now be a pdbqt output file.

6.2 Results for the Docking of the Chiral 12-mers

It was shown by ITC and HAC retention times that there was some difference in the binding of the two chiral peptoids to heparin, but what that difference was based upon the data available was unclear. Docking the two models, constructed in Spartan '08, to a fragment of heparin obtained from the RCSC protein data bank, designated as 1HPN³ yielded some fascinating and insightful data that may explain the difference between the two analogs. A jpeg file of the heparin fragment (six disaccharides in length) alone is presented in **Fig. 6.2.1**. In the case of the R analog, an image file is presented in **Fig. 6.2.2**, that shows the left-handed peptoid loosely attached to one face of the heparin fragment. The image files of the right-handed S analog attached to heparin is shown in **Fig. 6.2.3**. It is the latter image file that displays the character that is seen in the docking results with all ammonium-bearing S peptoid analogs: the peptoid interweaves into the helical groove of the heparin molecule. In comparison to the loose binding of the R form, the image for the S form provides significant insight into the actual binding phenomena between both chiral analogs and heparin. This would explain why the S peptoid analogs bind with enhanced affinity to heparin compared to the R form. The right-handed S peptoid interacts through wrapping around the groove of the helical heparin, which appears to be enhanced by the right-handedness of the peptoid. The left-handed R peptoid apparently can't fit into the groove due to the left-handedness interfering with the ability to enter the groove of the peptoid. This phenomena applies especially to the chiral peptoids, as there are other binding modalities that are possible that do not

require interlacing of the peptoid into the groove of heparin that also result in enhanced binding. These other binding modalities will be discussed below.

6.3. Results for the Docking of Ammonium-Bearing Peptoids to Heparin

The results of docking calculations for an s9-mer peptoid in ball and stick format docked to heparin, which is in molecular surface format with the atoms colored by atom type, is shown in **Fig.6.3.1**. The terminal nitrogens on the charge-bearing side chains are shown in their ammonium format with three hydrogens attached. The atoms on the heparin are given the following colors: red is oxygen; yellow is sulfur; carbon is white, and for the peptoid: blue are the nitrogens and the carbons are shown in grey. It should be noted that the dihedral angles of the backbone amide groups of the docked peptoids were a mixture of cis/trans amides. The amide bonds were allowed complete freedom, which resulted in the conformers undergoing cis/trans isomerism resulting in a mixture of some cis and some trans dihedral angles including ω . Measuring the dihedrals of S9-merBz gave the following ω ' dihedrals, starting from the C-terminus: $\omega_1 = -4.8^\circ$ (cis), $\omega_2 = -3.4^\circ$ (cis), $\omega_3 = -179^\circ$ (trans), $\omega_4 = -13.4^\circ$ (cis), $\omega_5 = 172^\circ$ (trans), $\omega_6 = -168^\circ$ (trans), $\omega_7 = 12.3^\circ$ (cis), $\omega_8 = -120^\circ$ (diminished trans) ignoring the amide at the C-terminal end. These measurements were taken by hiding the heparin molecule in Pymol viewer and measuring the dihedrals one at a time across the length of the peptoid. As can be seen, four of the ω dihedrals assume a cis conformation and four assume a trans conformation. This suggests that sections take up a cis conformation then switch to trans in order to

more tightly bind to the heparin. Eventually, through practice, it became possible to observe whether the dihedrals were cis or trans by inspection, without measurement. In this way a S9-mer gave the following dihedral pattern: starting from the C-terminus and ignoring the terminating amide, ω_1 (spe₁) = cis; ω_2 (Bu₁) = cis; ω_3 (Cad₁) = trans; ω_4 (spe₂) = trans; ω_5 (Bu₂) = trans; ω_6 (Cad₂) = trans; ω_7 (spe₃) = cis; ω_8 (Bu₃) = trans. As can be seen here most of the peptoid is in the trans conformation, which would result in a helix.

6.4 Results for the Docking of Guanidinium-bearing Peptoids to Heparin

The guanidinium-bearing peptoids docked to heparin by a similar means. An example of a peptoid expected to bind well to heparin is shown in **Fig. 6.4.1**. The sequence is H-[N(Cad)G-N(Et)-N(spe)]₃-NH₂. It was chosen based upon the binding studies of Chapters 4 and 5. This peptoid was not synthesized but a similar peptoid would be selected for future studies, which would be a culmination of everything learned in this research. It should be noticed that the peptoid lays along the face of the heparin molecule.

6.5 Results for the Docking of a Benzyl-bearing Peptoid to Heparin.

In the previous chapter, it was found that benzyl-bearing side chains in H-[N(Orn)-N(Bz)-N(spe)]₃-NH₂ yielded a peptoid with greatly enhanced binding affinity to heparin. Based upon that data, it was desirable to investigate the docking

of a benzyl-bearing peptoid to heparin to see if additional information could be obtained.

The results are shown in **Fig. 6.5.1**. The benzene rings in the figure can be seen to align suggesting that π - π stacking may be responsible for the enhanced binding affinity between peptoid and heparin.

6.6 Discussion and Conclusions

The examples shown in this chapter indicate three different binding modalities. The chiral S-ammonium-bearing 12-mer peptoid shown in **Fig. 6.2.3** and the S-ammonium bearing peptoids in general as seen also in **Fig.6.3.1** bind in a fashion typical for this class of peptoids. The S-peptoids with ammonium groups tend to fit into the groove that is evident in the molecular surface of heparin. This is also true for the guanidinium-bearing groups. They also fit into the groove and so bind in the groove of heparin, contrary to the original model discussed in Chapter One predicted. The enhanced binding affinity of the guanidinium-bearing peptoids is probably due to the increased hydrogen bonding of the guanidinium group over the ammonium group.

One peptoid with surprisingly high heparin binding affinity was the benzyl-bearing peptoid H-[N(Orn)-N(Bz)-N(spe)]₃-NH₂. The reason why this peptoid possessed enhanced binding affinity was hypothesized to be due to pi stacking between the multiple benzene rings from the benzyl groups and the spe monomers.

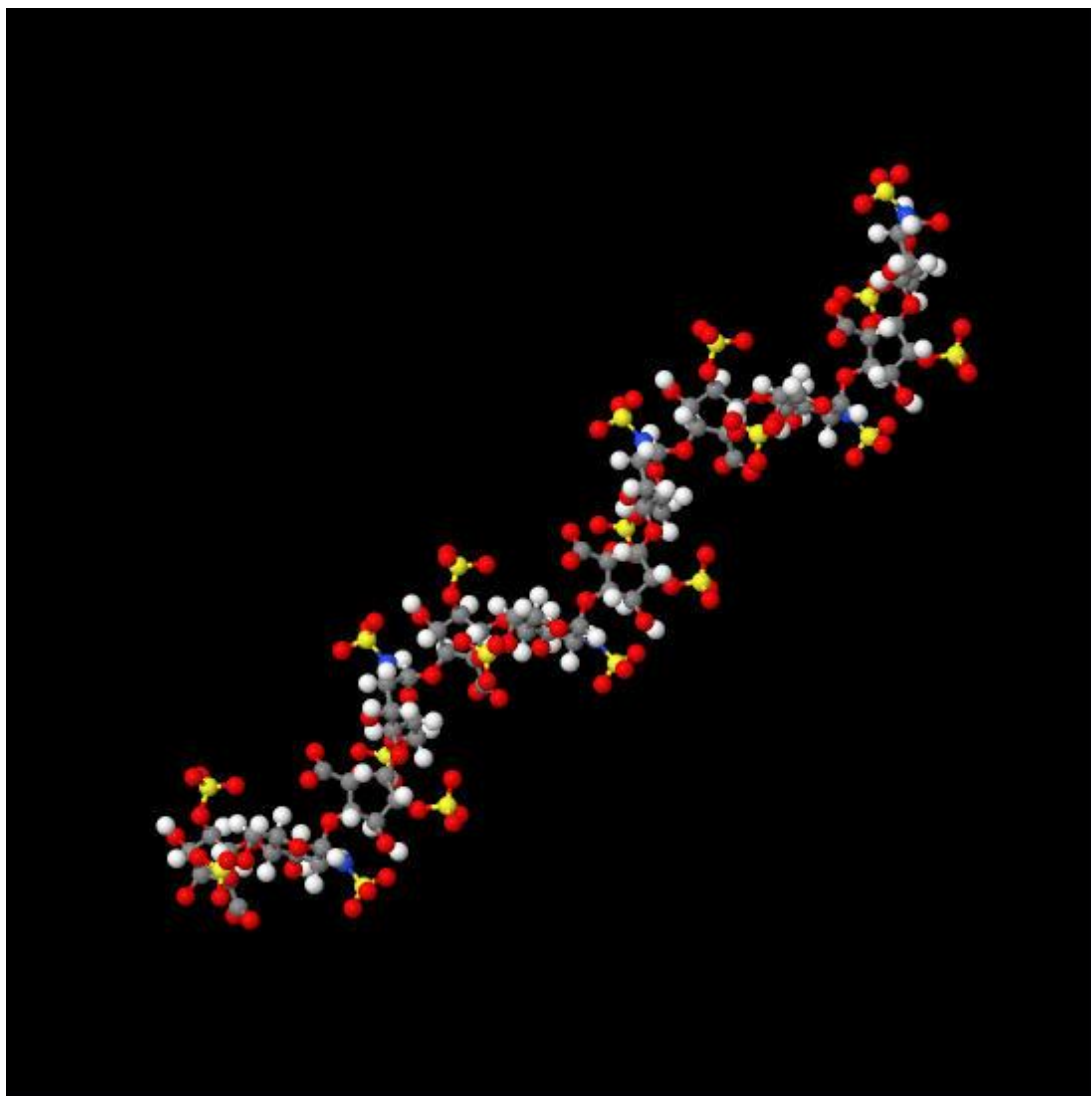


Fig. 6.2.1. Heparin hexadissacharide fragment obtained from the RCSB Protein Data Bank and used in these docking studies. Notice the helical structure of heparin. Also visible is the groove that winds around the heparin fragment. It is even more apparent in the molecular surface map format used in the docking images.

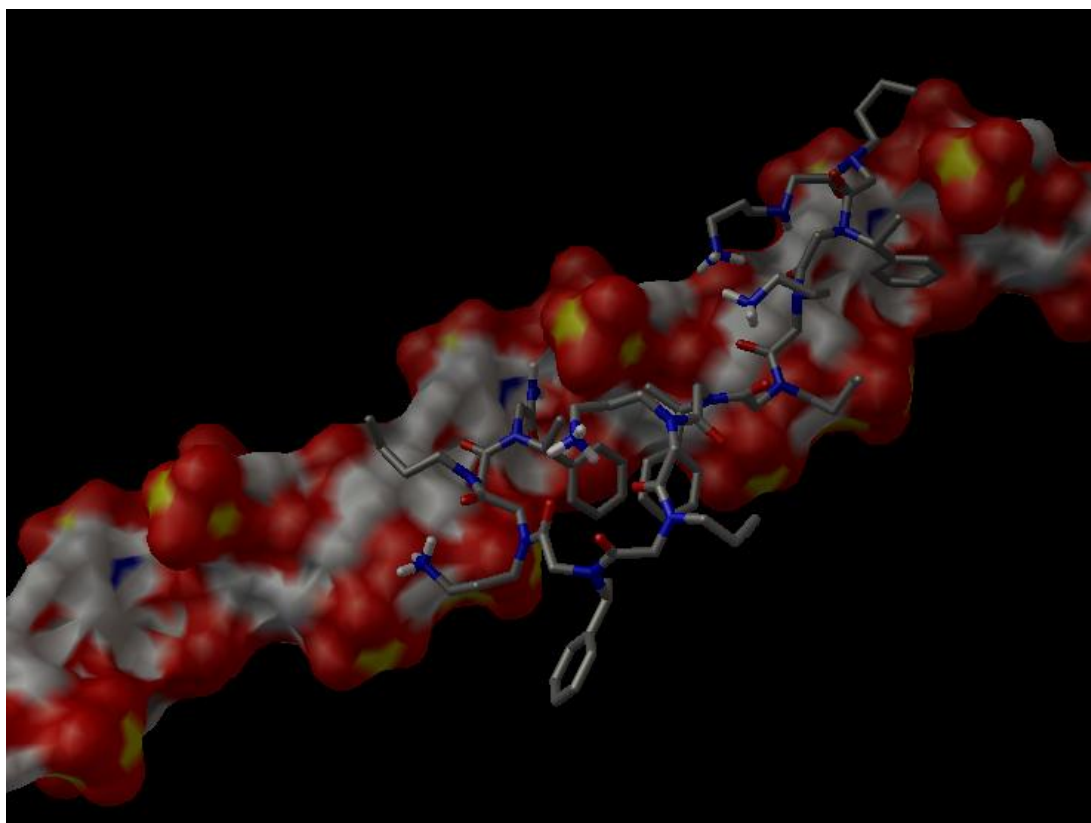


Fig. 6.2.2. The docking of the R12-mer peptoid analog. The loose binding of the R peptoid is apparent with a section of the peptoid out of contact with the heparin fragment.

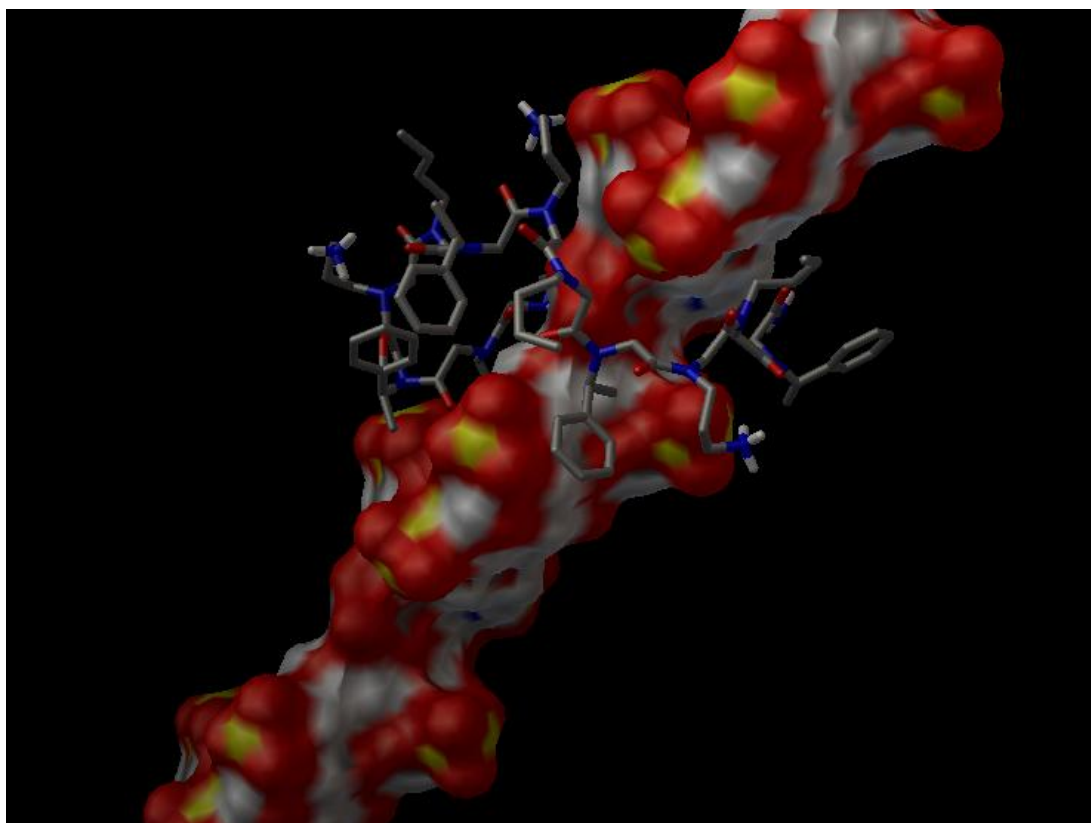


Fig. 6.2.3. The docking of the S12-mer peptoid analog demonstrates the ability of the right-handed conformer to wind around the groove of heparin resulting in a binding modality that results in higher binding affinity compared to the left-handed S peptoid analog.

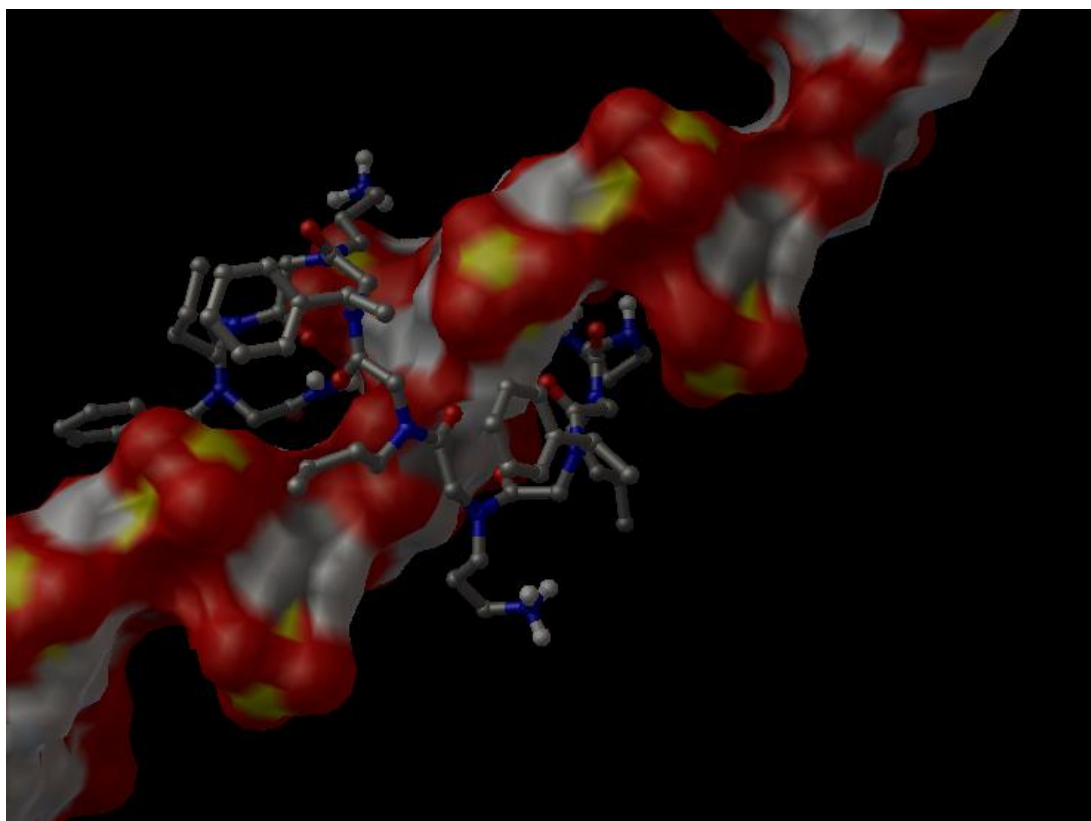


Fig.6.3.1. Ball and stick model of s9-mer docked to heparin, shown in molecular surface format. For heparin, the sulfur atoms are shown in yellow, the oxygens are shown in red and the carbons are shown in white. The peptoid can be seen to fit into a groove of heparin, a binding modality made possible by the smaller ammonium groups in comparison to guanidinium groups.

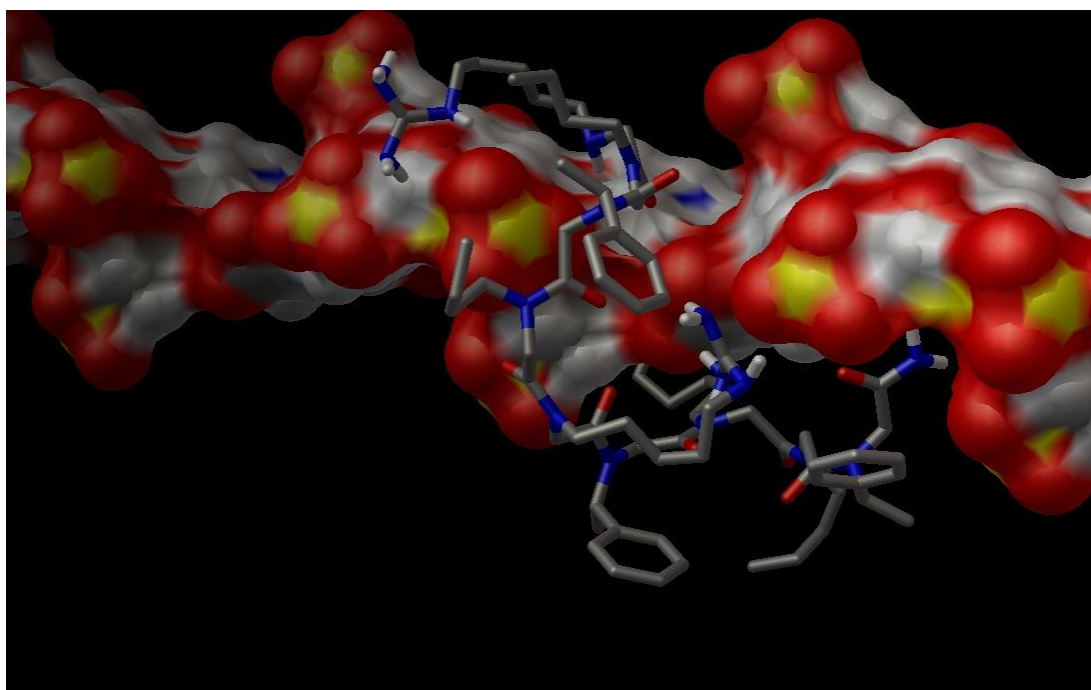


Fig. 6.4.1. A guanidinium-bearing s9mer docked to heparin. When the guanidinium groups are charged, the peptoid wraps itself around the helical groove of heparin. The dihedrals of this peptoid are starting from the C-terminus ignoring the amide: $\text{spe}_1 = \text{cis}$; $\text{Bu}_1 = \text{cis}$; $\text{Cad}_1 = \text{trans}$; $\text{spe}_2 = \text{trans}$; $\text{Bu}_2 = \text{trans}$, $\text{Cad}_2 = \text{trans}$; $\text{spe}_3 = \text{cis}$; $\text{Bu}_3 = \text{trans}$, and there is no dihedral at the N-terminus Cad . This suggests the peptoid has a central section that is a trans helix, with the beginning starting out as a cis helix. This would account for some helical character as measured by CD.

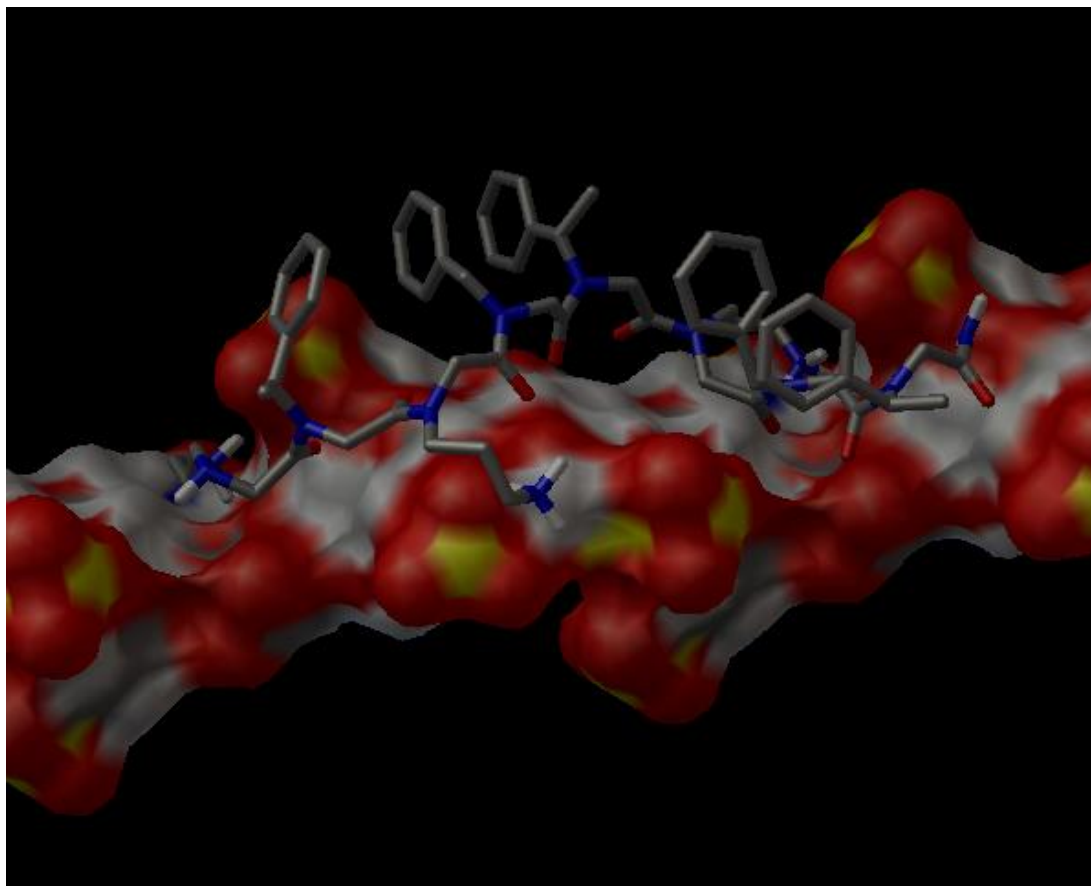


Fig. 6.5.1. A Bz-bearing peptoid is shown docked to heparin. As can be seen in the figure, three of the benzene rings are aligned on the left and the two on the right are also aligned with each other. The ammonium groups can also be seen to be in close proximity to the sulfonic esters.

The stacking would result in greater stability in secondary helical structure. The size also prevents the peptoid from falling into the groove as seen in the first peptoid shown in this chapter (**Fig. 6.3.2**). An alternative possibility is that bulky groups reinforce the helical secondary structure of the peptoid.

6.7 Summary

The docking studies done with AutoDoc Vina, yielded a significant amount of valuable data. It demonstrated three separate modalities and binding patterns for four classes of peptoids. The S right-handed ammonium and guanidinium-bearing peptoids, actually seem to interact with heparin by laying into a groove that runs along the helical structure of the heparin molecule. This is in contrast to the expected binding modality, which was discussed in Chapter One, which showed a peptoid docking to heparin along one face with all of the cationic groups on the same face. The R left-handed ammonium-bearing peptoid, while unable to fit into the groove, and thus use this method of tight binding, binds rather loosely along one face, but without the tightness provided by the hydrogen bonding of the guanidinium-bearing peptoids.

The guanidinium-bearing peptoids were shown by heparin affinity chromatography to possess enhanced binding, but ITC studies failed due to unknown binding events taking place. The docking of a guanidinium-bearing peptoid was shown in **Fig. 6.4.1** also seem to wrap around the helical groove of the heparin in contradiction to the rational design discussed in Chapter One. The guanidinium-

bearing peptoids probably gain their enhanced binding to heparin due to greater hydrogen bonding involved in comparison to the ammonium bearing peptoids.

The unexpectedly enhanced binding of the benzyl-bearing peptoid, an example of which is shown in **Fig. 6.5.1**, can be much easier to understand by viewing the docking image. The benzene rings are clearly aligned in a pi stacking configuration consistent with the hypothesis discussed in Chapter Five and also provide bulky substituents, which could reinforce the secondary structure of the peptoid.

6.8. References

1. Trott, O., Olsen, A.J. *J. Computational Chem.* **2010**, *81*, 455-461.
2. Spartan '08. Wavefunction, Inc, **2010**.
3. Mulloy, B., Forster, M.J., Jones, C., Davies, D.B. *Biochem.J.* **1993**, *293*, 849-858.

Chapter Seven: Summary and Conclusions

7.1 Introduction

The goal of this research was to design, synthesize and study a library of peptoids with the potential to replace protamine, which is in current medical usage to neutralize the anticoagulant activity of heparin when heparin is no longer needed in a medical setting such as a surgical operation requiring the extracorporeal circulation of blood through heart-lung machines or during kidney dialysis. Protamine is known to cause a myriad of side effects and there is a great desire to find a suitable replacement. It has already been shown that HIP¹, heparin interacting peptide and related analogs can bind with good affinity to heparin, and thereby restore the coagulation cascade that heparin inhibits.

Problems with peptides are that they possess low bioavailability due to vulnerability to proteases. In addition, peptides, because they possess a hydrogen on the backbone nitrogen, which allows hydrogen bonding, are subject to denaturation by high temperatures, solvents, or chemical denaturants such as urea or detergents.

Peptoids, which are N-substituted glycine oligomers, are superior to peptides as they are impervious to proteases, are nonimmunogenic, and are orally active. Also the number of commercially available amines is large, and generally inexpensive, allowing the synthesis of large libraries of peptoids. For these reasons, peptoids were a superior alternative choice to peptides, and peptoid-based heparin-binding ligands could be potential protamine replacements. To achieve the goal of producing a heparin binding

peptoid, rational drug design methodologies were used to guide the design and synthesis of a focused library of peptoids. A series of peptoid analogs were synthesized using solid phase methodologies and the resulting peptoids were studied by Isothermal Titration Calorimetry (ITC), Heparin Affinity Chromatography (HAC), and the secondary structures were determined by Circular Dichroism. *Ab initio* molecular modeling and docking to heparin by AutoDoc Vina², also provided intriguing information about how the peptoids potentially bind to heparin.

Peptoids were designed based upon a repeating trimer sequence consisting of H-[*N*(cationic side chain)-*N*(central alkyl and also 2 other side chains)-*N*(α -chiral side chain)]_n-NH₂, where n was 1—4.

An initial study was conducted to determine the choice of chiral side chain in the repeating trimer sequence. After synthesizing two enantiomeric 12-mers, it was determined by ITC, that the peptoid containing the *S*-analog possessed higher binding affinity to heparin. Subsequently (*S*)-(-)- α -methylbenzylamine was used to synthesize the remainder of peptoids with *spe* in this position. This resulted in peptoids with a higher percentage of right-handed helical secondary structure, which was confirmed by CD studies. However computational studies provided information that increased our understanding as to how peptoids dock to heparin and due to a combination of *cis*/*trans* isomerism and the interactions of cationic groups on the peptoids and their anionic counterpoints on heparin, a more complex set of binding modalities was discovered. The

computational studies helped to provide information that shed light on binding events detectable by ITC but not visible through ITC alone.

The second variable that was explored was the length of the peptoid, to determine the binding affinity of peptoids of increasing lengths from 3—12 monomer units in length. This showed by ITC and HAC that longer peptoids bind to heparin with greater affinity than shorter analogs. Analogs of insufficient length (shorter than 9 monomers) were not amenable to analysis by ITC due to insufficient binding affinities.

Ammonium-bearing peptoids were also converted to their guanidinylated counterparts by reaction with 1-*H*-pyrazole-1-carboxamidine HCl, thus producing peptoids with guanidinium groups in place of the ammonium groups. These peptoids were found by HAC to possess greater heparin-binding affinity relative to their ammonium-bearing analogs. ITC was of little use in providing binding constants or other thermodynamic parameters. ITC did show that there was a fundamental difference in its binding method to heparin compared to the ammonium-bearing peptoids. Possible answers to the question of how guanidinium-bearing peptoids bind differently than ammonium-bearing peptoids had to wait until computational studies were conducted later on in the research.

A series of analogs was then synthesized to explore the effect of lengthening the cationic side chain, which consists of a carbon chain terminating with either an ammonium group or a guanidinium group on the end. Three different lengths of carbon chains were used. The initial cationic side chain was designed to mimic arginine, so it bore a 3- carbon chain. Using this as a starting point, a design consideration was to

lengthen the carbon chain in order to allow the cationic ammonium and guanidinium groups to better interact with the anionic deprotonated esters and amides of heparin. MonoBoc protected 1,3-diaminopropane was used to produce the 3-carbon *N*(Orn) and *N*(Arg) monomers. It was found that monoBoc protected 1,4-diaminobutane and monoBoc Cadaverine were commercially available at reasonable cost, and these were used to extend the carbon chain from 3 to 5 carbons in length. After analysis of the resulting peptoids by ITC and HAC, it was found that longer carbon chains in this position did result in increased binding affinity to heparin.

The next position investigated was the central unit of the trimer. The initial peptoids studied bore a *N*(Bu) side chain. The design consideration was that by decreasing the length of the alkyl side chain, it may assist binding by decreasing steric interference with the cationic side chain. Therefore propyl, ethyl and finally methyl side chains were substituted in analogs and ITC and HAC provided data in support of the hypothesis that shorter alkyl chains enhanced peptoid binding to heparin. Two additional side chains were also used, an allyl group and a benzyl group, and the results of these two substitutes were peptoids that bound with increased affinity to heparin. The peptoid with the benzyl side chain, in particular demonstrated greatly enhanced binding to heparin. This phenomenon at first seemed counterintuitive, but it was hypothesized that pi stacking could result in stabilized helical structures of the peptoids. Additional data was provided by docking studies, that showed that not only did pi stacking result, but bulkier groups prevented the peptoids from wrapping the peptoid around and within a groove in the helical secondary structure of heparin. The results of decreasing the alkyl chain length

enhanced binding, but benzyl groups in this position possessed special features that resulted in greatly enhanced binding affinity to heparin.

Placing all of the modifications together that result in enhanced heparin binding, an ideal target peptoid can be postulated that would include a longer carbon chain on the charge bearing group. Guanidylation of the primary amine of this group is favored as all guanidylated peptoids were found to bind with greater affinity to heparin by HAC. The central monomer unit should bear a benzyl group, which enhances binding through pi stacking and steric prevention of the peptoid wrapping around the groove of the heparin molecule. The S form of the chiral side chain enhances binding affinity. The final factor is length, with 12 probably the best compromise between aqueous solubility and enhanced heparin affinity. The ideal target peptoid is proposed to have the following sequence: H-[N(Cad)G-N(Bz)-N(spe)]₄-NH₂.

In conclusion, through modification of side chains of heparin binding peptoids, an ideal target peptoid has been postulated that it is hypothesized could act as a replacement for protamine.

7.2 References

1. Rohde, L. H., Julian, J., Babaknia, A., Carson, D.D. *J. Biol. Chem.* **1996**, *271*, 11824-11830.
2. Trott, O., Olsen, A.J. *J. Computational Chem.* **2010**, *81*, 455-461.

Chapter Eight: Future Work

8.1 Introduction

In the last chapter on Summary and Conclusions, the work that has been done in this thesis and the meaning behind the research have been summarized. This chapter now carries that research forward to consider the next steps and future work. The design of the library of peptoids consisted in optimizing the features of the peptoids to investigate how changes affected the binding affinity of the peptoids for heparin. By making changes in the peptoid structure and evaluating the results compared to a control peptoid (the s9-mer), it was possible to arrive at the best possible configuration: H-[N(Cad)G-N(Bz)-N(spe)]₄-NH₂.

The starting point in all future research would be to synthesize the above peptoid sequence for conformation that it would, in fact, possess the highest heparin binding affinity. There are other possibilities that could also be synthesized as well. Substitution of a methyl group in place of the benzyl group could also be tried.

Following this, it would be of great interest to conduct tests of the efficacy of the peptoids for neutralizing the anticoagulant activity of heparin with the Coatest Assay¹. This assay would test the compound for the ability to not only bind to heparin, but to neutralize the anticoagulant activity of heparin.

Additionally, *in vivo* assays are also available such as the activated partial thromboplastin time (aPTT or APTT) test, or fibrinogen testing (using the Clauss method)².

The results of these tests would indicate the appropriateness of moving forward eventually toward animal testing before actual use in clinical studies can be conducted, but that would be far down the line in the development of this compound as a useful replacement for protamine.

8.2 References

1. Diapharma Inc. *<http://www.diapharma.com>* **2011**.
2. Tan, V., Doyle, C.J., Budzynski, A.Z. *Am J Clin Pathol* **1995**, *104*, 455-62.